University of Strathclyde

Strathclyde Institute of Pharmacy and Biomedical Sciences, University of Strathclyde,
Glasgow, G4 0RE

Analysis of the regulation mechanism of LmxMPK1, a *Leishmania mexicana* MAP kinase homologue.

A thesis submitted in fulfilment of the requirements for the degree of Doctor of Philosophy

Patrick Pearse McAleer

Glasgow, Scotland, September 2012

This thesis is the result of the author's original research. It has been composed by the author and has not been previously submitted for examination that has led to the award of a degree.

Signed:

Date:

We can only see a short distance ahead, but we can see plenty there that needs to be done.

- Alan M Turing, 1912 – 1954

Abstract

Abstract

Leishmaniasis is a disfiguring tropical disease, caused by various species of the protozoan parasite *Leishmania*. Two million new infections and 50,000 deaths occur annually. Currently 350 million people live in areas where leishmaniasis is endemic and are at risk of infection – a number that will increase with global warming. Access to treatment is inconsistent across the affected regions, moreover, the available treatments for leishmaniasis have changed little in the past century and are often toxic with resistance becoming more prevalent, thus underscoring the need for new treatment regimens. LmxMPK1 is an essential MAP kinase homologue in *Leishmania mexicana*. Previous work had suggested that it might be regulated in a novel manner that differed from that of MAP kinases in higher eukaryotes. This study found evidence to support this theory, although a definitive mechanism of regulation of kinase activity was not established. A residue outside of the MAPK phosphorylation lip was shown to be essential for regulation of kinase localisation *in vivo,* whilst *in vitro* results showed that it was a target for kinase autophosphorylation. The *in vitro* results also hinted that at least one other residue might also be subject to autophosphorylation, although to a lesser degree. An inhibitor-sensitised system for studying LmxMPK1 was optimised, with the phenylalanine-93 to glycine mutation shown to be optimal for retaining kinase activity in the absence of inhibitor and diminishing kinase activity when the inhibitor was present. The *in vivo* localisation of a novel *L. mexicana* phosphatase homologue, LmxPTP, was studied and evidence of endoplasmic reticulum localisation was found. Work was carried out to determine the essentiality of LmxPTP by attempting to delete the gene encoding it. However, this was not achieved and whether it was due to the phosphatase being essential, chromosome aneuploidy or unsuccessful transfection of the deletion fragments was not determined.

Abbreviations

-/-	double-allele deletion
°C	degrees Celsius
× g	times gravity
1Na	1-naphthyl-pyrazolo [3,4-d] pyrimidine
1Nm	1-naphthylmethyl-pyrazolo [3,4-d] pyrimidine
2Nm	2-naphthylmethyl-pyrazolo [3,4-d] pyrimidine
A	ampere
aa	amino acids
Amp	ampicillin
APS	ammonium persulfate
ATP	adenosine triphosphate
bp	base pairs
BSA	bovine serum albumin
cAMP	cyclic adenosine monophosphate
CL	cutaneous leishmaniasis
cpm	counts per minute
C-terminus	carboxy terminus
da	Dalton
DAPI	4′,6-diamidino-2-phenylindole dilactate
DCL	diffuse cutaneous leishmaniasis
ddH_2O	double distilled water
DMSO	dimethyl sulphoxide
DNA	deoxyribonucleic acid
dNTP	deoxyribonucleotide triphosphate
DTT	1,4-dithiothreitol
DUSP	dual-specificity phosphatase
E. coli	*Escherichia coli*
EDTA	ethylenediamine tetraacetic acid

EGTA	ethylene glycol bis(β-aminoethylether) tetraacetic acid
ER	endoplasmic reticulum
ERK	extracellular signal-regulated kinases
EtBr	ethidium bromide
FCS	foetal calf serum
g	gram
gDNA	genomic DNA
GDP	guanosine diphosphate
GFP	green fluorescent protein
GIPL	glycoinositol phospholipids
gp	glycoprotein
GSK	glycogen synthase kinase
GST	glutathione-S-transferase
h	hour
his	hexahistidine
HA	haemagglutinin
HCl	hydrochloric acid
HRE	hormone response element
HRP	horse radish peroxidase
HYG	hygromycin B resistance marker gene
iFCS	heat-inactivated FCS
iNOS	inducible nitric oxide synthase
InsP	inositol phosphate
InsP3	inositol 1,4,5-triphosphate
IPS	*myo*-inositol-1-phosphate synthase
IPTG	isopropyl-β-D-thiogalactopyranoside
IS	inhibitor-sensitive
kb	kilobase pairs
kDa	kilo-Dalton

kDNA	kinetoplast DNA
l	litres
L.	*Leishmania*
LB	Luria-Bertani (broth)
Lu.	*Lutzomyia*
LPG	lipophosphoglycan
M	molar
MAPK	mitogen-activated protein kinase
MAP2K	MAP kinase kinase
MAP3K	MAP kinase kinase kinase
MEK	MAPK/ERK kinase
MBP	myelin basic protein
MCL	mucocutaneous leishmaniasis
min	minute
ml	millilitres
MS	mass spectrometry
MS/MS	tandem MS
NaOH	sodium hydroxide
NaCl	sodium chloride
NEO	neomycin resistance marker gene
NOPP	nucleolar phosphoprotein
N-terminus	amino-terminus
OD	optical density
ORF	open reading frame
PBS	phosphate buffered saline
PCR	polymerase chain reaction
Phleo	phleomycin resistance marker gene
PMSF	phenylmethyl sulfonyl fluoride
PtdIns	phosphatidylinositol

PTP	protein-tyrosine phosphatase
PTPL	PTP-like
PV	parasitophorous vacuoles
PVDF	polyvinylidene fluoride
RNA	ribonucleic acid
RNAi	RNA interference
rpm	revolutions per minute
s	second
SAP	shrimp alkaline phosphatse
SDS	sodium dodecyl sulphate
SDS-PA	SDS-polyacrylamide
SDS-PAGE	SDS-PA gel electrophoresis
T.	*Trypanosoma*
TBS	tris-buffered saline
TEMED	N, N, N′, N′-tetramethylethylenediamine
TKL	tyrosine kinase-like
TLCK	Nα-tosyl-L-lysine chloromethyl ketone hydrochloride
tris	tris(hydroxymethyl)aminomethane
UV	ultraviolet
V	volt
v/v	volume per volume
VL	visceral leishmaniasis
w/v	weight per volume
WHO	World Health Organisation
WT	wild type
X-gal	5-Bromo-4-chloro-3-indolyl-β-D-galactopyranoside

1 Introduction

1.1 *Leishmania* and leishmaniasis

In 1903 two parasitologists working in India independently published papers in which they identified the causative agent of the tropical disease kala-azar. The Glasgow-born William Boog Leishman published an account in the British Medical Journal of small ovoid bodies in the liver of a patient who had died of, what was then called, “dum-dum fever” (Leishman, 1903). The Irish physician Charles Donovan published an account in the same journal of organisms he had seen in smears from patients in Madras (Donovan, 1903). It was later recognised that the two had identified the same organism and it was named *Leishmania donovani*. In addition to the *donovani* species, many other species of *Leishmania* are causative agents of the tropical disease leishmaniasis.

1.1.1 Taxonomy

Leishmania species are members of the Kinetoplastida class of organisms. This class is defined by the presence of the kinetoplast, which is a structure within the cell’s large, singular mitochondrion that contains the genome for the mitochondrion on densely coiled DNA. There are two orders within the Kinetoplastida class: the Trypanosomatidae and the Bodonidae. The Trypanosomatidae are uniflagellate (one flagellum) and generally obligatory parasites, whereas Bodonidae organisms are biflagellate (two flagella) and can be free-living as well as parasitic. Trypanosomatidae organisms fall within ten genera (nine living and one extinct), with species of *Crithidia*, *Trypanosoma* and *Leishmania* studied the most extensively due to their impact on human, animal and plant health.

Leishmania are split into two sub-genera, *L. (Leishmania)* and *L. (Viannia)*. The principal distinction between the sub-genera is that *L. (L.)* species develop exclusively in the midgut and foregut of the sand fly, whereas *L.* (*Viannia*) species have an additional developmental stage in the hindgut (Lainson *et al.*, 1987). It has recently been shown that members of the *Viannia* sub-genus have retained the cellular components necessary for RNAi, whereas *Leishmania* sub-genus members have lost it at some point in evolution (Lye *et al.*, 2010). The *Viannia* sub-genus only

contains a few *Leishmania* species (*L. braziliensis*, *L. guyanensis* and *L. panamensis*), which cause a relatively small proportion of the global disease burden of leishmaniasis. *Leishmania mexicana* (the species studied in this work) is a *L. (Leishmania)* species and thus is incapable of being studied using RNAi techniques.

1.1.2 Epidemiology and Clinical Manifestations

Leishmaniasis is a global problem with cases reported in 98 countries or territories (WHO, 2010). Cases occur in regions where Phlebotominae sand flies are found, namely the tropics and sub-tropics, with approximately 350 million people at risk of infection.

It is estimated that 12-14 million people have a current *Leishmania* infection and that 2 million new cases occur annually, of which 1.5 million are cutaneous leishmaniasis and 0.5 million are visceral leishmaniasis. Fatalities as a result of leishmaniasis are estimated to be 50,000 annually (WHO, 2010). The clinical symptoms, severity of disease and probability of death depend on the species of *Leishmania* that the patient is infected with.

Cutaneous leishmaniasis

Cutaneous leishmaniasis (CL) is the mildest form of disease caused by *Leishmania* species. Following infection by a bite by an infected sand fly, the symptoms present as a localised skin reaction, which develops into an ulcer that will resolve spontaneously in an immunocompetent host, but may cause a scar at the site of infection. In the majority of cases there is only a single lesion, however small “satellite” papules can develop in close proximity to the primary lesion (Salman *et al.*, 1999). These are believed to be due to localised reactions to antigens from the parasite or its secretions (Salman *et al.*, 1999).

In the Old World, *Leishmania aethiopica* (*L. aethiopica*), *L. major*, *L. infantum* and *L. tropica* are the causative agents of cutaneous leishmaniasis. In the New World (The Americas), *L. mexicana*, *L. venezuelensis* and *L. amazonensis* all cause Localised Cutaneous Leishmaniasis (LCL) (Berzunza-Cruz *et al.* 2008). Diffuse Cutaneous

Leishmaniasis (DCL), occurs when a primary lesion at the site of infection spreads to other areas of the skin causing painless plaques (Salman *et al.*, 1999). Although DCL responds poorly to treatment, it is very rarely fatal in immunocompetent patients. *L. aethiopica*, *L. amazonensis* and *L. mexicana* are currently the only species thought to cause DCL (Berzunza-Cruz *et al.*, 2008; Lucas *et al.*, 1998). The countries affected by cutaneous leishmaniasis are shown in Figure 1A. However, the disease burden is disproportionately borne by several countries: 90% of cutaneous leishmaniasis cases occur in Afghanistan, Brazil, Iran, Peru, Saudi Arabia and Syria (WHO, 2010).

Cases of CL are showing an upwards trend (Desjeux, 2004) and the regions affected are predicted to expand as a result of global warming (WHO, 2010). This has already been observed in Italy as cases are being reported further north than had been the case previously (Gramiccia & Gradoni, 2005). Development and industrialisation projects create the optimal blending of factors that increase disease transmission incidence. In many cases the workers on such projects are non-native to the area and will have no pre-existing immunity to the parasites as a result of endemic exposure, clearance of forests for logging or building does not remove the sand fly vector population and in cases where the development is water-based (i.e. a dam) the rodent reservoir population is often disturbed and moves to closer proximity to humans (Gramiccia & Gradoni, 2005).

Mucocutaneous leishmaniasis

The form of leishmaniasis with intermediate severity is mucocutaneous leishmaniasis (ML). The majority of cases are caused by *L. braziliensis*, *L. guyanensis* and *L. panamensis* species (Neuber, 2008). Cases of the disease are localised to South America and the majority of these occur in Bolivia, Brazil and Peru (WHO, 2010). Disease occurs when *Leishmania* organisms migrate to the mucous membranes, typically of the face, but rarely to the urogenital system (Schubach *et al.*, 1998; Babello *et al.*, 2002). Massive ulceration occurs across the lower jaw and nasal septum, which can eventually collapse due to degradation (Neuber, 2008). The pharynx and larynx are also destroyed during infection with death resulting either from aspiration pneumonia or secondary bacterial infections (Neuber, 2008).

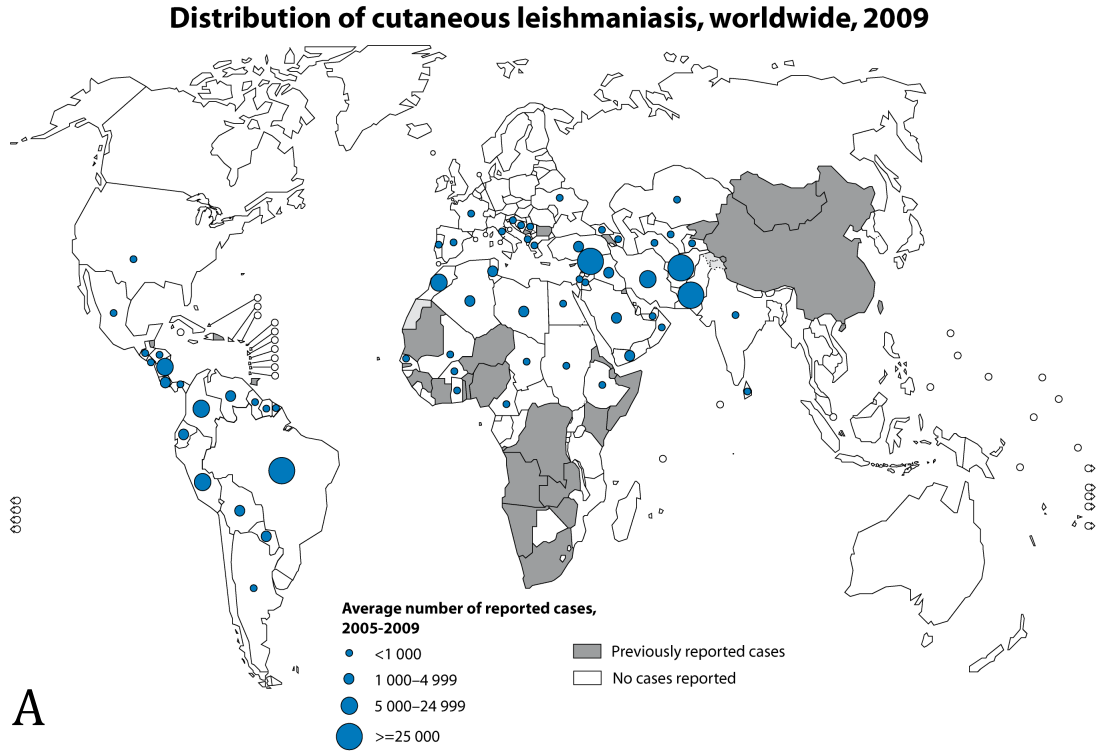

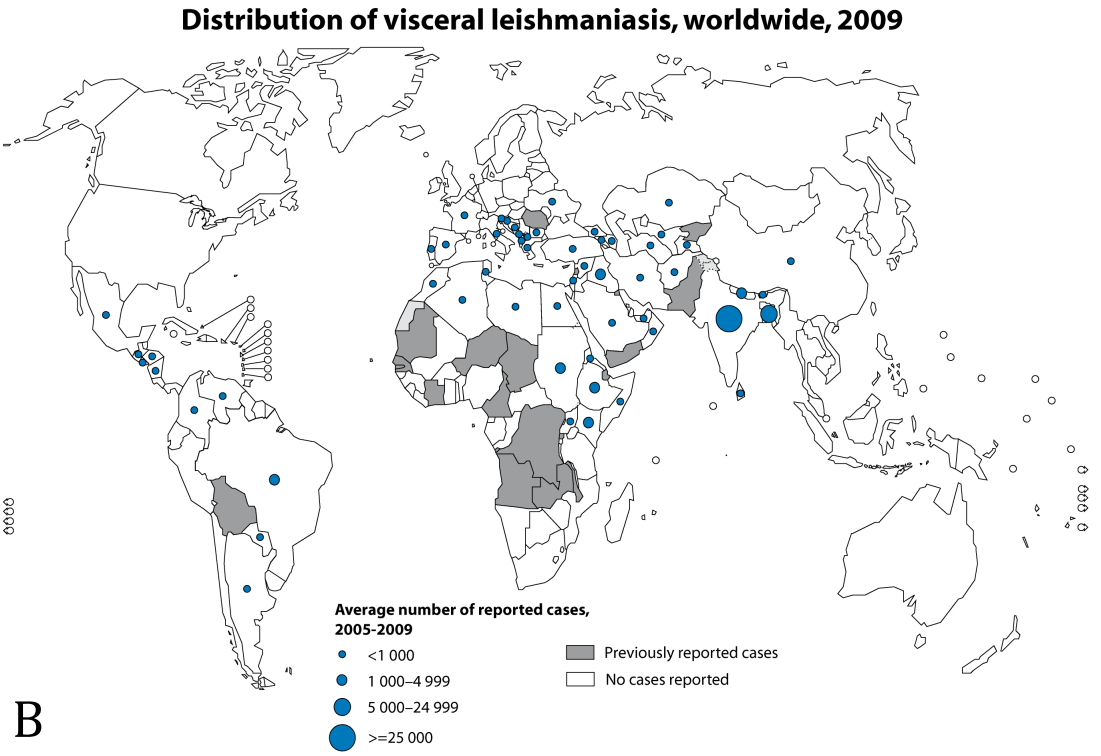

Figure 1: Countries affected by leishmaniasis.
A, Countries affected by cutaneous leishmaniasis; B, Countries affected by visceral leishmaniasis. (Source for both maps: WHO (http://gamapserver.who.int/mapLibrary/)

Visceral leishmaniasis

The most severe form of leishmaniasis is visceral leishmaniasis (VL). Species that cause this form of disease include *L. donovani*, *L. infantum*, and *L. chagasi*. Figure 1B shows that VL cases are less distributed than for CL, although they are found in Asia, Africa, southern Europe and South America, with 90% of cases occurring in Bangladesh, Brazil, Ethiopia, India, Nepal and North and South Sudan (WHO, 2010).

VL starts as a papule at the site of infection and may remain as such for many years (Neuber, 2008) before metastasising to the viscera, lymph nodes and bone marrow where an invasive destructive infection is established (McFarlane *et al.*, 2008; Neuber, 2008). This results in a non-specific lymphadenopathy and hepatosplenomegaly. The patient will also develop a double-quotidian fever (ie, one that spikes twice in every twenty-four hour period) (Neuber, 2008). Death occurs as a result either of haemorrhaging or from a secondary bacterial infection (Neuber, 2008).

Recent studies have suggested that cases of visceral leishmaniasis may increase rapidly in the future due to co-infection with HIV and VL-causing species of *Leishmania* (Desjeux *et al.*, 2003; Alvar *et al.*, 2008; Pandey *et al.*, 2008). This underscores the need to develop novel treatments for leishmaniasis and to bring them onto the market as quickly as possible. The manifestations of the forms of the disease are shown in Figure 2.

Figure 2: Clinical forms of leishmaniasis.
Cutaneous leishmaniasis (A, B), Mucocutaneous leishmaniasis (C) and Visceral leishmaniasis (D).
Sources: A is from USA Library of Congress collection;
B, Wikimedia Commons (Public Domain image);
C, http://tmcr.usuhs.mil/tmcr/chapter46/large46/46-18.jpg;
D, http://www.icp.ucl.ac.be/~opperd/parasites/images/WHO1.jpg

1.1.3 Current Treatments and Prevention

Currently there are several drugs used in the treatment of *Leishmania* infections in humans. Their use varies by country and access is often dependent on the patient's ability to pay. Drugs currently in use include: Amphotericin B (Fungizone®), Liposomal Amphotericin B (AmBisome®), Pentamidine, Miltefosine, Paromomycin, Sodium stibogluconate (Pentostam®) and meglumine antimonate (Glucantime®). Rifampicin and Ketoconazole are also used in patients who appear to be infected with a drug resistant strain of *Leishmania* or who are responding poorly to treatment with standard frontline medication. Miltefosine, Rifampicin and Ketoconazole are the only treatments administered orally, the others are either intramuscularly (IM) or intravenously (IV) administered.

One of the difficulties with treating leishmaniasis is that the majority of treatments require the medication to be injected. This can be problematic in remote, poor and/or politically unstable areas with limited or no healthcare provision. Intermittent provision of anti-leishmanials may also be a factor in the development of drug-resistant strains, as patients do not manage to complete a full course of treatment.

Another reason for failure to complete treatment is that although drugs like Meglumine antimonate, Sodium stibogluconate and Amphotericin B have cure rates exceeding 90% with low levels of resistance, they can be highly toxic to the patient; treatments with Antimony can be cardiotoxic and cause a decrease and even failure in hepatic and renal function. Amphotericin B can cause convulsions, fever and/or anaemia. For these reasons it is important that new, safer and equally effective treatments are developed for the treatment of leishmaniasis.

Prevention of leishmaniasis requires multiple strategies that must be adapted to local conditions. Elimination of the local sand fly population removes the disease vector and is achieved through annual treatment of domestic dwellings with insecticide (Desjeux, 2004), however it is expensive and protection only lasts for one year. Control of reservoir populations for *Leishmania* also contributes to a decline in

human cases of the disease. However, this is complicated by the fact that different *Leishmania* species have different reservoir hosts and that in some cases the reservoir species is unknown, for example, the reservoir host(s) for *L. major* in Chad, Cameroon, Nigeria and Yemen (WHO, 2010). Even in cases where the reservoir is known, culling of infected animals may be complicated due to emotional attachments that humans have with them (for example, domestic dogs) – particularly if the animal is asymptomatic. However, in cases where funds are available or if resistance to culling is insurmountable, insecticide-containing dog collars reduce feeding by sand flies (Quinnell & Courtenay, 2009) and thus transmission to humans is diminished.

Modification of people's behaviour can also reduce the likelihood of infection. The use of insecticide impregnated bed nets reduces the risk of infection whilst sleeping (Desjeux, 2004). As with all insect-transmitted diseases, the wearing of long-sleeved clothing at all times is a simple prophylactic measure, however, given the climate of endemic regions it is perhaps unreasonable to expect this to be widely adopted. Another measure that could reduce transmission is for people in affected regions to remain indoors during the sand fly's active period (dusk until dawn), however, yet again, after sundown in affected areas is when it is coolest and people may wish to remain outside.

Civil unrest and war are also linked to increased prevalence of leishmaniasis. During the civil war in Sudan many displaced people moved to camps in the Western Upper Nile region of the country, but due to their lack of exposure to the *Leishmania* species in the area and the high level of malnutrition in displaced persons camps, an outbreak of visceral leishmaniasis occurred that killed 100,000 people (out of a population of 300,000) (Seaman *et al.*, 1996). The socioeconomic effects of long-standing conflicts can also lead to large discrepancies in leishmaniasis cases on either side of a border: in the northern sector of the Palestinian territory of the West Bank seropositivity for *Leishmania* infection is almost triple the rate in the bordering region of northern Israel (8.4% and 3% respectively) (Alvar *et al.*, 2012). Cases of visceral leishmaniasis are also disparate (28 and 76 over a 14 year period).

1.1.4 Life cycle

Leishmania are eukaryotic protozoan organisms of the order *Trypanosomatida*. They are digenetic obligate parasites with two principal morphologies, a flagellated form in the sand fly vector stage of the life cycle (promastigote) and an aflagellate form in the mammalian host stage (amastigote). The morphologies and life cycle are shown in Figure 3.

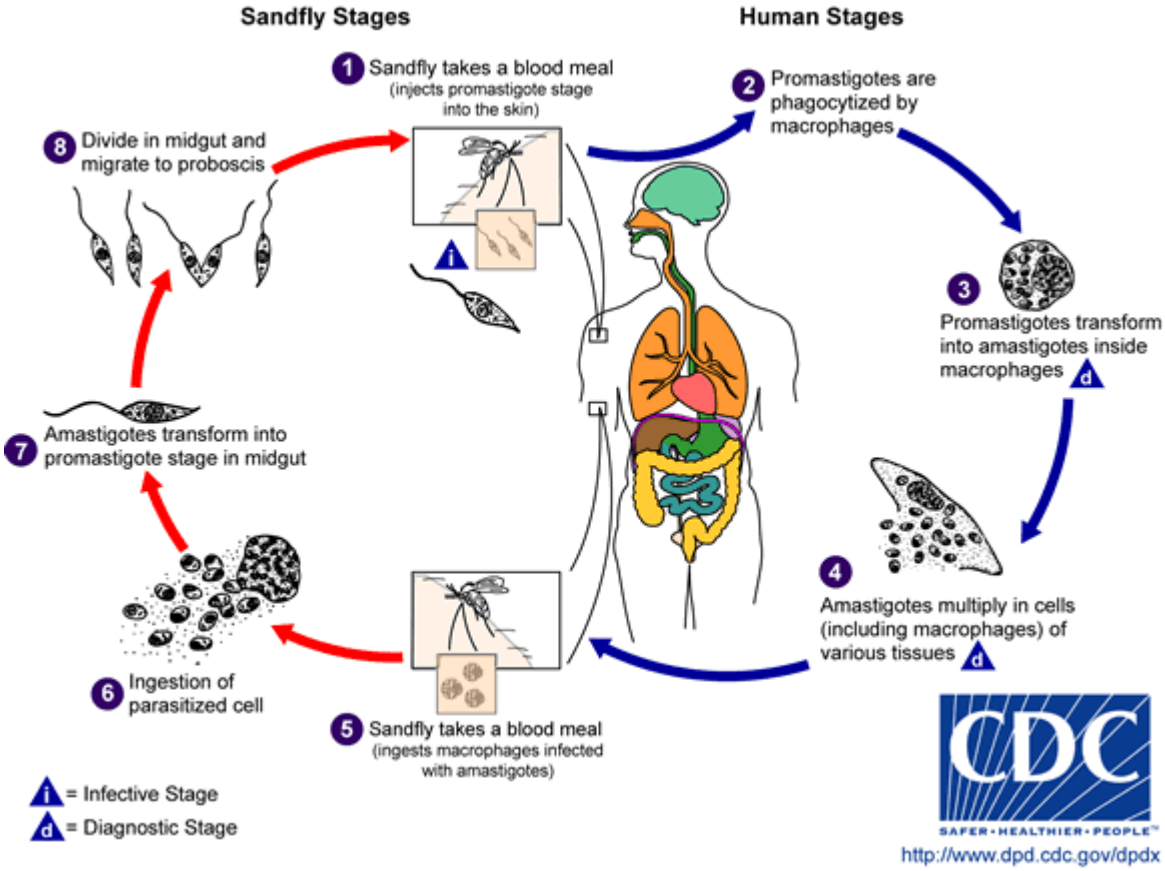

Figure 3: Life cycle and morphologies of *Leishmania* cells. (Source: http://dpd.cdc.gov/dpdx/html/imagelibrary/Leishmaniasis_il.asp?body=G-L/Leishmaniasis/body_Leishmaniasis_il_th.htm)

The principal vector for the various *Leishmania spp.* is the female sand fly (Bates, 2008). There are over one thousand species in the Phlebotomine subfamily of the Psychodidae family (Order: Diptera), but only seventy are implicated in the transmission of *Leishmania spp.* In the Old World (Africa, Asia and the Middle East) these are of the genera *Phlebotomus*, whereas in the New World (Central and South America) they are of the *Lutzomyia* genera (Bates *et al.*, 2008). Species involved in the transmission of *Leishmania* in the New World (including *L. mexicana*) include *Lutzomyia whitmani (Lu. whitmani), Lu. intermedia* and *Lu. migonei*.

Although the sand fly is the principal vector, there are reported cases, primarily in Europe, of injecting drug users acquiring *Leishmania* infections from sharing contaminated needles (Salman *et al.*, 1999; Desjeux *et al.*, 2003; Puig *et al.*, 2003).

During the vector stage of the life cycle *Leishmania* cells are flagellated and called promastigotes (Alexander and Russell, 1992). Different forms of promastigotes are found in different regions of the vector as the parasites pass through – see Figure 4. Within 48 hours of ingestion by the sand fly the parasites differentiate into the procyclic promastigote form while still enclosed in the peritrophic membrane (Kamhawi *et al.*, 2006), the cell body is generally less than 12 μm in length and is flagellated. At this stage the parasites are replicating rapidly (Mallinson and Coombs, 1989). Over the next 24 hours the parasites are released from the peritrophic membrane and attach to the midgut by hemidesmosome attachment (Alexander and Russell, 1992). At this stage replication is slower than in the initial 48 hours and the cell morphology has changed to be thinner and longer with parasites in this stage called nectomonad promastigotes. After 96 hours in the sand fly (4 days) the size of the cell body diminishes and a second wave of replication occurs, parasites in this stage are leptomonads (Kamhawi *et al.*, 2006). At this stage the parasites also produce a substance called the promastigote secretory gel (PSG), which forms a “plug” in the fly’s midgut and impairs the ability of the fly to feed, thus necessitating multiple attempts and the regurgitation (and transmission) of parasites to a new host (Kamhawi *et al.*, 2006). Five days after infection of the sand fly the parasites make their final stage differentiation to metacyclic promastigotes, these are non-replicating

parasites and are the population that will establish an infection in the new host following feeding by the sand fly. A further form of the parasite is observed after 5 days, namely the haptomonad form, however the precise role it plays in transmission of infection is currently unknown.

The parasite's glycocalyx is thicker in metacyclic promastigotes (17 μm compared with 7 μm in procyclic promastigotes), which has been attributed to modifications of the structure of lipophosphoglycan (LPG) (Pimenta *et al.*, 1989) and glycoprotein-63 (gp63) (Muskus and Marin-Villa, 2002). This is most likely due to the need for metacyclics to be able to attach to the midgut of the fly – a process dependent on LPG in many species of *Leishmania* (Kamhawi *et al.*, 2006).

Various proteins are found at different concentrations in the different promastigote forms. These include certain enzymes (Alexander and Russell, 1992) and surface proteins (as previously discussed). Enzymes involved in cell division such as Elongation Factor 2 and RNA helicase are found at higher levels in procyclic promastigotes (Mojtahedi *et al.,* 2008), whereas α-tubulin, β-tubulin and other proteins involved in cell motility are found at higher levels in metacyclic promastigotes (Mojtahedi *et al.*, 2008), thus suggesting that they may have a role in the more virulent nature of metacyclic promastigotes compared to procyclic promastigotes.

Following transfer of *Leishmania* promastigotes to a mammalian host the parasite must evade the innate immune response and also ensure uptake by macrophages. The complement system clears pathogens through the insertion of a lytic complex, consisting of C5b6789, into their cell membrane. *Leishmania* block the formation of the membrane attack complex (MAC) by discarding the components before the full MAC is assembled (Puentes *et al.*, 1990). They also secrete a kinase, leishmanial protein kinase-1 (LPK-1), which phosphorylates C3, C5 and C9, thus blocking the activating cleavage that promotes their assembly (Hermoso *et al.*, 1991). Phagocytosis of the parasite by macrophages is dependent on opsonisation by C3b,

but in order to prevent recruitment and activation of other components of the complement system the surface protease gp63 converts bound C3b to iC3b. Uptake of iC3b opsonised *Leishmania* is mediated by the complement receptors CR1 and CR3 (da Silva *et al.*, 1989). Macrophages are not the only cells that phagocytose *Leishmania*, dendritic cells and polymorphonuclear neutrophil granulocytes have also been identified as host cells (Bogdan & Röllinghoff, 1998; Sarkar *et al.*, 2012) but they are believed to be temporary before macrophages are infected.

Following phagocytosis the *Leishmania* cells are enclosed in a phagosome that fuses with lysosomes containing acid hydrolases. This new structure is called the parasitophorous vacuole and the number of *Leishmania* cells they contain depends on the *Leishmania* species, with multiple *L. amazonensis* or *L. mexicana* cells sharing a single vacuole, *L. major* and *L. donovani* have separate vacuoles for each *Leishmania* cell (Antoine *et al.*, 1998). The acidic pH of the vacuole and the higher temperature of the mammalian host stimulate differentiation from promastigotes to amastigotes. The principal phenotypic differences between amastigotes and promastigotes are the cell body decreases in size from 10-12 μm (for promastigotes) to 3-5 μm (for amastigotes) and the flagellum is shrunk so that it barely protrudes beyond the flagellar pocket (Alexander and Russell, 1992; Wiese, 2007; Bates, 2008). Differentiation to amastigotes can take up to 5 days (Zilberstein *et al.*, 1991), following that the cells proliferate until the burden on the host cell is too great and lysis occurs, the amastigotes are then phagocytosed as previously described.

Amastigotes lack several of the characteristic surface molecules that promastigotes possess including LPG and gp63 (Alexander and Russell, 1992; Bahr *et al.*, 1993). However, they retain glycoinositolphospholipids (GIPLs) on their surface. A 2004 study by Nugent *et al.* identified seven proteins that were only found in the amastigote stage of *Leishmania*. These included eukaryotic Initiation Factor-5α (eIF-5α), 40S Ribosomal S2 protein, Chaperonin 60.2, and Cysteine Proteinase B (Nugent *et al.*, 2004). There was some evidence that Heat Shock Protein-70 (HSP-70) and 83 (HSP-83) were only found in the amastigote stage.

LPG, GIPLs and gp63 all aid the evasion of cell killing mechanisms in macrophages. LPG inhibits protein kinase C activity, which diminishes generation of O_2^- (Olivier *et al.*, 2005). Both LPG and GIPLs block iNOS activity and, consequently, NO production. gp63 has been implicated in suppression of the respiratory burst (Sørensen *et al.*, 1994).

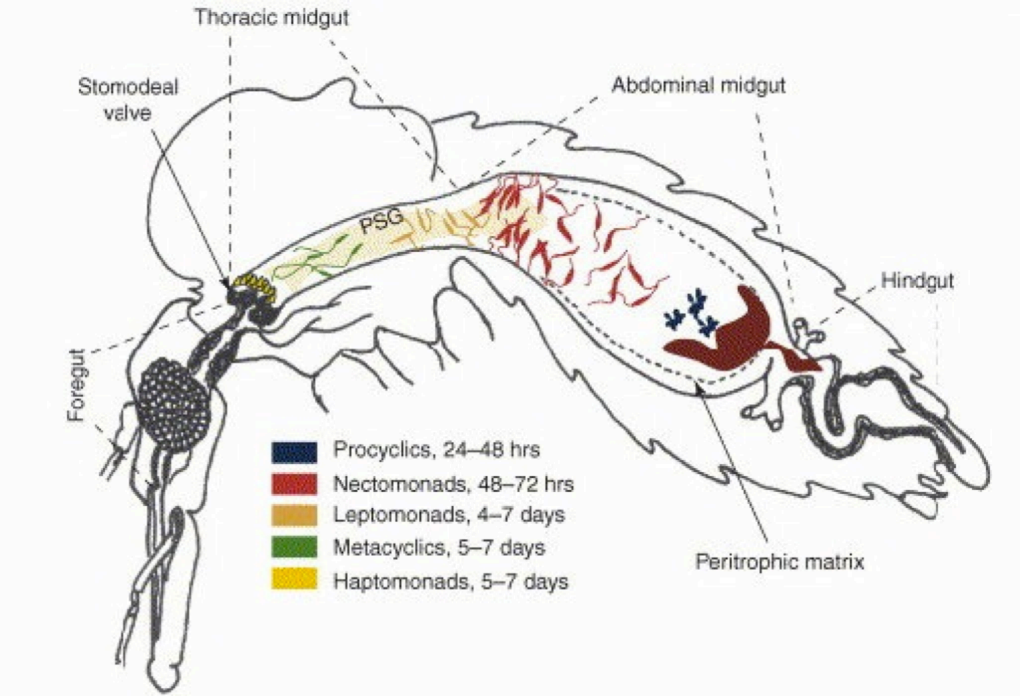

Figure 4: Different forms of *Leishmania* promastigotes during passage through the sand fly vector (From Kamhawi *et al.*, 2006).

There is evidence that *Leishmania* are also able to modulate host-cell signalling in a manner that benefits the parasites. Specifically that gp63 activates the host phosphatases SHP-1 and PTP1B (Shio *et al.*, 2012). These dephosphorylate mediators of the IFN-γ induced signalling pathway including ERK1/2 and JAK/STAT1, thus inactivating them. The effect of this modulation of host-cell signalling is a decrease in the secretion of pro-inflammatory cytokines, leading to a non-healing response by the host (Olivier *et al.*, 2005; Shio *et al.*, 2012).

1.2 Signal transduction in Eukaryotes

The ability of cells to detect and respond to changes in their environment is essential for survival and proliferation. In multicellular organisms homeostasis, growth and responses to pathogens are induced and regulated by endocrine signalling; in unicellular organisms, such as *Leishmania*, chemotaxis and differentiation are controlled by signalling events.

1.2.1 Signalling pathways in higher Eukaryotes

Cell signalling receptors can be divided into two main types based on their location in the cell: extracellular and intracellular. Extracellular receptors are found in the plasma membrane with a domain on the outside of the cell, the three principal types are ligand-gated ion channels, G protein-coupled receptors (GPCRs) and receptors with enzymatic activity.

Ligand-gated ion channels are transmembrane ion channels that change conformation upon binding of a ligand, such as serotonin or acetylcholine, and allow the entry or exit of ions from the cell. GPCRs (also called serpentine receptors) are activated by the binding of hormones or neurotransmitters following which they undergo a conformational change that allows them to exchange the GDP on the Gα subunit of the G protein for a GTP, thus stimulating cAMP signalling or the phosphatidylinositol pathway. Receptors with enzymatic activity include receptor tyrosine kinases (RTKs) and guanylate cyclase. RTKs are composed of an extracellular ligand-binding domain and an intracellular domain with tyrosine kinase activity. Binding of the ligand activates the kinase domain and allows phosphorylation of the substrate, typically itself, which in turn allows binding of other proteins to form a signalling complex. Ligands for this type of receptor include growth factors and

insulin.

Intracellular receptors detect substances that are soluble or capable of diffusing through the plasma membrane. Cytosolic guanylate cyclase is activated by Nitric Oxide, which leads to the production of cGMP. Activation of nuclear receptors is by lipophilic steroid hormones that have diffused into the cell. This causes translocation to the nucleus and binding to hormone response elements, which regulates transcription of certain genes.

1.2.2 Protein kinases

Protein kinases are a class of enzymes that transfer the terminal γ-phosphate group from adenosine triphosphate (ATP) onto a hydroxyl group in the kinase's substrate. Phosphorylation is a post-translational modification that can modulate the activity of an enzyme, stabilise protein-protein interactions, change the cellular localisation of a protein and influence the stability of a protein.

Protein kinases are split into two groups, the eukaryotic Protein Kinases (ePKs), which all have a highly conserved catalytic domain, and the atypical Protein Kinases (aPKs), which are kinases with low similarity to ePKs in the catalytic domain but that have been shown to exhibit kinase activity (Manning *et al.*, 2002). The vast majority of kinases are members of the ePK grouping with many organisms having only one aPKs. The ePK group is further divided into the AGC (Protein Kinases A, G and C), CAMK (Ca^{2+}/Calmodulin-dependent kinases), CMGC (Cyclin-dependent kinases, MAP kinases, GSK3 and CDK-like kinases), STE (homologues of yeast Sterile kinases 7, 11 and 20), TK (tyrosine kinases) and TKL (tyrosine kinase-like kinases) (Manning *et al.*, 2002).

The core structure of protein kinases is highly conserved and is divided into two domains linked by a hinge region (Figure 5A). The N-terminal domain (top of figure 5A) consists of five beta-sheets (β1- β5) and one alpha-helix (αC). The C-terminal domain is larger and is predominately alpha-helical. The hinge region includes the ATP and substrate binding domains (Krupa *et al.*, 2004).

Figure 5A: The 3-dimensional structure of the catalytic core of a serine/threonine or tyrosine protein kinase. a, phosphate anchor ribbon; b, Lys-Glu ionic bond; c, catalytic loop; d, catalytic Asp of subdomain VIb; e, activation loop. (Source: Krupa *et al.*, 2004)

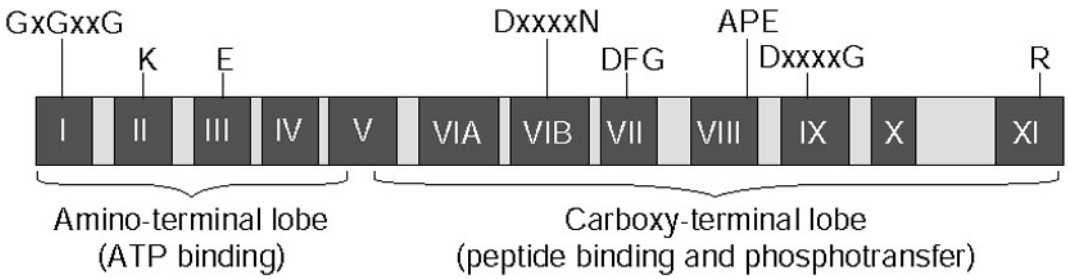

Figure 5B: Conserved sub-domains of the catalytic core of eukaryotic protein kinases.

Sub-domains are indicated by Roman numerals and conserved amino acid residues or motifs are indicated (X is any amino acid). Source: (Hanks, 2003)

The structure of protein kinases can be further divided into twelve subdomains separated by amino acid inserts of variable lengths (Figure 5B). Subdomain I contains the phosphate-anchor ribbon, which is a Glycine rich loop defined by the GxGxxG motif (Hanks and Hunter, 1995). Subdomain II contains a critical lysine residue that forms a salt bridge with a glutamate in subdomain III. This bond is essential for stabilising the interaction of the kinase with the α and β-phosphates of ATP (Hanks and Hunter, 1995). Mutation of the lysine to a methionine disrupts this bond and prevents phosphotransfer by the kinase. The catalytic loop is found in subdomain VIB and is defined by the invariant DxxxxN motif, with the aspartic acid (D) acting as the catalytic base by accepting a proton from the attacking substrate hydroxyl group during phosphotransfer. The DFG motif in subdomain VII assists in orientating ATP correctly. Both the APE and DxxxxG, of subdomains VIII and IX respectively, are involved in stabilising the C-terminus of the kinase. The activation lip is also found in subdomain VIII, that is, the residues that require phosphorylation to activate the kinase with the conformational changes that this induces linked to substrate recognition.

1.2.2.1 MAP kinases

Mitogen-activated Protein (MAP) kinases are a family of enzymes involved in cell signal transduction. They are part of the CMGC group of kinases and are ubiquitous to all eukaryotes, with the sole exception of *Encephalitozoon cuniculi* (Miranda-Saavedra *et al.*, 2007) and are involved in regulating processes such as differentiation, stress responses and proliferation. MAP kinases have a central role in the transduction of extracellular signals (also called ‘mitogens’). In higher eukaryotes the signal is transmitted via a cell membrane receptor that activates a MAP kinase kinase kinase (MAP3K), which in turn activates a MAP kinase kinase (MAP2K), which then activates a MAP kinase (MAPK) – in all cases by phosphorylation of the next kinase in the cascade. In higher eukaryotes the signal terminates often with the activation of a transcription factor or phosphorylation of another protein by the MAP kinase might occur.

MAP3Ks are activated by phosphorylation by an Ste20-like kinase or interaction with a G-protein scaffold (Avruch, 2007; Pearson *et al.*, 2001). The MAP3K then

phosphorylates a MAP2K on two serine and/or threonine residues, thus activating it. The MAP2Ks frequently have an N-terminal D-domain that binds to the common docking or CD-domain of the MAP kinase that it is activating (Avruch, 2007). The D-domain contains the consensus sequence (R/K)-X-(R/K)-$X_{2–4}$-(L/I)X(L/I) (Pearson *et al.*, 2001). The CD-domain consensus sequence is much simpler, DXXDE (Pearson *et al.*, 2001). MAPKs are activated by dual-phosphorylation of the TxY motif on both the threonine and tyrosine. MAPKs are serine/threonine kinases and their substrates include MAPKAPKs (MAPK-activated protein kinases), transcription factors or cytosolic proteins, such as heat shock proteins. MAPK inactivation is by dephosphorylation on one or both residues of the activation lip by a MAP kinase phosphatase (MKP), which is often a dual-specificity phosphatase (DUSP) (Jeffrey *et al.*, 2007).

1.3 Signal transduction in Trypanosomatids

In recent years the potential of developing signal transduction inhibitors as a means of treating leishmaniasis has attracted attention. However, this is hindered by the incomplete knowledge of what pathways are present and in what sequence the molecules within them interact (Parsons and Ruben, 2000; Naula *et al.*, 2005). It could be argued that it is not necessary for our knowledge of these pathways to ever reach completion: developing knock-out strains of known signal transducers that retain viability but do not lead to clinical symptoms could be used as live-organism vaccines (Wiese and Görcke, 2001). On the other hand, having a complete overview of the signalling sequences would enable the development of more refined treatments that target signalling molecules involved in different cascades and cellular processes.

1.3.1 Differences between higher eukaryotes and Trypanosomatids

Leishmania undergo significant morphological changes in response to changes in their environment as they move between hosts, this alone infers the presence of regulated signalling pathways that enable the parasites to adapt. Although complete signalling pathways have been determined for many processes in higher eukaryotes, particularly those of mammalian cells, their applicability to *Leishmania* is limited for several reasons. The first is that only some of the signalling pathways and the

molecules involved are found in *Leishmania spp.* (Figure 6) and for these an exact function has yet to be determined (Parsons and Ruben, 2000).

The differences and similarities between Trypanosomatid signalling and higher eukaryotes will be discussed in the same order as section 1.2.1.

Homologues of ligand-gated ion channels do not appear to be encoded in the *Leishmania* genome, however, control of the intracellular Ca^{2+} concentration does occur (Zilberstein, 1993), which suggests that it may be the inositol triphosphate (IP_3) pathway that regulates Ca^{2+} concentration. The precursor phosphatidylinositol (PtdIns) and enzymes phosphatidylinositol 3-kinase (PI3K) and phosphoinositide phospholipase C (PIPLC) are found in *Leishmania* along with the expected product, inositol triphosphate (InsP) (Parsons and Ruben, 2000).

InsP is one of the secondary effectors of GPCR stimulation in higher eukaryotes along with cAMP signalling. However, Trypanosomatids lack GPCRs, which is peculiar as adenylate cyclases are present in Trypanosomatids and adenylate cyclase signalling requires dimerisation with a G-protein in higher eukaryotes. It has been shown that adenylate cyclases are capable of transducing a signal following homodimerisation (Naula *et al.*, 2001). Indeed, adenylate cyclases are the only transmembrane receptor protein predicted in Trypanosomatids (Parsons and Ruben, 2000). No receptor tyrosine kinases exist in Trypanosomatids (Parsons *et al.*, 2005), which is notable as the most common transmembrane receptors that initiate signalling pathways in higher eukaryotes are receptor tyrosine kinases (Manning *et al.*, 2002).

A more fundamental, problem with investigating signal transduction in *Leishmania* is that many signalling pathways in higher eukaryotes culminate in the activation of a transcription factor and a change in the transcription of particular genes, yet no RNA Polymerase II transcription factors have been found in *Leishmania* to date. This does

not imply that there is no control exerted over protein production in *Leishmania* cells. Instead it appears likely that post-transcriptional regulation occurs at the mRNA stage (Parsons and Ruben, 2000; Wiese *et al.*, 2003), with eukaryotic Initiation Factors (eIFs) determining what mRNA sequences are translated into proteins (Barhoumi *et al.*, 2006; Singh *et al.*, 2008) and that *Leishmania* kinases might exert regulation at this level.

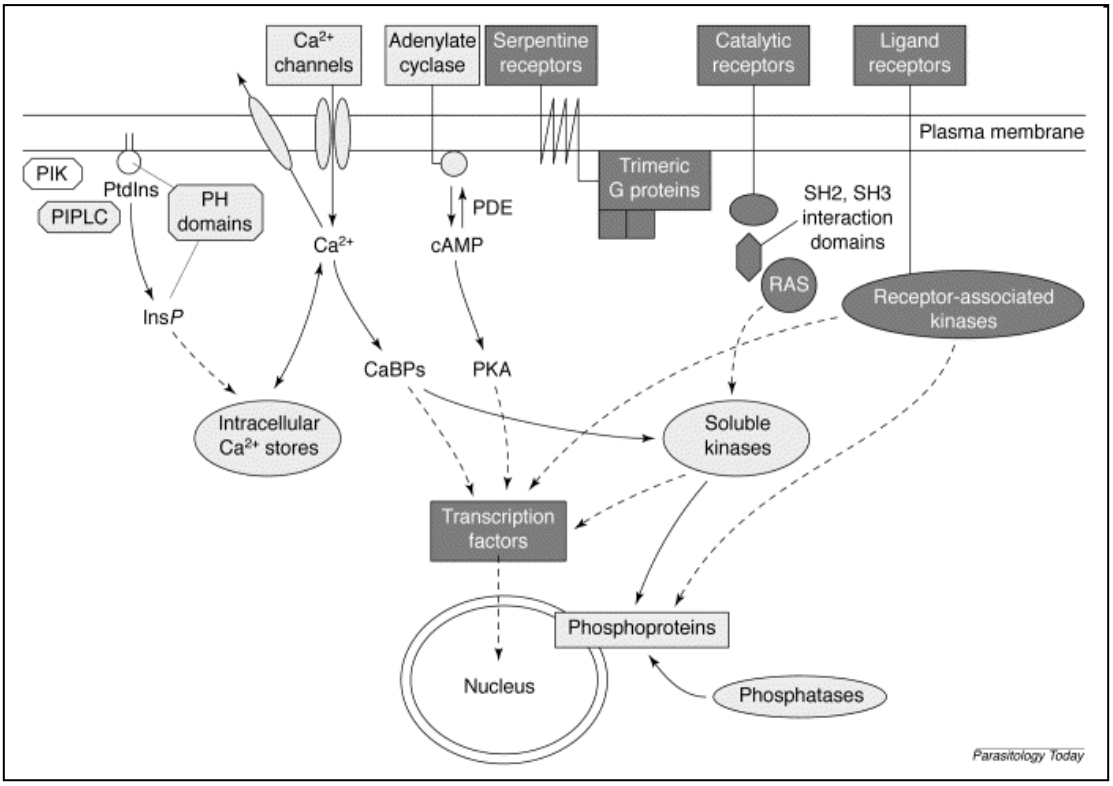

Figure 6: Differences between major signalling pathways in Trypanosomatids and higher eukaryotes. PDE, cAMP phosphodiesterase; PIK, phosphatidylinositol kinases; PIPLC, phosphoinositide phospholipase C; PKA, cAMP-dependent protein kinase; PtdIns, phosphatidylinositol; SH2, SRC homology region 2. Components shown in light grey are present in both; those shown in a darker grey are only present in higher eukaryotes. Source: (Parsons and Ruben, 2000).

Another difficulty with examining signal transduction pathways in trypanosomatids is that little is known about the nature of the external stimuli (Parsons and Ruben, 2000), thus it is difficult to determine what receptors are involved in communicating the stimulus to the inside of the cell.

The number of phosphatases predicted by the *Leishmania major* genome is 88 (Brenchley *et* al., 2007), which is approximately 63% of the number in humans. This is similar to the number predicted for *T. cruzi* and *T. brucei* (86 and 78, respectively) but double the number in *Saccharomyces cerevisiae* (38). The proportion of serine/threonine phosphatases is almost three times as great in the *L. major* phosphatome compared to in humans, whereas PTPs account for 30% of the human complement, in *L. major* it is only 3% (Brenchley *et al.*, 2007). This can be partially attributed to the greatly reduced proportion of tyrosine-kinases and TKLs in *Leishmania* (Parsons *et al.*, 2005).

1.3.2 *Leishmania* MAP kinases

Leishmania MAP kinases have the same general structure as other eukaryotic MAP kinases; a large kinase domain which is further divided into twelve kinase subdomains. The activation site TXY-motif is present on the activation loop (Wiese, 2003). Phosphorylation in this motif likely leads to a conformational change in the kinase structure, so that it is then able to transfer a phosphate group from a molecule of Adenosine Tri-Phosphate (ATP) to the substrate. In higher eukaryotes the signal terminates with the activation of a transcription factor or phosphorylation of another protein by the MAP kinase. The substrates of the *Leishmania* MAP kinases, however, are currently unknown.

Fifteen MAP Kinases have been identified in *Leishmania mexicana* since their presence was first described in 1998 (Wiese, 1998). Eight MAP Kinase Kinases (MKK) have been identified by bioinformatics (Parsons *et al.*, 2005). Two of these have been shown to be the activators of MAP kinases: LmxMKK activates LmxMPK3 (Erdmann *et al.*, 2006) and LmxMKK5 activates LmxMPK4 (John von Freyend *et al.*, 2010a). Additionally, there is evidence for the existence of MAP kinase kinase

kinases; this has been inferred from the need to artificially activate MKKs (Wiese *et al.*, 2003) and from bioinformatic analysis of the genome (Parsons *et al.*, 2005), which has suggested the existence of 23 MKKKs. This suggests the conservation of the MAP kinase core module of sequential activation by phosphorylation.

Of the 15 *Leishmania* MAPKs three have been validated as suitable drug targets, as amastigotes are unable to proliferate in the absence of the protein (LmxMPK1, LmxMPK2 and LmxMPK4 (Wiese, 1998; Wiese, 2007; John von Freyend *et al*., 2010a), whilst five have been confirmed as being of no value as a drug target due to the ability of parasites lacking the protein to remain infective (3, 9, 11, 12 and 13 (Erdmann *et al.*, 2006; Bengs *et al.*, 2005; Wiese, 2007). LmxMPK5 deletion mutants retained the ability to infect mice, however, without the production of a lesion (Wiese, 2007). Current data suggests that LmxMPK6 may be essential for the promastigote (and potentially amastigote) stage of the parasite as it was not possible to generate a deletion mutant (John von Freyend, 2010b). LmxMPK7 and 8 have not been categorised, however the lack of homologue in *T. brucei* or *T. cruzi* suggests that they may be essential for the intracellular stage of the life cycle. The roles of LmxMPK10, 14 and 15 have not been studied.

Although the external stimuli that initiate pathways that involve Mitogen-Activated Protein kinases (MAP kinases) are uncharacterised (Wiese, 2007), it is known that changes in temperature, pH and nutrient concentrations can initiate differentiation between the different life stages and this is likely to be mediated by MAP kinases (Parsons and Ruben, 2000; Naula *et al.*, 2005; Wiese, 2007), thus making them a worthwhile area of research as greater understanding may contribute to better drugs for the treatment of leishmaniasis.

At present the substrate(s) of the various *Leishmania* MAPKs are unknown. An aquaglyceroporin (LmjAQP1) is postulated to be the substrate of LmjMPK2 as it has been shown to have altered phosphorylation and activity in LmjMPK2 null mutant cells (Mandal *et al.*, 2012), although it has not been shown definitively that LmjMPK2

directly phosphorylates LmjAQP1, rather than an intermediary kinase. Analysis of antimony-resistant strains of *L. donovani* revealed down-regulation of LdMPK1 expression (Ashutosh *et al*., 2012). This suggests that both LmxMPK1 and LmxMPK2 (the *L. mexicana* homologue of LmjMPK2) may have similar substrates, an outcome that would not be entirely unexpected as together they comprise a subfamily of *Leishmania* MAPKs (Figure 7).

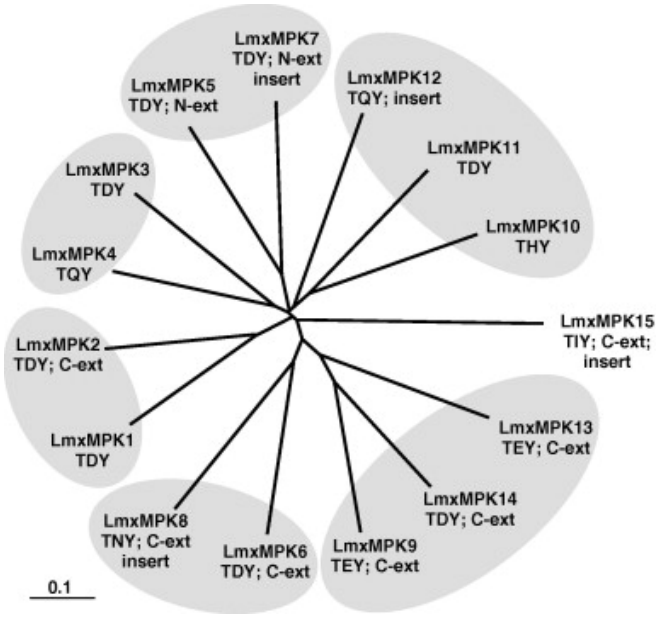

Figure 7: Phylogenetic tree of the *Leishmania mexicana* MAP kinases. The residues of the TXY motif are indicated. N-ext, N-terminal extension longer than 40 amino acids; C-ext, C-terminal extension longer than 100 amino acids; insert, denotes the presence of insert(s). (From: Wiese, 2007)

1.4 State of knowledge and research objectives

The *Leishmania mexicana* Mitogen-activated Protein Kinase 1 (LmxMPK1) was first described in 1998 (Wiese, 1998) (Genbank accession number Z95887). The gene encoding it was found in the 11.5 kb intergenic region between two stretches of DNA coding for two Secreted Acid Phosphatases and is 1,074 bp long. The protein it encodes, LmxMPK1, is composed of 358 amino acids and has a molecular mass of 41 kDa, making it the smallest of the known MAP kinases in *L. mexicana* (Wiese, 2003). It is an essential MAPK as deletion of the gene results in parasites that are unable to establish a footpad infection in Balb/c mice (Wiese, 1998).

The protein displays a high degree of amino acid identity to homologues in other *Leishmania* species: *L. amazonensis* 98%, *L. tropica*, *L. major*, *L. aethiopica*, *L. donovani* and *L. infantum* 97%. Among *Trypanosoma* species there is less of an identity match: *T. brucei* and T. *cruzi* have homologues that are 56% identical. The closest human homologue is MPK15 (ERK7/8), which has a 48% match.

Previous work in the Wiese group had suggested that extended incubation of His-LmxMPK1 with ATP decreased phosphotransferase activity when subsequently incubated with myelin basic protein (MBP). It had also found that autophosphorylation was occurring on tyrosine, with the tyrosine of the TDY motif thought to be the most likely residue for this to be occurring on. Due to the decrease in activity after extended autophosphorylation it was hypothesised that autophosphorylation on tyrosine-178 reduced the activity of the kinase. To test this, TDY mutants were generated and *in vitro* kinase assays were performed, as were mouse footpad infections with *LmxMPK1* -/- parasites expressing the mutant kinases (replacement of a residue with an alanine or phenylalanine was to mimic a non-phosphorylatable residue, while glutamate was to mimic a phosphoresidue). These experiments showed (Figure 8) that autophosphorylation of LmxMPK1 is intramolecular (Figure 8C), that the ADY and EDY were active in kinase assays (Figure 8A, B) and that only the EDY and TDF mutants were infective in footpad infections (Figure 8D). This suggested that the activation mechanism for LmxMPK1 might be different from that of MAPKs in higher eukaryotes, as even in the absence

of a phosphorylatable residue at the 178th residue (TDF) the kinase was capable of rescuing the null mutant in footpad infections (Figure 8D). Furthermore, the inactivity of the TDF mutant during kinase assays, whilst the EDY mutant, which was also infective, was active suggests that phosphothreonine-176 (actual or mimicking residue) is essential for kinase activity. This was also suggested by the inactivity and non-infectiveness of the ADF mutant.

Therefore, the following mechanism of activation and regulation of kinase activity was proposed: phosphorylation of tyrosine-178 inactivates LmxMPK1 (TDE is inactive in assays and not infective); monophosphorylation of threonine-176 activates LmxMPK1 and must be by a separate activating kinase (only EDY is active and infective; TDF is infective only suggesting an upstream kinase that phosphorylates threonine) and dual phosphorylation of both Thr176 and Tyr178 leads to an inactive kinase (TDE is neither active nor infective).

Hypothesis to be tested in this study: dephosphorylated LmxMPK1 will be capable of autophosphorylation on tyrosine, however, once autophosphorylation reaches a peak substrate phosphorylation activity will then decline. Localisation of the TDY kinase mutants in *L. mexicana* cells will be different for mutants that are enzymatically active and/or are capable of causing an infection in mice (WT, EDY, TDF) compared to inactive and non-infective mutants (KM, ADF, ADY, TDE).

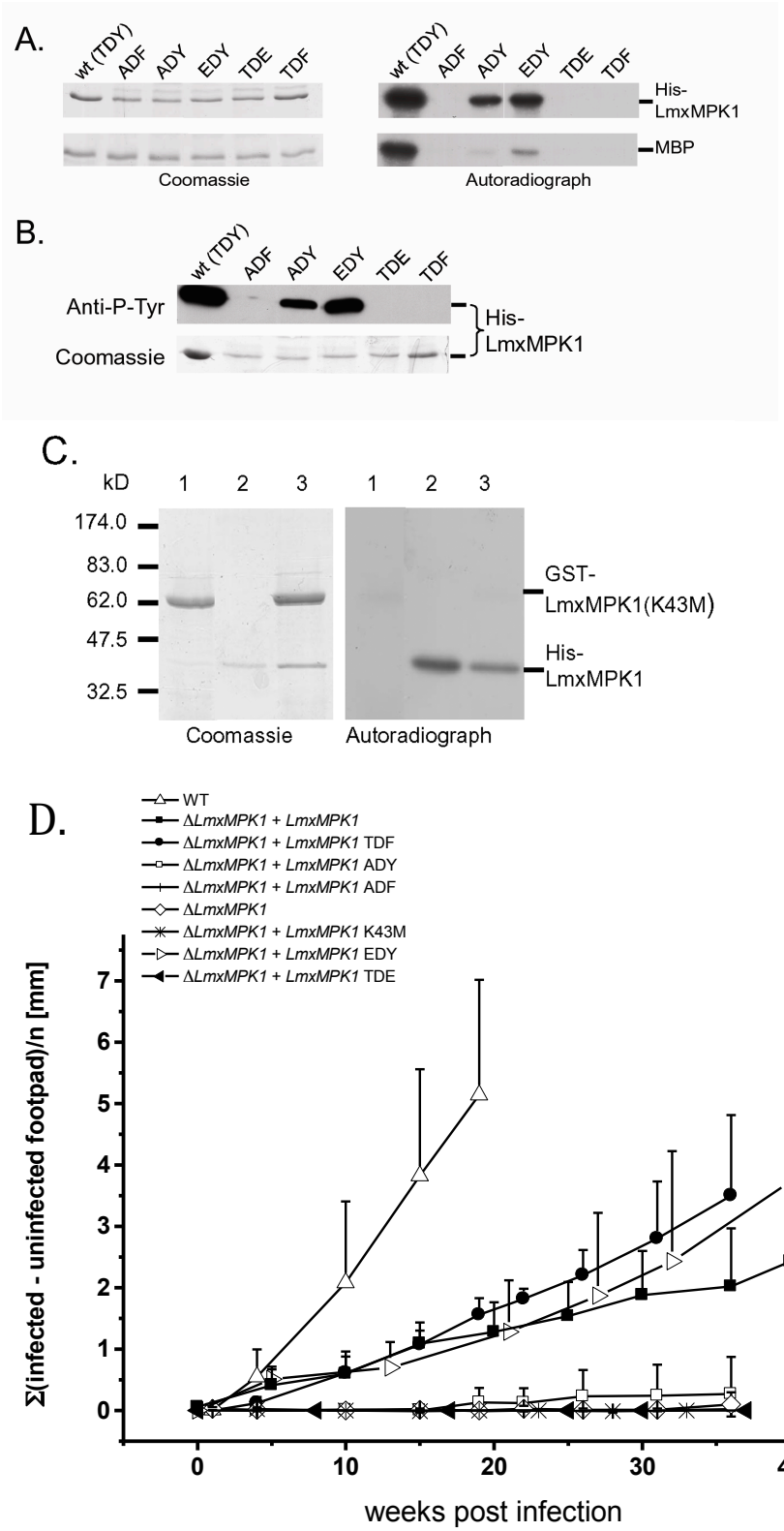

Figure 8: *In vitro* and *in vivo* results of kinase assays and footpad infections with LmxMPK1 TDY mutants.

A, Kinase assays with recombinant His-LmxMPK1 mutants to assess auto- and substrate phosphorylation capabilities. Kinase was incubated with radiolabelled ATP and MBP for 1 h at 34°C. B, Tyrosine phosphorylation of TDY mutants following a 1 h kinase assay with unlabelled ATP.

C, Assessment of mechanism of autophosphorylation to determine if it is intra- or intermolecular.

D, Footpad swelling of Balb/c mice infected with WT *L. mexicana*, ΔLmxMPK1 parasites and ΔLmxMPK1 parasites expressing various TDY mutants to assess the ability of the mutants to restore infectivity to null mutant parasites.

The aims of this project were:

a) Optimise an inhibitor-sensitised system for LmxMPK1 to allow selective *in vivo* inhibition of the kinase.
b) Generate dephosphorylated recombinant kinase for use in kinase assays.
c) Generate green fluorescent protein (GFP)-tagged versions of wild type LmxMPK1, a kinase dead mutant (K43M) and various activation lip motif mutants and express them in a null mutant background. The GFP-tag will allow purification of the protein in its natural *in vivo* state and localisation of the kinase, which should allow the relationship between TDY phosphorylation, activity and *in vivo* localisation to be examined. Figure 8D shows that the different TDY mutants exert different effects on null mutant parasites.
d) Assess the *in vivo* localisation of a novel *Leishmania mexicana* phosphatase, LmxPTP and attempt deletion of its gene to assess whether it is essential for parasite viability.

The results generated fulfilling aims (b) and (c) should also allow a conclusion to be made about the mechanism of activation and regulation of the activity of LmxMPK1.

2 Materials

2.1 Laboratory equipment

Centrifuges

Centriguge 5424	Eppendorf, Hamburg, Germany
Centrifuge 5415R	Eppendorf, Hamburg, Germany
HERMLE Z 400 K	Hermle Labortechnik, Wehingen, Germany

CO2 incubator

BBK 6220	Kendro Laboratory Products, Hanau, Germany

Electrophoresis equipment

Minigel (Twin) Tank	Biometra, Göttingen, Germany
Power supply: Consort E734	Consort, Turnhout, Belgium
Power supply: Gene Power Supply GPS 200/400	Amersham Biosciences, Freiburg, Germany

Immunoblotting equipment

Fastblot B33 / B34	Biometra, Göttingen, Germany

Heat block

Thermomixer comfort	Eppendorf, Cambridge, UK

Microscopes

Axiovert 25	Carl Zeiss, Jena, Germany
Axiostar plus	Carl Zeiss, Jena, Germany
Nikon TE2000S	Nikon Instruments, Derby, UK

(inverted epifluorescent)

CFI Plan Fluor DLL-100X objective lens

Camera: Hamamatsu Orca-285

pH Meter

Digital-pH-Meter CG 820	Schott, Hofheim am Taunus, Germany

Photometer

BioPhotometer 6131	Eppendorf, Hamburg, Germany
Pharmacia LKB Ultrospec III	Pharmacia, Milton Keynes, UK

Shaking incubators

Innova 4230/4400	New Brunswick Scientific, Edison, NJ, USA

Shaking water baths

GFL 1083	GFL, Burgwedel, Germany
mgw LAUDA M3	Heidolph Electro, Kehlheim, Germany

Sonicator

Branson Sonifier 250	Branson, Danbury, CT, USA

Thermocyclers

Gene Amp PCR System 9700	PE Applied Biosystems, Weiterstadt, Germany
Gene Amp PCR System 2400	PE Applied Biosystems, Weiterstadt, Germany

Tissue Culture Hood

Thermo SAFE 2020, Class II Safety Cabinet	Fischer Scientific, Loughborough, UK

Transfector

Nucleofector II	Amaxa Biosystems, Gaithersburg, MD, USA

Vortex

IKA-VIBRO-FIX VF2	IKA Labortechnik, Staufen, Germany

UV transilluminators

VWR Genosmart	VWR International, Lutterworth, UK
High Performance UV Transilluminator	UVP, Cambridge, UK

2.2 Glassware and consumables

Biodyne A nylon membrane	Pall, Dreieich, Germany
Complete EDTA-free protease inhibitor tablets	Roche Diagnostics, Burgess Hill, UK
Gel drying frames	Sigma-Aldrich, Gillingham, UK
Immobilon-P PVDF membrane	Millipore, Schwalbach, Germany
Neubauer counting chambers	VWR International, Darmstadt, Germany
OctoMACS™ Separator, MACS stand, M Columns	Miltenyi Biotec, Surrey, UK
Parafilm M	Brand GmbH, Wertheim, Germany
Plastic consumables	Eppendorf, Cambridge, UK Sarstedt, Leicester, UK Greiner Bio-One, Solingen, Germany Nunc, Langenselbold, Germany VWR International, Lutterworth, UK
X-ray films	Fotochemische Werke, Berlin, Germany

2.3 Chemicals

[γ-^{32}P]-ATP	Hartmann Analytics GmbH, Braunschweig, Germany
Acetic acid	Carl Roth, Karlsruhe, Germany
Acrylamide 30% (w/v) /Bis-acrylamide 0.8% (w/v)	VWR, Lutterworth, UK
Adenosine triphosphate (ATP)	Roche Diagnostics, Sussex, UK
Agar-Agar	Techmate Ltd, Milton Keyes, UK
Agarose (electrophoresis grade)	Techmate Ltd, Milton Keyes, UK
Ammonium chloride	Sigma-Aldrich, Steinheim, Germany
Ammonium persulfate (APS)	VWR, Lutterworth, UK
Ampicillin	Sigma-Aldrich, Steinheim, Germany
Bacto Tryptone	Becton Dickinson, Heidelberg, Germany
Boric acid	Techmate Ltd, Milton Keyes, UK
Bovine serum albumin (BSA)	Sigma-Aldrich, Steinheim, Germany
Bromophenol blue	Sigma-Aldrich, Steinheim, Germany
Calcium chloride	Techmate Ltd, Milton Keyes, UK
Chelating sepharose fast flow	GE Healthcare, Little Chalfont, UK
Chloroform	Techmate Ltd, Milton Keyes, UK
Cobalt chloride	Carl Roth, Karlsruhe, Germany
Coomassie Brilliant Blue G250	Techmate Ltd, Milton Keyes, UK
Coomassie Brilliant Blue R250	Techmate Ltd, Milton Keyes, UK
DABCO	Sigma-Aldrich, Steinheim, Germany
DAPI	Sigma-Aldrich, Steinheim, Germany

Disodium hydrogen phosphate dihydrate	Techmate Ltd, Milton Keyes, UK
DMSO	Techmate Ltd, Milton Keyes, UK
dNTP mix	Roche Diagnostics, Mannheim, Germany
DTT	Biomol, Hamburg, Germany
EDTA disodium dihydrate	Techmate Ltd, Milton Keyes, UK
EGTA	Techmate Ltd, Milton Keyes, UK
Ethanol	Techmate Ltd, Milton Keyes, UK
Ethidium bromide	Sigma-Aldrich, Steinheim, Germany
FCS	PAN Biotech, Aidenbach, Germany
Formaldehyde 37% (Formaline)	Carl Roth, Karlsruhe, Germany
Formamide	Techmate Ltd, Milton Keyes, UK
Glucose	Techmate Ltd, Milton Keyes, UK
Glutaraldehyde	Merck, Darmstadt, Germany
Glutathione, reduced	Sigma-Aldrich, Steinheim, Germany
Glutathione Sepharose 4B	GE Healthcare, UK
Glycerol	Techmate Ltd, Milton Keyes, UK
Glycine	Techmate Ltd, Milton Keyes, UK
Hemin	Sigma-Aldrich, Steinheim, Germany
HEPES	Techmate Ltd, Milton Keyes, UK
Hydrochloric acid	Techmate Ltd, Milton Keyes, UK
Hygromycin B	Merck Biosciences, Schwalbach, Germany
Imidazole	Techmate Ltd, Milton Keyes, UK
IPTG	Gerbu Biochemicals, Gaiberg, Germany

Isoamyl alcohol	Techmate Ltd, Milton Keyes, UK
Isopropanol	Techmate Ltd, Milton Keyes, UK
Kanamycin sulfate	VWR, Lutterworth, UK
Leupeptin	Sigma-Aldrich, Steinheim, Germany
L-Glutamine	PAN Biotech, Aidenbach, Germany
Lithium chloride	Sigma-Aldrich, Steinheim, Germany
Magnesium chloride hexahydrate	Techmate Ltd, Milton Keyes, UK
Magnesium sulfate	Merck, Darmstadt, Germany
Maleic acid	Techmate Ltd, Milton Keyes, UK
Manganese chloride	Merck, Darmstadt, Germany
MBP dephosphorylated	Millipore,
MES	Fischer Scientific, Loughborough, UK
Methanol	Carl Roth, Karlsruhe, Germany
Milk powder	Carl Roth, Karlsruhe, Germany
MOPS	Sigma-Aldrich, Gillingham, UK
Mowiol 4-88	Merck, Darmstadt, Germany
Neomycin (G418)	Roche Diagnostics, Mannheim, Germany
N-Lauroyl sarcosine sodium salt	VWR, Lutterworth, UK
Okadaic acid	Merck, Darmstadt, Germany
ortho-Phenanthroline	Sigma-Aldrich, Steinheim, Germany
ortho-Phosphoric acid	Carl Roth, Karlsruhe, Germany
Paraformaldehyde	VWR, Lutterworth, UK
Penstrep (1000 U/ml Penicillin,	Life Technologies, Carlsbad, USA

10 mg/ml Streptomycin)	
Phenol, equilibrated in TE buffer (pH 7.5-8.0)	Techmate Ltd, Milton Keyes, UK
Phleomycin (Bleomycin)	Merck Biosciences, Schwalbach, Germany
PMSF	Sigma-Aldrich, Steinheim, Germany
Poly-L-Lysine hydrobromide	Sigma-Aldrich, Steinheim, Germany
Potassium acetate	Techmate Ltd, Milton Keyes, UK
Potassium chloride	Sigma-Aldrich, Gillingham, UK
Potassium dihydrogen phosphate	Merck, Darmstadt, Germany
Puromycin dihydrochloride	Techmate Ltd, Milton Keyes, UK
Rubidium chloride	Sigma-Aldrich, Gillingham, UK
Saponin	Carl Roth, Karlsruhe, Germany
SDM medium	Generon, Maidenhead, UK
Silver nitrate	Techmate Ltd, Milton Keyes, UK
Sodium acetate trihydrate	Techmate Ltd, Milton Keyes, UK
Sodium carbonate	Techmate Ltd, Milton Keyes, UK
Sodium chloride	Sigma-Aldrich, Gillingham, UK
Sodium dihydrogen phosphate	Merck, Darmstadt, Germany
Sodium dodecyl sulfate (SDS)	Fischer Scientific, Loughborough, UK
Sodium fluoride	Merck, Darmstadt, Germany
Sodium hydroxide	Techmate Ltd, Milton Keyes, UK
Sodium orthovanadate	Sigma-Aldrich, Steinheim, Germany
Sodium thiosulfate pentahydrate	Techmate Ltd, Milton Keyes, UK

TEMED	Sigma-Aldrich, Steinheim, Germany
Tetracycline	Sigma-Aldrich, Steinheim, Germany
Trisodium citrate	Techmate Ltd, Milton Keyes, UK
TLCK	Sigma-Aldrich, Steinheim, Germany
Triton X-100	Techmate Ltd, Milton Keyes, UK
Trizma	Sigma-Aldrich, Gillingham, UK
Tween 20	Techmate Ltd, Milton Keyes, UK
X-Gal	Roche Diagnostics, Mannheim, Germany
Xylenecyanol	Sigma-Aldrich, Steinheim, Germany
Yeast extract	Fluka, Gillingham, UK
β-mercaptoethanol	Techmate Ltd, Milton Keyes, UK
1-Na-PP1	Tocris Bioscience, Bristol, UK
1-Nm-PP1	K Shah, Purdue University, USA
2-Nm-PP1	K Shah, Purdue University, USA

2.4 Media and Buffers

Ammonium Persulphate (10%)	10% (w/v) Ammonium Persulphate dissolved in ddH_2O
Agarose gel loading buffer (10X)	0.1 M EDTA pH 8.0 0.1% (w/v) bromophenol blue 0.1% (w/v) xylenecyanol 0.5 x TBE 50 % (v/v) glycerol
Bradford reagent	5% (v/v) ethanol 0.01% (w/v) Coomassie Brilliant Blue G250 10% (v/v) phosphoric acid filtered and stored at 4°C in the dark
Coomassie Staining Solution	0.1% (w/v) Coomassie Brilliant Blue R250 50% (v/v) methanol 40% (v/v) ddH_2O 10% (v/v) acetic acid
Coomassie Destaining Solution	30% (v/v) methanol 60% (v/v) ddH_2O 10% (v/v) acetic acid
Drying solution for SDS-PAGE gels	20% (v/v) ethanol 10% (v/v) glycerol
Fixing solution for counting *Leishmania*	10% (v/v) formaldehyde in 1 x PBS
Freezing Solution for *Leishmania* stabilates	10% (v/v) Sterile DMSO 90% (v/v) iFCS
GFP-purification Lysis Buffer	1 % (v/v) Benzonase 150 mM NaCl 1 % (v/v) Triton X-100 50 mM Tris-HCl, pH 8.0 0.25 % (v/v) CHAPS 10mM Ortho-phenanthroline 1 × Complete Protease Inhibitor Cocktail (EDTA free)
Hemin stock solution	2.5 mg/ml in 50 mM NaOH
His-tag purification Elution Buffer	50 mM Tris-HCl pH 8.0 300 mM NaCl 500 mM Imidazol 10% Glycerol 1mM PMSF

His-tag purification Wash Buffer	50 mM Tris-HCl pH 8.0 1 M NaCl 10 mM Imidazol 10% Glycerol
His-tag purification Binding Buffer	50 mM Tris-HCl pH 8.0 1 M NaCl 20 mM Imidazol 10% Glycerol
iFCS	FCS heated to 56°C for 45 min then filter sterilised
Immunoblot Blocking Solution I	3 % (w/v) BSA in TBST
Immunoblot Blocking Solution II	5 % (w/v) Milk Powder in PBST 20 mM Tris-HCl pH 7.5
Immunoblot stripping solution	62.5 mM Tris-HCl pH 6.7 2 % (w/v) SDS 0.78 % (v/v) β-mercaptoethanol
Immunoblot transfer buffer	25 mM Trizma 150 mM glycine 10% (v/v) methanol
Kinase reaction buffer for LmxMPK1 (10 x)	500 mM MOPS pH 7.5 50 mM $MnCl_2$ 1 M NaCl
LB Agar	1.5 % (w/v) agar-agar in LB Medium. Sterilised by autoclaving then allowed to cool to ~50°C, antibiotics were added (if required) and poured into plates.
LB Medium	1% (w/v) bacto tryptone 0.5% (w/v) yeast extract 1 % (w/v) NaCl Sterilised by autoclaving, allowed to cool to ~50°C then antibiotics were added (if required)
Lysis Buffer for *Leishmania* promastigotes	1 × PBS 0.1% (w/v) SDS 50 µM Leupeptin 25 µM TLCK 1 mM PMSF 10 mM o-Phenanthroline 50 µM DTT 1 × Sample Buffer (without DTT)
Phosphate Buffered Saline (PBS) (10x)	1.37 M NaCl 27 mM KCl 101 mM Na_2HPO_4 18 mM KH_2PO_4

PBST	0.2% (v/v) Tween-20 in 1 × PBS
Resolving Gel Buffer for SDS-PAGE (4x)	1.5 M Tris-HCl pH 8.8 0.4% (w/v) SDS
RF1	100 mM RbCl 50 mM $MnCl_2.4H_2O$ 30 mM $K^+CH_3COO^-$ (Potassium Acetate) 10mM $CaCl_2.2H_2O$ 15% Glycerol pH adjusted to 5.8 using 10% acetic Acid. Filter sterilised
RF2	10 mM MOPS 10 mM RbCl 75 mM $CaCl_2.2H_2O$ 15% Glycerol pH adjusted to 6.8 using 0.5M NaOH Filter sterilised
SDM Medium for Promastigote Culture	10% (v/v) iFCS 1% (v/v) penstrep 7.5 µg/ml hemin in 500 ml SDM Medium
SDS-PAGE Running Buffer (10x)	0.25 M Tris-HCl pH 8.3 1.92 M Glycine 1% (w/v) SDS
SDS-PAGE Sample Buffer (5x)	62.5 mM Tris-HCl pH6.8 20% (v/v) glycerol 2% (w/v) SDS 0.001% (w/v) bromophenol blue 200 mM DTT
20× SSC	3 M NaCl 0.3 M Sodium Citrate pH adjusted to 7.0
Stacking Gel Buffer for SDS-PAGE (4x)	0.5 M Tris-HCl pH 6.8 0.4% (w/v) SDS
TELT Buffer	50 mM Tris-HCl pH 8.0 62.5 mM EDTA pH 8.0 2.5 M LiCl 4% (v/v) Triton X-100
TBE (5x)	0.45 M Trizma 0.45 M Boric acid 10 mM EDTA pH 8.0

Tris-Buffered Saline (TBS) (10x)	200 mM Tris-HCl pH 7.5 1.37 M NaCl
TBST	0.2% (v/v) Tween-20 in 1 × TBS
TENS solution	10 mM Tris-HCl pH 8.0 1 mM EDTA 100 mM NaOH 0.5% (w/v) SDS

2.5 Bacterial strains

Description	Genotype	Source
BL21(DE3) [pAP*lac*IQ]	B F^- *dcm ompT hsdS*(r_B^- m_B^-) *gal* λ(DE3) [pAP*lac*IQ]	Joachim Clos, Hamburg, Germany
OneShot TOP10F'	F´{*lac*I^q Tn*10* (Tet^R)} *mcr*A Δ(*mrr-hsd*RMS-*mcr*BC) Φ80*lac*ZΔM15 Δ*lac*X74 *rec*A1 *ara*D139 Δ(*ara-leu*)7697 *gal*U *gal*K *rps*L *end*A1 *nup*G	Invitrogen Life Technologies, Paisley, Scotland
XL1-Blue	*ecA endA gyrA96 thi-1 hsdR17 supE44 rel A1 lac* [F' *proAB* $lac^qZ\Delta M15$ Tn*10* (Tet^R)]	Stratagene, La Jolla, CA, USA
BL21(DE3)	B F^- *dcm ompT hsdS*(r_B^- m_B^-) *gal* λ(DE3)	Stratagene, La Jolla, CA, USA

2.6 *Leishmania* strain

Leishmania mexicana mexicana MNYC/BZ/62/M379, clone 2

2.7 Oligonucleotides

Description	Sequence
F93A.for	5’ AC ATA GAT CTG TAC CTC GTC GCG GAG TTG ATA GAG ACC GAT 3’
MPK1BglII.rev	5’ GTG TAG ATC TTC TCG TCG ACG AGG GGC AGC ACG AGT 3’
LmexPTP.for	5’ ACT AGT GGC ATC AAG GAC ATG TAC CTG 3’
LmexPTP.rev	5’ GAT ATC CGC CGA CTT CTT CGA CCT CTC 3’
PTP1B.for	5’ ACT AGT GAG ATG GAA AAG GAG TTC GAG 3’
PTP1B.rev	5’ GTT AAC TCG CGA ATT GTG TGG CTC CAG GAT TCG 3’
Lambda Phos.for	5’ ACT AGT CGC TAT TAC GAA AAA ATT GAT 3’
Lambda Phos.rev	5’ GAT ATC TGC GCC TTC TCC CTG TAC CTG 3’

2.8 DNA vectors and plasmid constructs

Name	Source
pCR2.1-TOPO	Invitrogen Life Technologies, Paisley, Scotland
pGEX-KG-mpk1F93G	Melzer, PhD Thesis, 2007
pGEX-KG-mpk1F93GF144L	Melzer, PhD Thesis, 2007
p-ampR-PTP1B	D Barford, ICR, London, gift, 2009
p-ampR-λ-phosphatase	D Barford, ICR, London, gift, 2009
pJC-mpk1	M Wiese, unpublished
pMA-triple-HA	Mr Gene, Regensburg, Germany
pMK-mpk1HA	Mr Gene, Regensburg, Germany
pQE8W-mpk1	Melzer, PhD Thesis, 2007
pX63polPhleo	M Wiese, unpublished
pX5lmpk	M Wiese, unpublished
pX6lmpk K43➔M	M Wiese, unpublished
pX19lmpkADF	M Wiese, unpublished
pX13lmpkADY	M Wiese, unpublished
pX4mpk1 T to E	M Wiese, unpublished
pX1lmpk TDE	M Wiese, unpublished
pX5lmpkTDF	M Wiese, unpublished
pX5lmpkF93G	Melzer, PhD Thesis, 2007
pX5lmpkF93GF144L	Melzer, PhD Thesis, 2007
pTH6nGFPc	Dubessay *et al.*, 2006
pUC57-delLmxPTP	Proteogenix, Oberhausbergen, France
pUC57-MPK1TA-MKK-DQED	Proteogenix, Oberhausbergen, France
pUC57-MPK1TE-MKK-AQEA	Proteogenix, Oberhausbergen, France

2.9 Antibodies

Primary antibodies

Antigen / Name	Host	Dilution	Source
Phosphotyrosine / 4G10 (hybridoma cell supernatant)	mouse	1:2500	Bernhard Fleischer, BNI, Hamburg
anti-LmxMPK1	rabbit	1:500	Wiese, 1998
anti-IPS	rabbit	1:500	Ilg, 2002

Secondary antibodies

Antigen / Name	Host	Dilution	Source
Mouse IgG (HRP-conjugated)	rabbit	1:2000	DAKO, Hamburg, Germany
Rabbit IgG (HRP-conjugated)	goat	1:5000	Dianova, Hamburg, Germany

One-step antibody

Antigen / Name	Host	Dilution	Source
anti-GFP coupled directly to HRP	Mouse	1:1000	Miltenyi Biotec, Surrey, UK

2.10 Enzymes

Alkaline phosphatase, shrimp	Roche Diagnostics, Mannheim, Germany
Basemuncher	Expedeon, Cambridge, UK
Expand High Fidelity PCR System	Roche Diagnostics, Mannheim, Germany
Klenow enzyme	New England Biolabs, Hitchin, UK
Restriction endonucleases	New England Biolabs, Hitchin, UK
RNase A (bovine pancreas)	Roche Diagnostics, Mannheim, Germany
T4 DNA ligase	Roche Diagnostics, Mannheim, Germany
λ-phosphatase	New England Biolabs, Hitchin, UK

2.11 Molecular biology kits

Human T Cell Nucleofector Kit	Amaxa Biosystems, Gaithersburg, USA
M&N NucleoSpin Extract II Kit	Macherey & Nagel, Düren, Germany
M&N NucleoSpin Plasmid Kit	Macherey & Nagel, Düren, Germany
M&N NucleoBond Xtra Midi Kit	Macherey & Nagel, Düren, Germany
SuperSignal West Pico Chemiluminescent Substrate Kit	Pierce/Perbio Science, Bonn, Germany
TOPO TA Cloning Kit	Life Technologies, Carlsbad, USA formerly: Invitrogen Life Technologies
µMACS GFP Isolation Kit	Miltenyi Biotec, Surrey, UK

2.12 DNA and Protein Molecular Weight markers

1kb DNA Ladder	New England Biolabs, Hitchin, UK
PCR Marker	New England Biolabs, Hitchin, UK
Prestained Protein Marker, Broad Range	New England Biolabs, Hitchin, UK

3 Methods

3.1 Cell Biology

3.1.1 Culturing of *E. coli*

3.1.1.1 Culturing on agar plates

A maximum volume of 200 µl of a suspension of *E. coli* cells were evenly spread on LB agar plates using a Drigalski spatula that had been sterilised in 100 % Ethanol. If the colonies required selective pressure antibiotics were used at the following concentrations: Ampicillin (100 µg/ml), Kanamycin (50 µg/ml) and Tetracycline (20 µg/ml). After spreading the plates were incubated upside down overnight at 37°C.

3.1.1.2 Culturing in liquid medium

LB medium was inoculated with either a single colony of transformed *E. coli* picked from an LB agar plate using a sterile 200 µl pipette tip or an appropriate volume of a liquid culture was added to a final concentration of 1 % (v/v). The cultures were grown in a shaker incubator at 37°C and 220 rpm overnight or until the desired optical density was achieved. Antibiotics were added, if required, at the same concentrations as 3.1.1.1.

3.1.1.3 Preparation of glycerol stocks

500 µl of an overnight bacterial culture was mixed with 500 µl of sterile glycerol in a sterile cryo-tube (Nunc). The tube was vortexed to ensure adequate mixing, incubated for 30 min on ice then stored at -80°C.

3.1.2 Culturing of *Leishmania*

3.1.2.1 Culturing of *L. mexicana* promastigotes

Promastigotes were grown in complete SDM medium (Brun and Schönenberger, 1979) at 27°C. Antibiotics were added, if required, at the following concentrations: bleocin (phleomycin) (5 µg/ml), G418 (neomycin) (10 µg/ml), hygromycin B (20 µg/ml) and puromycin (40 µM). Cells were passaged every 3-4 days by inoculating a fresh culture 1:1000 using a sterile Pasteur pipette.

The standard culture method for *L. mexicana* was in 10 ml SDM medium (complete) in a 25 cm^2 non-vented tissue culture flask (Sarstedt). Flasks were incubated lying down. If necessary parasites were cultured in 6, 12, 24 and 96-well plates, in which

case the plate was wrapped in Parafilm (Pechiney) to prevent evaporation of the medium.

3.1.2.2 Preparation of *Leishmania* stabilates

Freezing solution (2.0 ml/culture) was prepared and chilled on ice. A 10 ml late log-phase promastigote culture (2-3 × 10^7 cells/ml) was centrifuged for 10 min at 5,200 × g, 4°C. The supernatant was removed and the cell pellet was resuspended in 2 ml of freezing solution, then distributed to four cryotubes (500 µl/tube). The cryotubes were placed in the gas phase of liquid nitrogen overnight and then in the liquid phase for long-term storage.

3.1.2.2.1 Defrosting and reculturing of *Leishmania* stabilates

Cryotubes with frozen cells were removed from liquid nitrogen and rapidly defrosted in a water bath at 37°C then the contents were immediately used to inoculate 10 ml of SDM medium including antibiotic(s), if required. After 24 hours the cells were sub-cultured to a fresh 10 ml of SDM medium (with antibiotic(s) if required), as the original culture would contain a high concentration of DMSO, which could lead to growth inhibition.

3.1.2.3 Growth curves of *L. mexicana* in the presence of inhibitors

Proliferation assays of *L. mexicana* promastigotes were carried out in 2 ml of SDM (complete) incubated in 24-well plates. Each well was seeded with 5 × 10^5 cells/ml and inhibitor was added (no more than 5 µl/well). For control wells 5 µl of DMSO was added instead. Samples were taken for counting at the same time each day for the next 5-7 days. A 1 ml pipette was used to mix the contents of each well after the inhibitor was added and before a sample was removed for counting to ensure homogeneity.

3.1.2.4 Counting *Leishmania* cells

A sample of *Leishmania* culture (10 – 50 µl) was removed and diluted in fixing solution at an appropriate ratio (1:5 -1: 50). Both sides of a Neubauer counting chamber (0.1 mm, 0.0025 mm^2) were loaded with 10 µl of the fixed cells and the cells in the square areas were counted by eye using a light microscope. The mean of the two sides was calculated and used to calculate the number of cells/ml by multiplying the mean value by the dilution factor and the chamber factor (10^4).

3.1.2.5 Microscopy of *Leishmania* cells

To ensure the adhesion of live *Leishmania* cells to a microscope slide, it was first treated with 20 µl poly-lysine. This was applied to a spot on the slide, left for 5 min then removed. The cells were immediately added and a cover slip was placed over them. For microscopy with an inverted light source the cover slip was attached to the slide using an adhesive.

3.2 Molecular Biology

3.2.1 Preparation of competent *E. coli*

A disposable streak-loop was used to plate cells from the glycerol stock of the required genotype onto an LB agar plate, containing the required antibiotic. For XL1-Blue this was tetracycline (20 µg/ml) and for BL21 (DE3) [pAPlaclQ] kanamycin (50 µg/ml) was used. BL21 (DE3) does not have any endogenous resistance so no antibiotics were included. The plate was incubated at 37°C overnight and a single colony was picked and used to inoculate a 2 ml LB culture containing antibiotics, if required (for XL1-Blue cells the tetracycline concentration was increased to 40 µg/ml). The 2 ml culture was incubated overnight at 37°C, 225 rpm in a shaking incubator (Innova 44). The next day 500 µl of the pre-culture was used to inoculate 100 ml of LB medium (again, 40 µg/ml tetracycline for XL1-Blue). This was incubated at 37°C, 225 rpm for 3-5 hours until the culture reached an OD_{600} of 0.2. The culture was cooled on ice for 15 min then centrifuged for 15 min at 4,000 × g, 4°C. The cell pellet was resuspended in 32 ml of RF1, vortexed and left on ice for 90 min. The suspension was then centrifuged for 15 min at 4,000 × g, 4°C. The supernatant was discarded and the pellet was resuspended in 8 ml of RF2, left on ice for 15 min then 200 µl aliquots were made, which were frozen in liquid Nitrogen and stored at -80°C.

3.2.2 Heat-shock transformation of *E. coli*

Competent cells were retrieved from the -80°C and gently defrosted on ice. (For BL21 (DE3) [pAPlaclQ] it was possible to split the vial of cells into 5 × 20 µl aliquots). Up to 10 µl of DNA (pure plasmid or ligation mixture) was added and mixed gently before returning the cells to ice for 30 – 60 min. The cells were then heat-shocked at 42°C for 90 s (or 45 s for BL21 (DE3) [pAPlaclQ] cells that had been split), then returned to ice for 5 min. 800 µl LB medium (500 µl for BL21 (DE3) [pAPlaclQ]) without antibiotics was added and the cells were incubated at 37°C, 500 rpm in a Thermomixer (Eppendorf) for 1 hour. Cells were plated at volumes according to the

expected transformation efficiency (typically 50 – 200 µl) on LB agar plates containing any necessary antibiotics and incubated overnight upside-down at 37°C.

If blue/white selection of transformants was available the plates were spread with 40 µl X-gal (40 mg/ml in DMF) and 40 µl IPTG (100 mM) and the plates were warmed to 37°C for a minimum of 30 min before the transformed cells were plated.

3.2.3 Transformation of *Leishmania* by electroporation

3×10^7 late log-phase *L. mexicana* promastigotes were sedimented by centrifugation at 5,000 × g for 30 secs and immediately resuspended in 100 µl of Human T-Cell Nucleofector solution containing the provided supplement. The cell suspension was transferred to an electroporation cuvette and 1-5 µg of linear DNA or 5 µg of plasmid DNA was added and gently mixed with the suspension. The DNA was electroporated using an *Amaxa* Nucleofector II set to program V-033, following which the cells were placed on ice for 10 min then added to 10 ml of SDM medium without antibiotic(s) using the supplied pastettes. After 24 hours incubation at 27°C, 30 ml SDM medium (containing the appropriate antibiotics(s)) was added and the cells were plated out on a 96-well plate (200 µl/well). Two ml of the cell suspension was further diluted in 18 ml SDM medium (with antibiotic(s)) (1:10 dilution) and plated on a 96-well plate (200 µl/well). The plates were wrapped in Parafilm and incubated at 27°C for 2 weeks until antibiotic-resistant cells had grown. These were transferred to 2 ml of SDM medium (still under antibiotic selective pressure), which was subsequently increased to 10 ml.

3.2.4 Isolation of plasmid DNA from *E.coli*

3.2.4.1 Mini-preparation of plasmid DNA (Zhou et al., 1990)

A single colony was picked from a streak plate of transformed *E. coli* and used to inoculate 3 ml of LB medium containing the appropriate antibiotic(s). This was incubated overnight at 37°C, 225 rpm in a shaker incubator. The next day 1.5 ml of the culture was transferred into a 1.5 ml microcentrifuge tube and centrifuged at 11,000 × g for 30 s. The majority of the supernatant was decanted and the cell pellet was resuspended in the remaining ca. 100 µl by vortexing vigorously. 300 µl of TENS solution was added, the mixture was vortexed for 4 s and placed on ice before 150 µl of 3M sodium acetate (pH 5.2) was added and the solution was vortexed for 3 s. The mixture was then centrifuged at 11,000 × g, 4°C for 15 min. The particle-free supernatant was transferred to a fresh microcentrifuge tube and the DNA was

precipitated by the addition of 900 µl of ice-cold 100% ethanol. Following centrifugation under the same conditions as before, the pellet was washed with 1 ml of ice-cold 70% ethanol, centrifuged for 5 min at 11,000 × g, 4°C. The supernatant was discarded and the pellet was air-dried before being resuspended in 40 µl of ddH_2O.

3.2.4.2 Mini-preparation of plasmid DNA using the Macherey & Nagel Nucelospin Plasmid Kit

A single colony was picked from a streak plate of transformed *E. coli* and used to inoculate 3 ml of LB medium containing the appropriate antibiotic(s). This was incubated overnight at 37°C, 225 rpm in a shaker incubator. The next day 1.5 ml of the culture was transferred into a 1.5 ml microcentrifuge tube and centrifuged for at 11,000 × g for 30 s. For the rest of the procedure the kit manufacturer's instructions in the chapter of the manual titled "Using a microcentrifuge" were followed.

3.2.4.3 Midi-preparation of plasmid DNA using the Macherey & Nagel Nucleobond Xtra Midi Kit

100 ml of LB medium containing the appropriate antibiotic(s) was inoculated with a single colony from a streak plate of transformed *E. coli*. The culture was incubated at 37°C, 225 rpm in a shaker incubator overnight. (A sterile glycerol stock was made as per section 3.1.1.3.) The overnight culture was centrifuged for 15 min at 4,000 × g, 4°C. Steps 4 to 12 of the "Plasmid DNA Purification" kit protocol (Macherey-Nagel) for Midi preparation were followed. After step 12 was carried out the 5 ml of eluate was distributed between six 1.5 ml microcentrifuge tubes; 833 µl of eluate and 583 µl of Isopropanol. The mixture was vortexed briefly and left at room temperature for 2 min before being centrifuged for 30 min at 11,000 × g, 4°C. The supernatant was decanted and the DNA pellets were washed with 1 ml of 70% ice-cold ethanol then centrifuged for 10 min at 11,000 × g, 4°C. The pellets were air-dried, resuspended in 20 µl of ddH_2O and then combined. The DNA was stored at -20°C.

3.2.5 Isolation of genomic DNA from *Leishmania*

2.8 ml (2 × 1.4 ml) of a stationary phase promastigote culture was sedimented by sequential centrifugation (16,000 × g for 30 s, 4°C). The pellets were either immediately frozen in liquid nitrogen and stored at -70°C or the procedure was continued thus: the pellets were resuspended in 400 µl of freshly prepared TELT buffer and incubated at room temperature for 5 min. 400 µl of cold phenol was added

and the mixture was rotated for 5 min at 4°C, following which it was centrifuged for 10 min at 4°C, 16,100 × g. The upper (aqueous) phase was carefully removed and transferred to a fresh 1.5 ml microcentrifuge tube, 400 µl of chloroform/isoamyl alcohol (24:1) was added and the mixture was rotated for 5 min at 4°C, following which it was centrifuged for 10 min at 4°C, 16,100 × g. The upper (aqueous) phase was transferred to another fresh microcentrifuge tube, 1 ml of ice-cold 100% ethanol was added to precipitate the genomic DNA (gDNA) and the mixture was rotated and centrifuged as before. The gDNA pellet was washed by adding 400 µl of ice-cold 70% ethanol and centrifuging for 10 min at 4°C at 16,100 × g. The pellet was then dried and resuspended in 100 µl of TE buffer and stored at 4°C.

3.2.6 Phenol/chloroform extraction of DNA solutions

An equal volume of a DNA solution (typically 100 µl of a restriction endonuclease digest) was mixed with TE-equilibrated phenol and vortexed for 30 s. To separate the solution into different phases it was centrifuged at 16,100 × g for 5 min. The upper aqueous phase was carefully removed and transferred into a fresh microcentrifuge tube, 100 µl chloroform/isoamyl alcohol (24:1) was added and the mixture was vortexed for 30 s before being centrifuged as before. The upper aqueous phase was removed and transferred to a fresh microcentrifuge tube where it was ethanol precipitated (section 3.2.7).

3.2.7 Ethanol precipitation of DNA

The DNA solution was mixed with 2.5 volumes 100% ethanol and 1/9 volume 3 M sodium acetate, pH 5.2, vortexed to ensure thorough mixing and incubated at -70°C for 30 min. The solution was then centrifuged for 15 min at 16,100 × g, 4°C. The supernatant was discarded and the pellet was washed with 1 ml 70% ethanol and centrifuged for 10 min at 16, 100 × g, 4°C. The pellet was air-dried then dissolved in an appropriate volume of ddH_20.

3.2.8 Determination of DNA concentration in aqueous solutions

The DNA solution was diluted 1:100 in ddH_2O, 100 µl was pipetted into a UV cuvette (UVette, Eppendorf) and the concentration was determined using a BioPhotometer (Eppendorf) in DNA mode.

3.2.9 Reactions with DNA-modifying enzymes

3.2.9.1 Cleavage with Type II restriction endonucleases

All restriction digests were performed using restriction endonucleases purchased from New England Biolabs (NEB). Digests were carried out using the supplied buffers and BSA, if required. Analytical digests of plasmid DNA were carried out in a total volume of 15 µl using 1.0 µg of DNA and 5-10 U of each restriction enzyme and were incubated for 2-3 h at the recommended temperature. When the DNA was isolated using the Zhou method, 2 µg of RNase A were also added to the digest. Preparative digests of plasmid DNA were performed in a total volume of 50-100 µl using 10-20 µg of DNA and 40-60 U of each restriction enzyme. After three hours incubation at the recommended temperature a sample of the digest was electrophoresed on a 0.8% agarose gel to ensure the digest was complete, if not the incubation was extended by another 1.5 hours or left overnight if none of the restriction enzymes exhibited star activity.

3.2.9.2 Complete fill-in of a 5' overhang to create blunt-end DNA using Klenow polymerase

The DNA fragment that was to be treated was extracted from an agarose gel following restriction digest and electrophoresis. The fragment was dissolved in 30 µl of ddH_2O and an additional 13.25 µl ddH_2O was added along with 5 µl 10× Klenow Buffer and 1 µl dNTPs. 0.75 µl Klenow polymerase was added last and the mixure was incubated for 15 min at 25°C, 400 rpm. The enzyme was inactivated by heating to 75°C for 20 min.

3.2.9.3 Dephosphorylation of 5'-ends of DNA fragments

In cases where endonuclease digestion had resulted in blunt ends or complementary overhangs of the linearised vector molecule it was necessary to dephosphorylate the 5'-end to reduce the likelihood of spontaneous self-ligation. The DNA was purified from the restriction digest mixture by phenol/chloroform extraction and ethanol precipitation. The DNA pellet was resuspended in 25.5 µl ddH_2O, 3 µl of 10 × SAP buffer (Roche) and 1.5 µl Shrimp Alkaline Phosphatase (SAP) were added and the mixture was incubated for 2 hours at 37°C. To inactivate the enzyme it was heated for 20 min at 65°C.

3.2.9.4 Ligation of DNA fragments

Ligation mixes consisted of approximately 50 – 100 ng vector and three times as much insert DNA, 1.5 µl 10 × ligation buffer and 0.8 µl T4 DNA Ligase (Roche). The total volume was made up to 15 µl with ddH_2O and incubated overnight at 13°C. The ligation mixture was then kept on ice until required for bacterial transformation.

3.2.10 Agarose gel electrophoresis

Agarose gels were prepared at an agarose concentration of 0.8 – 1.2% (w/v) in 0.5 × TBE and 0.3 µg/ml Ethidium Bromide. 10× Agarose gel loading buffer was added to DNA samples to a final concentration of 1×, the samples were loaded into gel pockets and separated at a speed of 1.4 – 10 V/cm in 0.5 × TBE until the dye-front reached three quarters of the length of the gel. DNA bands were then visualized using UV illumination and sizes of the bands could be estimated by comparison to a DNA molecular weight marker.

3.2.11 Extraction of DNA fragments from agarose gels using the Macherey & Nagel Nucleospin Extract II Kit

DNA fragments were excised from agarose gels using a clean scalpel under low-intensity UV light (λ = 365 nm) then purified from the gel fragment using the manufacturer's instructions. The only deviation was in the final stage when the DNA was eluted using 20 – 30 µl ddH_2O.

3.2.12 Polymerase Chain Reaction (PCR)

PCRs were performed using the Expand High Fidelity PCR System from *Roche*. Reactions were carried out in a 200 µl PCR tube using a *PE* thermocycler.

Reaction mixture:

DNA template	10-200 ng
Primer A (10 µM)	5 µl
Primer B (10 µM)	5 µl
10 × PCR buffer (15 mM $MgCl_2$)	5 µl
dNTPs (10 mM)	2 µl
Hi-Fidelity Polymerase	0.75 µl

ddH_2O was used to attain a final volume to 50 µl

PCR Temperature Sequence:

94 °C	2 min	
94 °C	20 s	
54 °C	30 s	20 - 30 ×
72 °C	50 s	

72 °C 7 min
4 °C Unlimited

3.2.13 Cloning of a PCR product using the TOPO TA Cloning Kit

The TOPO cloning kit supplies the vector pCR2.1-TOPO in a linearized form with 3'-Thymidine overhangs. This allows the direct insertion and ligation of *Taq* polymerase-amplified PCR products. All TOPO cloning was carried out according to the manufacturers instructions and TOP10F' *E. coli* used (Invitrogen, Paisley, UK).

3.2.14 DNA Sequencing

DNA sequencing was performed by Geneservice (Cambridge, UK). Samples for sequencing were prepared according to the company's instructions.

3.3 Protein biochemistry

3.3.1 Expression of recombinant proteins in *E. coli*

Competent *E. coli* cells were transformed with plasmids encoding the protein(s) of interest as detailed in 3.2.2. The agar plates were incubated at 37°C overnight and the colonies of transformed bacteria were harvested by washing the plates with 2 ml of sterile LB medium, which was then used to inoculate 100-200 ml of LB medium containing the appropriate antibiotic(s). This was incubated at 37°C, 225 rpm in a shaking incubator and the optical density at 600nm (OD_{600}) was monitored until an OD_{600} of 0.9 was reached. The culture was then cooled to 18°C and protein expression was induced by the addition of Isopropyl β-D-1-thiogalactopyranoside (IPTG) to a concentration of 100 μM. The cells were then incubated overnight at 18°C, 225 rpm in a shaker incubator.

Following overnight incubation at 18°C, the cells were sedimented by centrifugation for 15 min at 4,000 × g, 4°C. The supernatant was discarded and the pellet was resuspended in 10 ml cold 1× PBS per 100 ml original culture volume. The centrifugation was repeated and the pellet was resuspended in 5 ml cold 1× PBS per 100ml original culture volume and kept on ice. The cells were then lysed (while still on ice) using a Branson sonifier fitted with a 6mm tip. Each sonication intensity was used three times for 20 s each interspaced with a 20 s break, with increasing intensity from 2-4. Triton X-100 (10%) was added to a final concentration of 1% (v/v) and mixed by rolling at 4°C for 30 min. The cell lysate(s) was distributed to 2 ml tubes

and centrifuged for 10 min at 16,100 × g, 4°C. The supernatants were immediately used for protein purification.

3.3.2 Affinity purification of recombinant proteins

Co^{2+} sepharose beads were prepared concurrently with the centrifugation and wash steps. 200 µl of Chelating Sepharose Fast Flow bead suspension per 100 ml original culture volume (1:1 mixture of beads: slurry) was centrifuged for 2 min at 1000 × g, 4°C. The supernatant was carefully removed and the beads were washed in 1 ml of ddH_2O, rotated at room temperature for 5 min then centrifuged as before. The beads were washed in this way again with 1 ml of ddH_2O, once with 200 µl of 0.1 M $CoCl_2$, three times with 1 ml ddH_2O and finally with 200 µl of binding buffer.

The supernatants from 3.3.1 were collected, mixed with an equal volume of binding buffer, added to the equilibrated Co^{2+} beads and rolled at 4°C for 1 hour. The beads were sedimented by centrifuging for 5 min at 11,000 × g , 4°C, then washed consecutively with 6 ml wash buffer, 1 ml binding buffer and 1 ml wash buffer by rolling for 10 min at 4°C then centrifuging for 5 min at 1000 × g, 4°C. To elute the protein from the beads 200 µl His-elution buffer was added and the suspension was rotated and centrifuged as previously described. (If the protein was not eluted from the beads they were stored in an equal volume of 1× MPK1 kinase buffer.)

Purified protein was stored on ice at 4°C.

3.3.3 Preparation of *Leishmania* cell lysates

Pellets of 2×10^8 late log-phase promastigotes were prepared by centrifuging at 4°C for either 30 seconds at 17,000 × g or 90 seconds at 6,000 × g. The supernatant was discarded and the pellets were resuspended in 200 µl of lysis buffer and heated at 98°C for 10 min. The 1.5 ml tubes were then given a brief spin to remove any condensation from the lid. The lysate was left on ice for 5 min then stored at -80°C.

3.3.4 µMACS purification of GFP-tagged proteins from *Leishmania*

4×10^8 logarithmic phase promastigote cells were pelleted by centrifuging for 10 min at 3,000 rpm, 4°C. The supernatant was discarded and the cells were resuspended in 10 ml cold 1 × PBS (with 1 × complete protease inhibitor solution (Roche) and ortho-phenanthroline) and centrifuged as before. The supernatant was discarded and the pellet was snap-frozen in liquid Nitrogen and stored at -80°C until needed.

The cell pellet that had been previously prepared was gently defrosted on ice then 1 ml of ice-cold GFP Lysis Buffer was added and the pellet was dissolved by gently pipetting up and down. The dissolved cell pellet was incubated on ice for 30 min and was gently mixed every 10 min by inverting the tube. The solution was then centrifuged at 10,000 × g, 4°C for 10 min and the supernatant was carefully transferred to a fresh 1.5 ml microcentrifuge tube where it was mixed with 50 µl of anti-GFP magnetic beads then incubated for 30 min on ice. Steps 3-9 of section 2.4 “Magnetic labelling and separation for subsequent analysis by SDS-PAGE” from the “MultiMACS™ Epitope Tag Isolation Kits” manual were followed with the following modifications: for step 3 the supplied lysis buffer was substituted with GFP Lysis Buffer and for step 6 three washes were performed with GFP Lysis Buffer and the final wash was performed using the supplied Wash Buffer 1. Following the elution step 2.6 µl 5 × SSB/DTT and 2.4 µl 25 × Complete Protease Inhibitor solution (with ortho-phenanthroline) were added, the eluate was boiled at 98°C for 10 min the stored at -20°C.

3.3.5 Determination of protein concentration by Bradford assay

10 µl of eluted protein was mixed with 500 µl Bradford’s solution in a cuvette, incubated at RT for 2 min then the concentration was determined using a BioPhotometer (Eppendorf) using the Bradford Assay mode.

3.3.6 Discontinuous SDS polyacrylamide gel electrophoresis (SDS-PAGE)

Sodium Dodecyl Sulphate-Polyacrylamide Gel Electrophoresis (SDS-PAGE) was used to separate proteins. Stacking gels were a universal 4% acrylamide whereas resolving gels were either 10 or 12% acrylamide. SDS Sample Buffer (5 × SSB) was added to the sample to be separated and it was heated at 95°C for 10 min then 25-30 µl was loaded on the gel along with 15 µl of NEB pre-stained, broad range (7-175 kDa), protein molecular weight marker (NEB, UK). The samples were separated at 20 mA in the stacking gel and 30 mA in the resolving gel. The current was switched off when the dye in the samples reached the end of the gel.

3.3.7 Staining of SDS-PA gels

Following SDS-PAGE and Immunoblotting (if performed) the gel was placed in Coomassie staining solution and agitated for approximately 10 – 30 min. The staining solution was then replaced with destaining solution, which was changed several

times until the bands of protein were easily distinguished and the blue background was minimised. The gels were either dried or stored in ddH_2O.

3.3.8 Drying of PA gels

Following staining and destaining of the gel it was agitated at RT for 30 min in gel drying solution. Cellophane sheets were soaked in tap water and the gel was placed in between two sheets and a gel-drying frame. To ensure the gel did not crack it was essential to ensure there were no air-bubbles trapped. The set-up was placed in a fume-hood for a minimum of 12 hours.

3.3.9 Immunoblot analysis

Proteins were resolved by electrophoresis on SDS-PAGE then blotted to a Polyvinylidene Difluoride (PVDF) membrane by semi-dry electroblotting using a Fastblot B33/B34 (Biometra) current of 4 mA/cm^2 of gel for 30 min, or 45 min if two gels were being blotted simultaneously. The membrane was then incubated for one hour at 37°C in blocking solution; this was then replaced with blocking solution containing the primary antibody and incubated overnight at 4°C or for one hour at 37°C. The membrane was then washed four times for 5 min with either TBST or PBST (depending on the antibody used) at room temperature. It was then incubated for one hour at 37°C with the secondary antibody diluted in blocking solution, washed three times for 5 min in TBST or PBST then twice for 5 min in TBS or PBS. The blot was developed by incubating the membrane with a 1:1 mix of Supersignal Peroxide solution and Signal Enhancer and exposing to X-ray film for times ranging from 1 s to 1 hour.

3.3.10 Stripping-off antibodies from an Immunoblot

Antibodies were removed from PVDF membranes that had been previously probed by incubation in 100 ml of immunoblot stripping solution at 65°C in a shaking water-bath for 30 min. The membrane was then washed twice with 50 ml TBST or PBST before being re-blocked and probed with a different antibody.

3.3.11 *In vitro* kinase assays

Approximately 1 µg of recombinant kinase (either eluted or still bound to Co^{2+} sepharose beads) was incubated with 1 × Kinase Buffer, 5 µg MBP and 5 µl 1mM ATP (either “cold” or 5 µCi γ-^{32}P ATP (6000 Ci/mmol) for one hour at 34°C with agitation (typically end-over-end rotation) in a total volume of 50 µl. The reaction was

stopped by adding 12.5 µl SSB/DTT and heating at 95°C for ten minutes then placing on ice. 20-25 µl of each sample was separated on SDS-PAGE. Radioactive gels were stained and dried then exposed to X-ray films in a radiograph cassette at -70°C for several hours or days. Non-radioactive gels were immunoblotted as described in section 3.3.9.

4 Results

4.1 Optimisation of selective inhibition of LmxMPK1 through the use of inhibitor-sensitising mutations

LmxMPK1 is not essential for the promastigote stage of the *Leishmania* life cycle (Wiese, 1998), however null mutants do exhibit a slower growth rate when compared to the wild type (Melzer, 2007). Gene deletion is a blunt tool that does not allow the immediate effects of ablating the protein of interest to be examined and *Leishmania mexicana* is not suited for study using RNA interference due to the absence of several of the components of the RNAi pathway (Lye *et al.*, 2010; Kolev *et al.*, 2011). The use of a silent mutation of the gatekeeper residue in the ATP binding pocket allows the kinase to be specifically inhibited by certain small molecule inhibitors (Bishop *et al.*, 2000).

The small molecules that worked best as specific inhibitors of sensitised kinases were derivatives of pyrazolo [3,4-d] pyrimidine (PP1) (Bishop *et al.*, 2001). For this study the derivatives 1-naphthyl PP1 (1Na), 1-naphthylmethyl PP1 (1Nm) and 2-naphthylmethyl PP1 (2Nm) were used. 1Na was purchased commercially (Tocris Bioscience, UK) and 1Nm and 2Nm were gifts from K. Shah (Purdue University, USA).

4.1.1 *In vitro* analysis

Phosphotransferase activity and concentration-dependent inhibition of GST-tagged MPK1F93G with 1Na, 1Nm and 2Nm had already been established (Melzer, PhD Thesis, 2007). However, it was necessary to confirm that this was also the case for His-tagged MPK1F93G and for two new mutants, MPK1F93GF144L and MPK1F93A. Wild type and inhibitor-sensitised LmxMPK1 mutants were expressed in *E. coli* then subjected to radiometric kinase assays.

4.1.1.1 Generation of expression constructs

The primers F93A.for and MPK1BglII.rev were used to amplify a 745 bp fragment from pGEX-KG-MPK1F93G by PCR. This changed the glycine-93 to an alanine and introduced a *Hinc*II restriction site. The fragment was cloned into the pCR2.1-TOPO vector and the presence of the mutation was verified by sequencing (Geneservice) with the positive plasmid designated pCR2.1-TOPO-MPK1F93A. *Bgl*II was used to liberate a 731 bp fragment from pCR2.1-TOPO-MPK1F93A; this was ligated with a

5418 bp fragment that was liberated from pGEX-KG-MPK1F93G using *Bgl*II and *Acc*65I to give the plasmid pGEX-KG-MPK1F93A.

The plasmid pGEX-KG-MPK1F93G was cleaved with *Eco*NI and *Acc*65I to liberate a 421 bp fragment, this was ligated with the 4079 bp fragment that had been released from pQE8W-MPK1 following digestion with the same endonucleases to generate pQE8W-MPK1F93G.

pQE8W-MPK1F93G was then digested with *Acc*65I and *Bgl*II to liberate a 3769 bp fragment. This was ligated with the 731 bp *Bgl*II fragment that had been liberated from pCR2.1-TOPO-MPK1F93A to give pQE8W-MPK1F93A. The 3769 bp fragment was also ligated with a 731 bp fragment that had been released from pGEX-KG-MPK1F93GF144L following digestion with *Bgl*II to give pQE8W-MPK1F93GF144L.

4.1.1.2 Phosphotransferase activity of His-tagged mutants and assessment of specific inhibition

Hexa-histidine tagged wild type LmxMPK1, and the three inhibitor-sensitised mutants (F93G, F93A and F93GF144L) were expressed in BL21 (DE3) [paplaclQ] cells and purified. While still bound to Co^{2+} Sepharose beads approximately 1 µg of protein was incubated in 1 × Kinase Buffer, 5 µg MBP, 5 µl 1mM ATP containing 5 µCi γ-^{32}P ATP (6000 Ci/mmol) and 5 µl of either DMSO or one of the inhibitors (1Na, 1Nm or 2Nm) for 1 hour at 34°C with end-over-end rotation in a total volume of 50 µl. The reaction was stopped by adding 12.5 µl SSB/DTT and heating at 95°C for ten minutes then placing on ice. Twenty-five µl of each sample was separated by SDS-PAGE, the gel was Coomassie-stained, dried and then exposed to X-ray film at -80°C.

Wild type LmxMPK1 (Figure 9) shows no sensitivity to any of the three inhibitors, although the autoradiograph shows a weaker signal for 100 µM 1Na this is expected due to the lower quantity of LmxMPK1 and MBP present in the SDS gel.

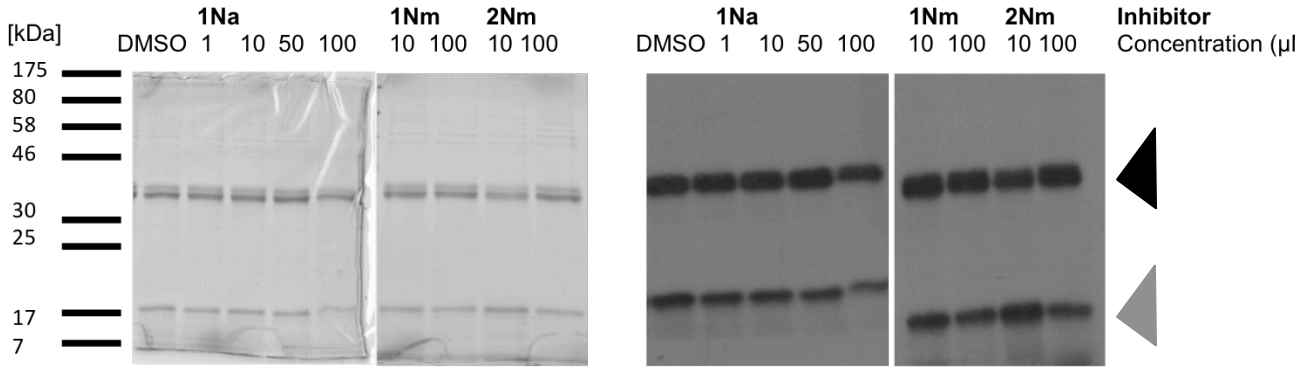

Figure 9: Effect of inhibitors on wild type MPK1.
Left panels show Coomassie-stained SDS-PAGE gels, right panels show autoradiographs following 110 hours exposure; black arrowhead indicates His-LmxMPK1, grey arrowhead indicates MBP; molecular masses of standard proteins are indicated in kDa.

His-tagged MPK1F93G (Figure 10) shows concentration-dependent sensitivity to 1Na, with decreased autophosphorylation for concentrations of 50 μM and 100 μM and a decrease in MBP phosphorylation at 10 μM and the ablation of MBP phosphorylation at 50 μM and 100 μM. The inhibitor 1Nm shows no autophosphorylation inhibition and only moderate inhibition of MBP phosphorylation at 10 μM; there is slight inhibition of autophosphorylation at 100 μM but total ablation of MBP phosphorylation. The inhibitor 2Nm appears to have no effect on either autophosphorylation or MBP phosphorylation.

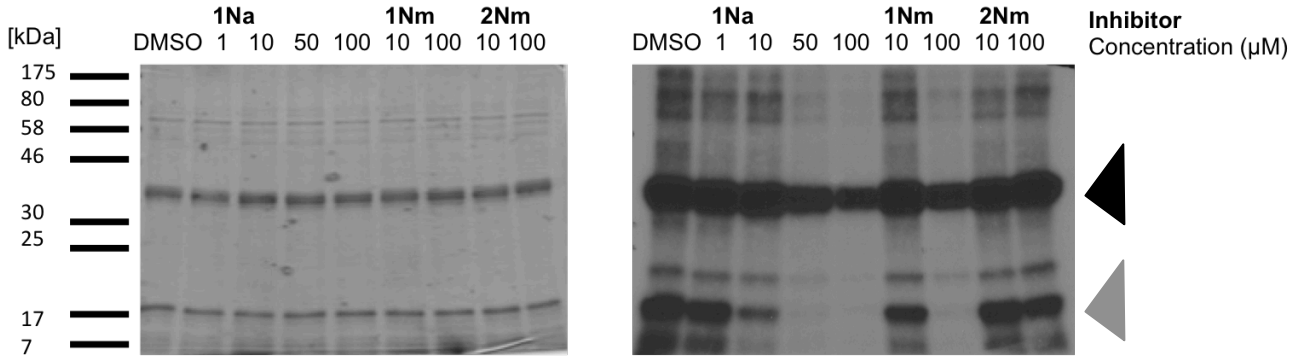

Figure 10: Effect of inhibitors on MPK1F93G.
Left panel shows Coomassie-stained SDS-PAGE gel, right panel shows autoradiograph following 110 hours exposure; black arrowhead indicates His-LmxMPK1F93G, grey arrowhead indicates MBP; molecular masses of standard proteins are indicated in kDa.

Figure 11 shows that MPK1F93A has moderate autophosphorylation activity in DMSO (negative control) but extremely weak phosphotransferase activity towards MBP. Autophosphorylation is only minimally inhibited by 1 and 10 μM 1Na, while the limited MBP phosphorylation observed in the absence of inhibitor is barely detectable. Increasing the concentration of 1Na to 50 and 100 μM completely ablates MBP phosphorylation and decreases autophosphorylation activity. For both 1Nm and 2Nm 10 μM of these inhibitors appears to have a minimal effect on autophosphorylation, while completely eliminating MBP phosphorylation. Increasing the concentration of 1Nm to 100 μM markedly inhibits autophosphorylation and also eliminates MBP phosphorylation; 100 μM of 2Nm eliminates MBP phosphorylation while having little effect on autophosphorylation.

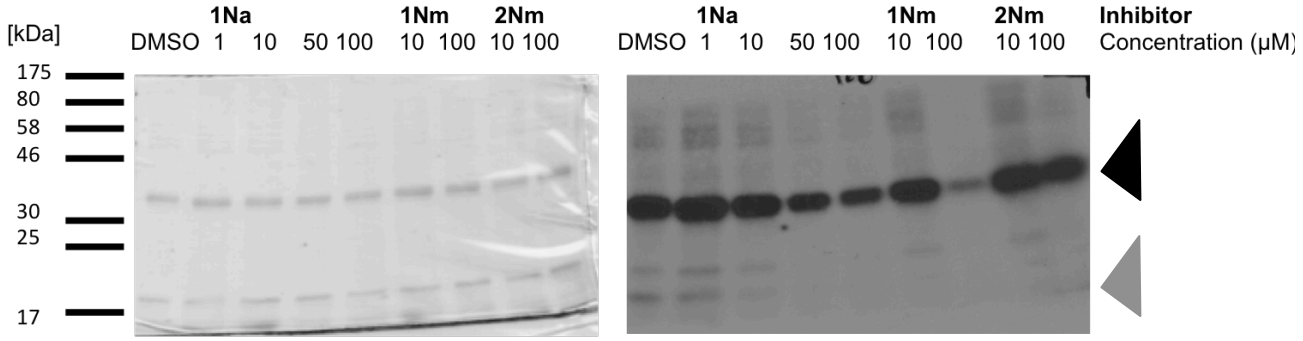

Figure 11: Effect of inhibitors on MPK1F93A.
Left panel shows Coomassie-stained SDS-PAGE gel, right panel shows autoradiograph following 110 hours exposure; black arrowhead indicates His-LmxMPK1F93A, grey arrowhead indicates MBP; molecular masses of standard proteins are indicated in kDa.

The double mutant, MPK1F93GF144L, shows decreasing autophosphorylation (Figure 12) and MBP phosphorylation activity as the concentration of 1Na increases. Autophosphorylation is diminished for both 1Nm and 2Nm at concentrations of 10 μM, although weak MBP phosphorylation can be seen. For both 1Nm and 2Nm autophosphorylation is markedly reduced and MBP phosphorylation appears completely extinguished at concentrations of 100 μM.

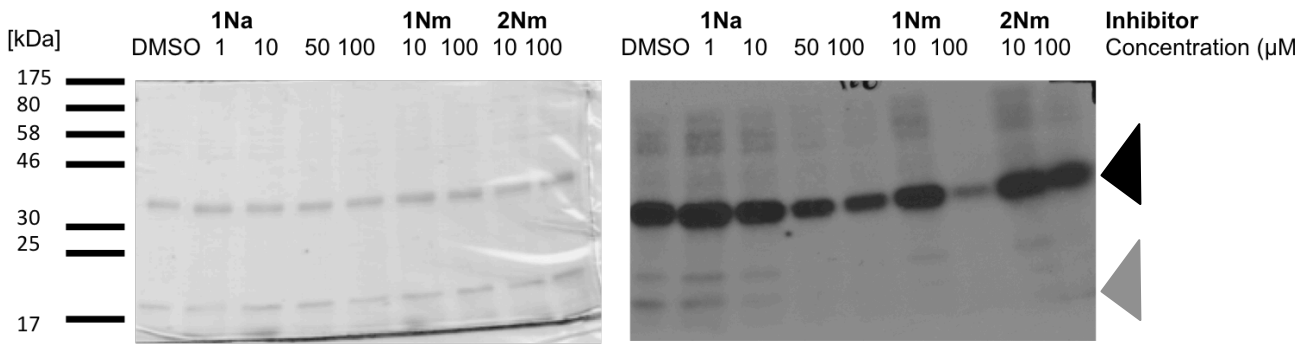

Figure 12: Effect of inhibitors on MPK1F93GF144L.
Left panel shows Coomassie-stained SDS-PAGE gel, right panel shows autoradiograph following 110 hours exposure; black arrowhead indicates His-LmxMPK1, grey arrowhead indicates MBP; molecular masses of standard proteins are indicated in kDa.

4.1.2 *In vivo* analysis

Following *in vitro* analysis of the phosphotransferase activity of the inhibitor-sensitised mutants, which showed activity for all three mutants, it was decided to take all three forward to *in vivo* analysis. 1Na had shown consistent inhibition at lower concentrations for all three mutants so inhibition was only attempted using it.

4.1.2.1 Generation of transfection constructs

The production of the plasmids encoding haemagglutinin-green fluorescent protein (HA-GFP) double-tagged inhibitor-sensitised LmxMPK1 is described in section 4.4.1. The plasmids were transfected into an LmxMPK1 deletion background (Δ*LmxMPK1*) and three clones were selected for each mutant. The clones were selected for by continuous phleomycin selection pressure and verification of protein expression by fluorescent microscopy of live cells. The most fluorescent clone for each mutant was chosen for use in growth curves.

4.1.2.2 Effects of inhibitors on promastigote growth

Wild type *Leishmania mexicana* (WT 0906) and the three inhibitor-sensitised clones were grown in the presence of inhibitor to test for any effect on proliferation. Cells were seeded in 2 ml of SDM-79 medium at a concentration of 5×10^5 cells/ml, with either 5 µl of DMSO or inhibitor at the appropriate concentration and incubated at 27°C for 5 days, with samples for counting taken at the same time each day. Growth was assessed relative to cells expressing the same kinase variant grown with DMSO alone for each time point (i.e. F93A cells grown in presence of inhibitor/F93A cells grown in DMSO alone).

The significance of the data was determined using an unpaired, one-tail t-test. Where the p-value is <0.05 the observed difference was significant and is indicated by an asterisk on the graph (*) (Figure 13). In cases where growth was significantly lower for more than one concentration of 1Na t-tests were used to determine if the growth difference between the inhibitor concentrations was significant, indicated by a delta on the graph (Δ).

For the wild type and all three inhibitor-sensitised mutants 0.1 µM 1Na did not cause a statistically significant decrease in cell growth at any stage in the growth curve.

After 72 hours incubation with 1Na the wild type and the three inhibitor-sensitised mutants all showed a significant growth decrease. For the wild type growth was

81.1% (±7.9), F93G was 63.6% (±8.3), F93A was 62.7% (±4.4) and F93GF144L was 64.1% (±5.1) – all for 10 μM 1Na. After 96 hours wild type growth remains decreased but not to a significant degree (90.2 ± 9.7%). The three inhibitor-sensitised mutants all continued to show a significant decrease in growth: F93G (67.9 ± 2.7%), F93A (78.2 ± 5.0%) and F93GF144L (75.3 ± 5.7%).

On the final day of the growth curve (120 hours incubation), the wild type and the inhibitor-sensitised mutants all showed a certain degree of growth inhibition for cells grown in the presence of 1 and 10 μM 1Na. However, the extent of inhibition was extremely varied. For 10 μM 1Na the wild type showed growth 88.6 ± 9.1% of cells grown in DMSO alone, the F93G mutant showed growth of 53.2 ± 6.0%, for the F93A mutant growth was 80.2 ± 9.5% of DMSO alone and for F93GF144L growth was 65.2 ± 6.2% of cell grown in DMSO.

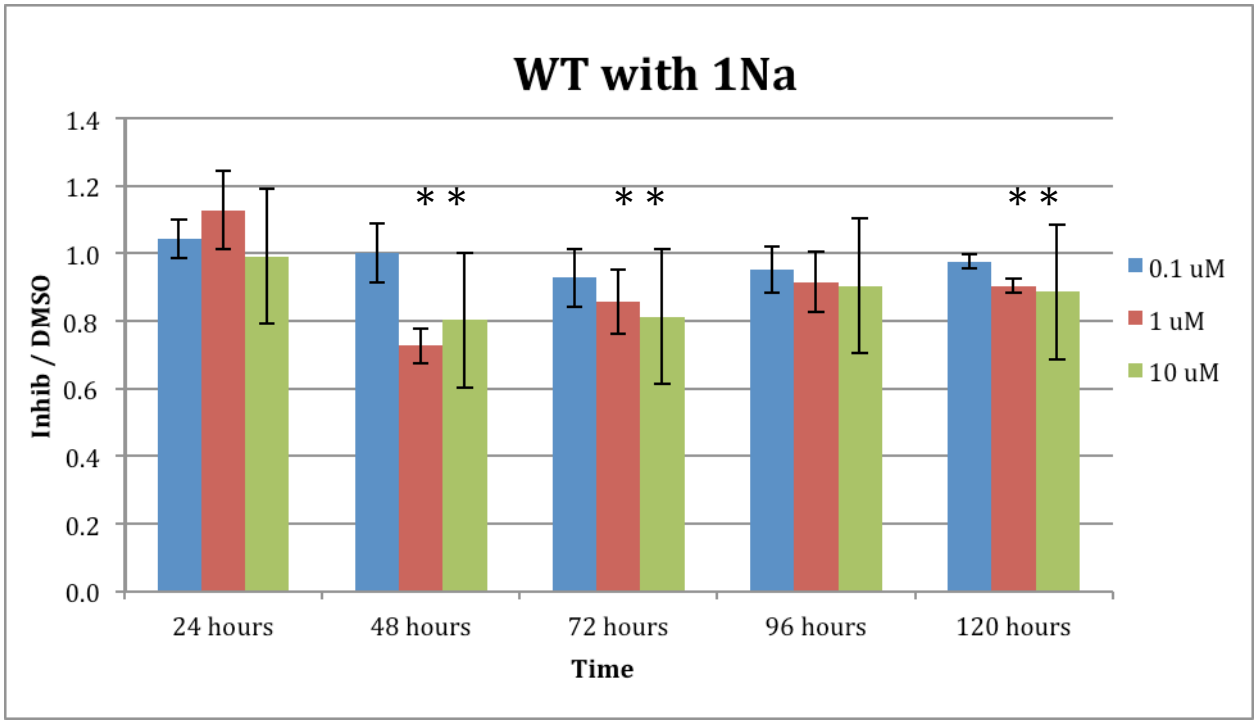
WT with 1Na
Inhib / DMSO
1.4
1.2
1.0
0.8
0.6
0.4
0.2
0.0
* *
* *
* *
24 hours
48 hours
72 hours
96 hours
120 hours
Time
0.1 uM
1 uM
10 uM

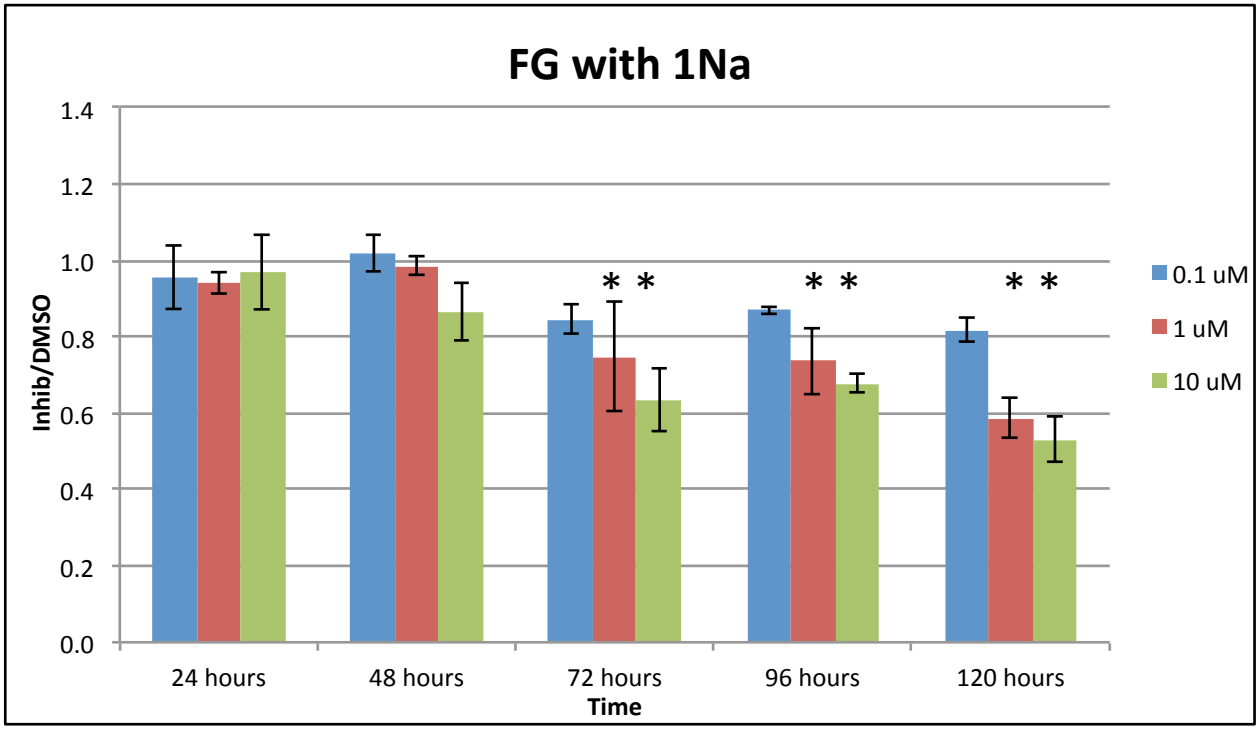
FG with 1Na
Inhib/DMSO
1.4
1.2
1.0
0.8
0.6
0.4
0.2
0.0
* *
* *
* *
24 hours
48 hours
72 hours
96 hours
120 hours
Time
0.1 uM
1 uM
10 uM

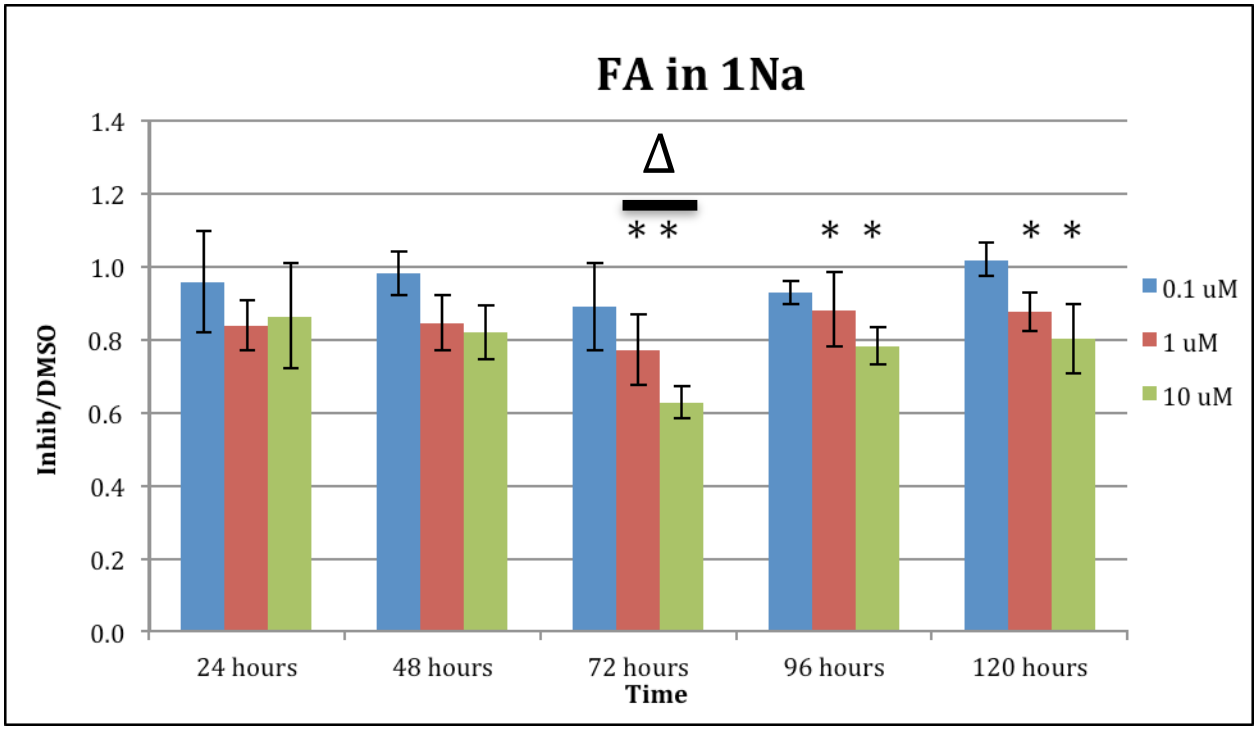

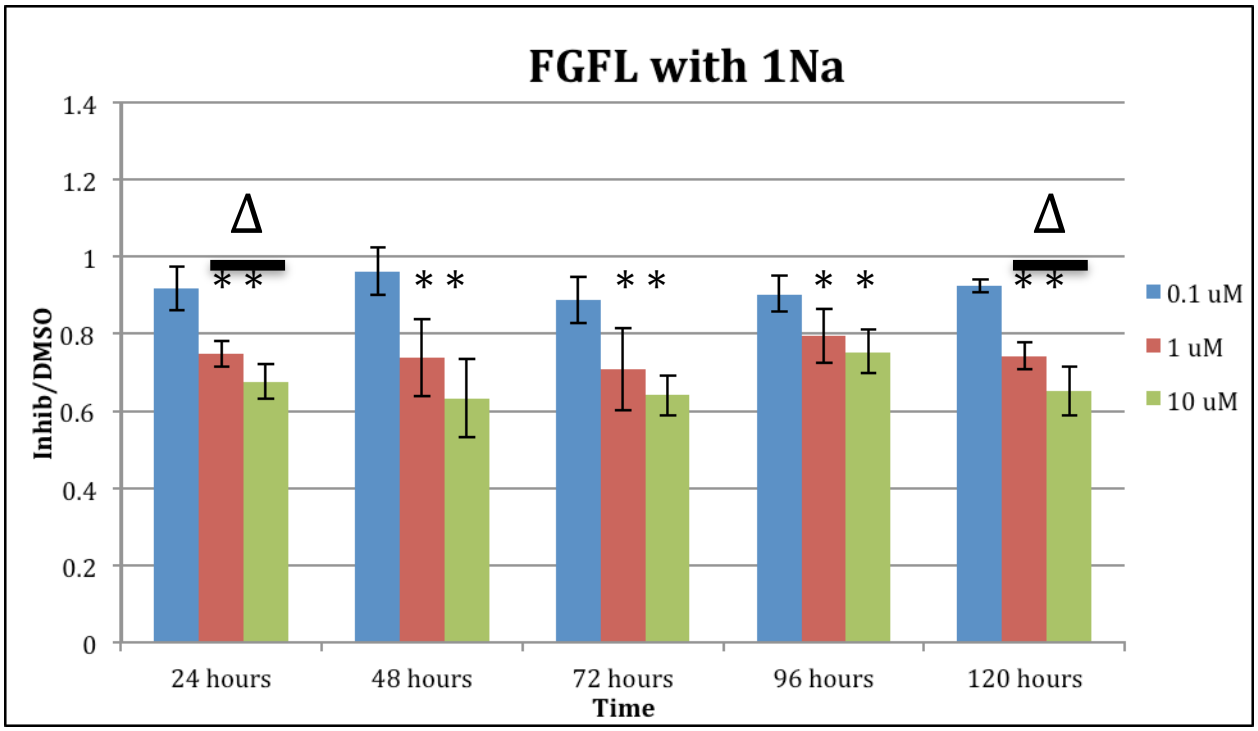

Figure 13: Growth of wild type and inhibitor-sensitised mutants under different concentrations of 1Na – relative to growth in DMSO alone.
WT, WT0906 *L. mexicana*; FG, FA and FGFL, Δ*LmxMPK1* + pX63polPhleoMPK1(F93G/F93A/F93GF144L) HAgfp, respectively.

4.2 Production of dephosphorylated LmxMPK1 through a novel co-expression vector system

LmxMPK1 is phosphorylated when purified from *E. coli* and is active in kinase assays. Attempts to dephosphorylate it using commercial λ-phosphatase had proven inconsistent in their performance (data not shown). In order to produce consistently dephosphorylated recombinant kinase it was decided to co-express LmxMPK1 with one of three phosphatases: human PTP1B, the bacteriophage λ-phosphatase and a novel PTP homologue from *Leishmania mexicana*, LmxPTP (see 4.5 for background information). LmxPTP was chosen as mass spectrometry had detected its presence in the lysates of both amastigotes and promastigotes (H Rosenqvist, unpublished data), it is a small protein so should be possible to express in *E. coli* easily and genome annotation had classed it as a PTP (TriTrypDB: Aslett *et al.*, 2010).

Furthermore, the use of tyrosine phosphatases and dual-specificity lambda phosphatase should enable a comparison of the effects of differential phosphorylation on LmxMPK1 activity and may provide insights to kinase regulation *in vivo*.

Mass-spectrometry had shown that wild type LmxMPK1 is phosphorylated in both stages of the life cycle but in different patterns: both threonine-176 and tyrosine-178 of the activation lip of LmxMPK1 are phosphorylated in promastigotes and axenic amastigotes. In lesion-derived amastigotes only single tyrosine-phosphorylation could be detected so far. Mono-phosphorylation of tyrosine-178 as well as threonine-224 phosphorylation was found in promastigotes, axenic amastigotes and lesion-derived amastigotes (mass spectrometry performed by H Rosenqvist – see appendix).

4.2.1 Generation of expression constructs

Plasmids encoding human PTP1B and λ-phosphatase were provided by Prof David Barford (ICR, London, UK) and were designated p-ampR-PTP1B and p-ampR-λ–phosphatase. The plasmid encoding a triple-haemagglutinin tag, pMA-triple-HA, was generated by de novo gene synthesis by Mr Gene (Regensburg, Germany).

pMA-triple-HA was cleaved with *Nde*I and *Nru*I to release a 155 bp fragment. This was ligated with the 4356 bp fragment that was obtained following digestion of pJC-MPK1 with *Nde*I and *Nru*I; this gave a plasmid named pJC-MPK1-triple-HA.

The genes for PTP1B, λ -phosphatase and LmxPTP were amplified using the primer pairs PTP1B.for/PTP1B.rev, Lambda Phos.for/Lambda Phos.rev and LmexPTP.for/LmexPTP.rev to perform PCRs on the template DNA p-ampR-PTP1B, p-ampR-λ–phosphatase and *L. mexicana* gDNA, respectively. The amplified DNA was cloned into pCR2.1-TOPO and sequenced (Geneservice). Then the lambda phosphatase and LmxPTP genes were released using *Eco*RV and *Spe*I, while PTP1B was released using *Hpa*I and *Spe*I.

pJC-MPK1-triple-HA was cleaved variously with either *Hpa*I and *Spe*I or *Eco*RV and *Nhe*I. The phosphatase gene fragments that were released from pCR2.1-TOPO were then ligated with each of these fragments (i.e., six ligations in total). Ligating the phosphatase fragments with the *Hpa*I/*Spe*I vector fragment resulted in plasmids that encoded hexa-His-LmxMPK1 and a triple-haemagglutinin C-terminally tagged phosphatase, with the general plasmid name pJC-LmxMPK1-*phosphatase*-3HA. Ligation of the phosphatase fragments with the *Eco*RV/*Spe*I vector fragment generated plasmids that encoded LmxMPK1 and a triple-HA N-terminally tagged phosphatase, with the general plasmid name pJC-LmxMPK1-3HA-*phosphatase*.

4.2.2 Assessment of tyrosine phosphorylation of co-expressed protein

Hexa-histidine tagged wild type LmxMPK1, and phosphatase co-expressed LmxMPK1 were expressed in BL21 (DE3) [paplacIQ] cells and purified (For the sake of clarity it should be emphasised that only LmxMPK1 was purified and used in assays, the phosphatases were 3HA tagged and were discarded with the rest of the cell lysate). While still bound to Co^{2+} sepharose beads approximately 1 µg of protein was incubated in 1 × Kinase Buffer, 100 µM ATP for varying lengths of time at 34°C with end-over-end rotation in a total volume of 50 µl. The reaction was stopped by adding 12.5 µl SSB/DTT and heating at 95°C for ten minutes then placing on ice. Twenty-five µl of each sample was separated by SDS-PAGE, blotted onto a PVDF membrane and probed using the monoclonal anti-phosphotyrosine antibody, 4G10. Following blotting the SDS-PA gels were Coomassie-stained to visualise the proteins.

Figure 14 shows wild type, singly expressed LmxMPK1 before incubation with ATP (0 min) and after 20 min incubation with ATP at 34°C. Tyrosine phosphorylation is present following purification from *E. coli* (0 min) and further autophosphorylation on tyrosine can be observed (20 min).

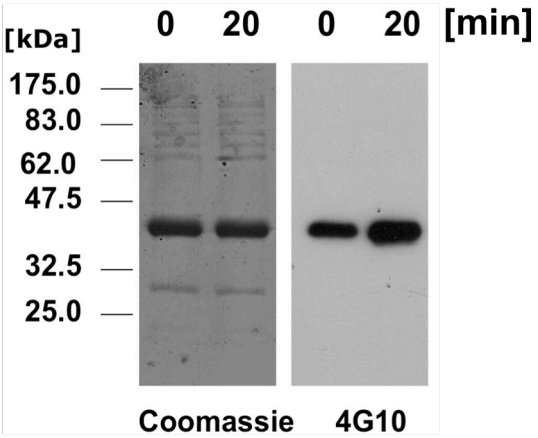

Figure 14: Tyrosine phosphorylation of wild type, singly expressed LmxMPK1.
Left panel shows Coomassie-stained SDS-PA gel following immunoblotting, right panel shows result of immunoblot with 4G10 antibody; molecular masses of standard proteins are indicated in kDa.

Figure 15 shows tyrosine phosphorylation of LmxMPK1 co-expressed with PTP1B before incubation with ATP (0 min) and after 20, 40 and 60 min incubation with ATP at 34°C. For LmxMPK1 co-expressed with C-terminally tagged PTP1B (left panels), tyrosine phosphorylation is present following purification from *E. coli* (0 min) and further autophosphorylation on tyrosine can be observed (20-60 min). Kinase co-expressed with N-terminally tagged PTP1B (right panels) shows no evidence of tyrosine phosphorylation prior to incubation with ATP (0 min), however increasing autophosphorylation on tyrosine is observed (20-60 min).

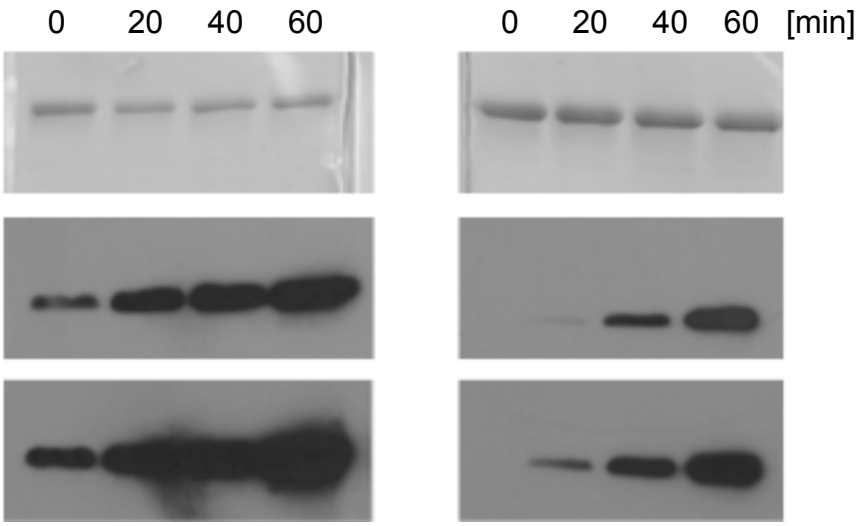

Figure 15: Tyrosine phosphorylation of PTP1B co-expressed LmxMPK1.
LmxMPK1 was co-expressed with PTP1B tagged at either the C- or N-terminus with a triple-haemagglutinin tag. Left panels show the result of an immunoblot using kinase co-expressed with C-terminally tagged PTP1B, right panels show kinase co-expressed with N-terminally tagged PTP1B. For both sides the top panel shows Coomassie-stained SDS-PA gel following immunoblotting; middle panel shows result of immunoblot with 4G10 antibody after 10 s exposure; bottom panel shows result of immunoblot after 30 s exposure.

Tyrosine phosphorylation of λ-phosphatase co-expressed LmxMPK1 is shown in Figure 16. Co-expression of the kinase with C-terminally tagged λ-phosphatase (left panels) resulted in complete dephosphorylation of tyrosine residues, whereas co-expression with N-terminally tagged λ-phosphatase (right panels) did not result in full tyrosine dephosphorylation. In both cases tyrosine autophosphorylation was observed during kinase assays (20-60 min).

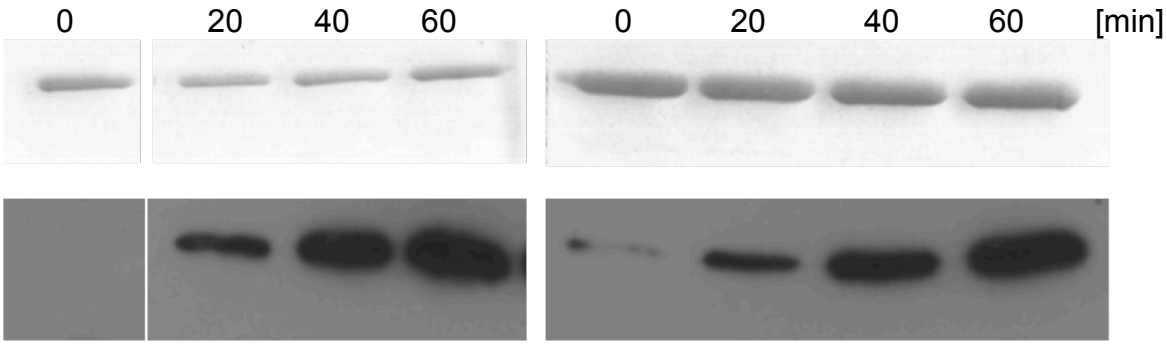

Figure 16: Tyrosine phosphorylation of λ-phosphatase co-expressed LmxMPK1. LmxMPK1 was co-expressed with λ-phosphatase tagged at either the C- or N-terminus with a triple-haemagglutinin tag. Left panels show the result of an immunoblot using kinase co-expressed with C-terminally tagged λ-phosphatase, right panels show kinase co-expressed with N-terminally tagged λ-phosphatase. For both sides the top panel shows Coomassie-stained SDS-PA gel following immunoblotting and the bottom panel shows result of immunoblot with 4G10 antibody after 10 s exposure.

LmxMPK1 was also co-expressed with LmxPTP (Figure 17) tagged at either the C- or N-terminus with the triple-HA tag, then subjected to kinase assay and immunoblotting. Co-expression with C-terminally tagged LmxPTP resulted in complete tyrosine dephosphorylation (left panels); however, this was not the case for kinase co-expressed with N-terminally tagged LmxPTP (right panels). In both cases LmxMPK1 was able to tyrosine autophosphorylate and appears to have reached saturation within the first 20 min of the assay. The stronger signal visible for kinase co-expressed with N-terminally tagged phosphatase is most likely due to the higher protein quantities on the SDS-PA gel, rather than a higher degree of tyrosine phosphorylation.

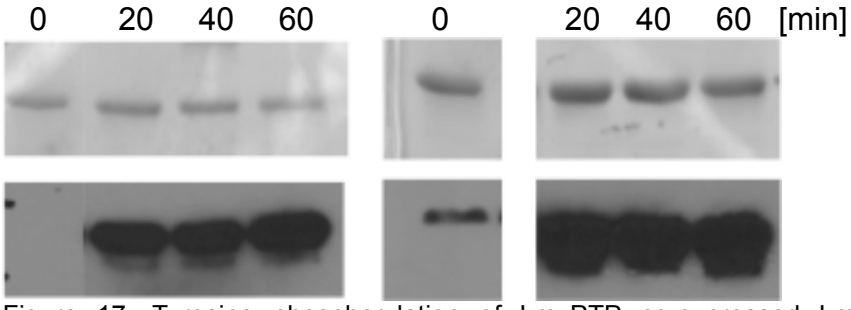

Figure 17: Tyrosine phosphorylation of LmxPTP co-expressed LmxMPK1. LmxMPK1 was co-expressed with LmxPTP tagged at either the C- or N-terminus with a triple-haemagglutinin tag.
Left panels show the result of an immunoblot using kinase co-expressed with C-terminally tagged LmxPTP, right panels show kinase co-expressed with N-terminally tagged LmxPTP. For both sides the top panel shows Coomassie-stained SDS-PA gel following immunoblotting and the bottom panel shows result of immunoblot with 4G10 antibody (15 s exposure).

4.2.3 Assessment of threonine phosphorylation of co-expressed protein

Hexa-histidine tagged singly expressed LmxMPK1, C-terminally 3-HA tagged λ-phosphatase co-expressed LmxMPK1 and N-terminally 3-HA tagged PTP1B co-expressed LmxMPK1 were expressed in BL21 (DE3) [paplaclQ] cells and purified. While still bound to Co^{2+} sepharose beads approximately 1 µg of protein was incubated in 1 × Kinase Buffer, 100 µM ATP for 60 min at 34°C with end-over-end rotation in a total volume of 50 µl. The reaction was stopped by adding 12.5 µl SSB/DTT and heating at 95°C for ten minutes then placing on ice. Twenty-five µl of each sample was separated by SDS-PAGE, blotted onto a PVDF membrane and probed using the polyclonal anti-phosphothreonine antibody 71-8200 (Invitrogen, UK).

Figure 18 shows that singly expressed LmxMPK1 is already phosphorylated on threonine when purified from *E. coli* (Lane 1) and that it undergoes autophosphorylation on threonine when incubated in the presence of ATP (Lane 1'). Kinase co-expressed with λ-phosphatase and (intriguingly) PTP1B show no threonine phosphorylation when purified (Lanes 2 and 3), however, in both cases threonine autophosphorylation is observed following incubation with ATP for 60 min (Lanes 2' and 3').

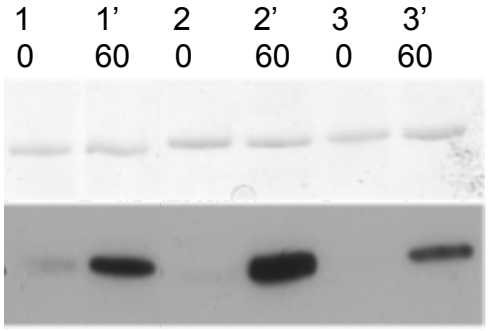

Figure 18: Threonine phosphorylation of LmxMPK1 when expressed singly and when co-expressed with phosphatases.
Kinase was expressed in *E. coli* and purified (0 min) then a kinase assay was performed (60 min), following which an immunoblot using an anti-phosphothreonine antibody was carried out. 1, 1', Singly expressed LmxMPK1; 2, 2', λ-phosphatase co-expressed LmxMPK1; 3, 3', PTP1B co-expressed LmxMPK1.

4.2.4 Phosphotransferase activity of dephosphorylated proteins

Following recombinant expression and purification of LmxMPK1, both singly expressed and with phosphatases, kinase assays were carried out to examine the effect of dephosphorylation on phosphotransferase activity of LmxMPK1. For the majority of kinases dephosphorylation is used to inactivate the kinase so it was expected that co-expressed LmxMPK1 would either be inactive or display a very low level of activity.

Previous work (Melzer, PhD Thesis, 2007) had suggested that extended incubation of LmxMPK1 with ATP decreased further autophosphorylation (as expected) but also diminished kinase activity towards MBP (not as expected). In order to confirm this observation recombinant kinase (both singly expressed and co-expressed with phosphatases) was incubated with non-radioactive ATP for varying lengths of time then incubated with radioactive ATP and MBP to assess autophosphorylation and phosphotransferase activity.

4.2.4.1 Time-course kinase assays

Hexa-histidine tagged wild type LmxMPK1, and LmxMPK1 co-expressed with one of the phosphatases (PTP1B, λ-phosphatase and LmxPTP) were expressed in BL21 (DE3) [paplaclQ] cells and purified. While still bound to Co^{2+} sepharose beads approximately 1 µg of protein was incubated in 1 × Kinase Buffer, 5 µg MBP and 5 µl 1mM ATP containing 5 µCi γ-^{32}P ATP (6000 Ci/mmol) for varying lengths of time (5-80 min) at 34°C with end-over-end rotation in a total volume of 50 µl. The reaction was stopped by adding 12.5 µl SSB/DTT and heating at 95°C for ten minutes then placing on ice. Twenty-five µl of each sample was separated by SDS-PAGE, the gel was stained with Coomassie, dried and then exposed to X-ray film at -80°C.

All results in this section are of kinase assays carried out simultaneously with radiation from a single stock to ensure equal levels of radioactive activity in each assay. Assays shown are representative of three repeats.

Figure 19 shows a kinase assay performed with singly expressed LmxMPK1. Autophosphorylation of the kinase is evident from the beginning of the time-course and occurs for the full 80 min. MBP phosphorylation appears to begin after a delay of approximately 10 min.

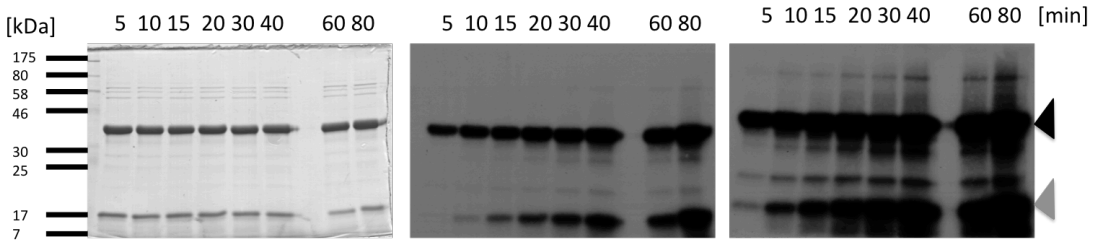

Figure 19: Radiometric kinase assay with singly expressed LmxMPK1 incubated with MBP and γ-^{32}P ATP for between 5 and 80 min.
Left panel, Coomassie-stained SDS-PA gel; middle panel, autoradiograph after 3 h exposure; right panel, autoradiograph of the same experiment after 18 h exposure; black arrowhead indicates His-LmxMPK1, grey arrowhead indicates MBP; molecular masses of standard proteins are indicated in kDa.

Kinase activity of LmxMPK1 co-expressed with PTP1B (N-terminal triple-HA tag) was analysed in the same manner (Figure 20). Kinase autophosphorylation activity was present from the beginning and appeared to continue for the full 80 min. MBP phosphorylation appeared to start after a 10 min delay, similar to singly expressed LmxMPK1.

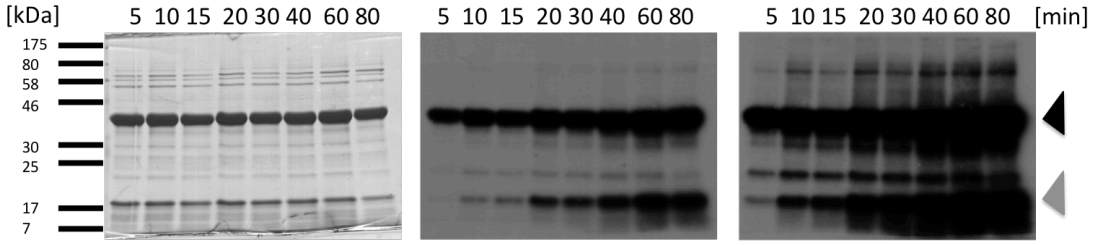

Figure 20: Radiometric kinase assay with PTP1B co-expressed LmxMPK1 incubated with MBP and γ-^{32}P ATP for between 5 and 80 min.
Left panel, Coomassie-stained SDS-PA gel; middle panel, autoradiograph after 3 h exposure; right panel, autoradiograph of the same experiment after 18 h exposure; black arrowhead indicates His-LmxMPK1, grey arrowhead indicates MBP; molecular masses of standard proteins are indicated in kDa.

Figure 21 shows that following co-expression with λ-phosphatase (C-terminal triple-HA tag) autophosphorylation activity was still present from the outset (5 min) but appears to plateau after 15-20 min. MBP phosphorylation starts after approximately 15 min – a longer delay than is exhibited by singly expressed and PTP1B co-expressed kinase.

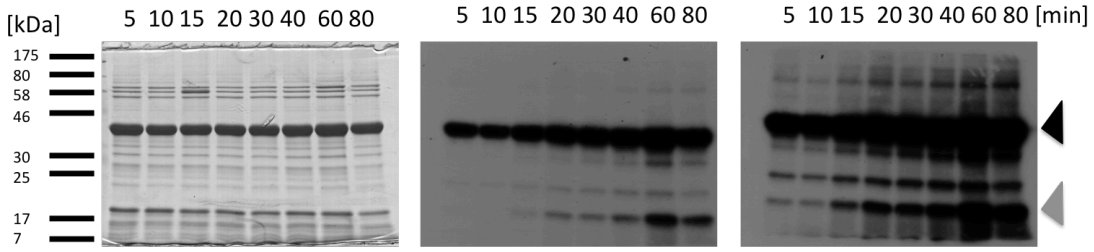

Figure 21: Radiometric kinase assay with λ-phosphatase co-expressed LmxMPK1 incubated with MBP and γ-^{32}P ATP for between 5 and 80 min.
Left panel, Coomassie-stained SDS-PA gel; middle panel, autoradiograph after 3 h exposure; right panel, autoradiograph of the same experiment after 18 h exposure; black arrowhead indicates His-LmxMPK1, grey arrowhead indicates MBP; molecular masses of standard proteins are indicated in kDa.

LmxPTP (C-terminal triple-HA tag) co-expressed LmxMPK1 (Figure 22) exhibited similar activity to that of PTP1B co-expressed LmxMPK1, as it autophosphorylated from the outset (5 min) and for the duration of the experiment (80 min). MBP phosphorylation also began after a 10 min delay.

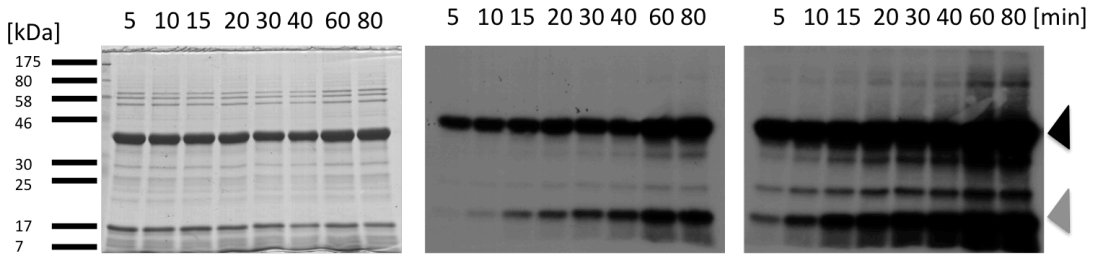

Figure 22: Radiometric kinase assay with LmxPTP co-expressed LmxMPK1 incubated with MBP and γ-^{32}P ATP for between 5 and 80 min.
Left panel, Coomassie-stained SDS-PA gel; middle panel, autoradiograph after 3 h exposure; right panel, autoradiograph of the same experiment after 18 h exposure; black arrowhead indicates His-LmxMPK1, grey arrowhead indicates MBP; molecular masses of standard proteins are indicated in kDa.

In order to better assess the activity of LmxMPK1 after expression with the different phosphatases the computer program ImageJ (NIH, USA) was used to quantify both the amount of protein in the SDS-PA gel and the intensity of the signal on the autoradiograph (3 hours exposure). ImageJ 64 for Mac OS X was downloaded from the NIH website (http://rsbweb.nih.gov/ij/) and installed. The SDS-PA gels and associated autoradiographs were scanned and opened with ImageJ. Each lane of protein was selected using the lane tool and the density of the protein bands was measured for LmxMPK1 and MBP. The signal on the X-ray film was similarly quantified and all numerical data was imported to Excel.

To normalise the data, first the protein loading ratios were calculated: for example, of the LmxMPK1 bands in the first gel the 80 min time point had the most protein so the values for all the other bands of LmxMPK1 on the gel were divided by it. The value obtained for signal on the autoradiograph was then divided by the ratio value:

$$a = b/g_{adj}$$

a is the adjusted value for the autoradiograph; b is the signal on autoradiograph and g_{adj} is the quantity of protein in the lane divided by the maximum.

The adjusted values were then plotted on a scatter graph against time, although to enable comparisons to be made between data set intensities were plotted as a percentage of the maximum for each group of proteins on the individual gels (e.g. 100% is calculated independently for LmxMPK1 and MBP).

Figure 23 shows the result of adjusting the results shown in Figures 19, 20, 21 and 22.

At this point it should be noted that unflashed X-ray film was used during the autoradiography. Consequently, this means that the linearity of the signal/radioactivity ratio is diminished (Laskey, 1993). Although the differences in the trends observed for each experiment are unaffected, it is not possible to ascribe absolute values for the signals that were recorded.

Furthermore, the graphs shown in Figure 23 are merely adjusted representations of what is shown – unprocessed – in Figures 19, 20, 21 and 22.

Adjusting the signal data for singly expressed LmxMPK1 shows gradual autophosphorylation for the first 15 min, a sudden increase between 15 and 20 min then plateauing of autophosphorylation activity thereafter. Although the adjusting process suggests a decrease for kinase that was incubated for 80 min, this is more likely to be attributable to the difficulty discerning what part of the signal on the radiograph for the 80 min time point is from LmxMPK1 and what is from phosphorylated contaminants (see Figure 19). MBP phosphorylation appears to occur at a fairly steady rate up until 60 min, thereafter only a small rise seen in the next 20 min. It is not possible to say with certainty whether the calculated value for 20 min is too high or if the 30 min one is too low (note the slight dip between 20 and 30 min).

PTP1B co-expressed LmxMPK1 autophosphorylated for the full 80 min, although at a faster rate for the first 40 min than it did in the last 40 min, which appears to confirm what is seen in Figure 20. MBP phosphorylation starts after a slightly longer delay than is seen in singly expressed kinase and occurs at a more gradual rate until the last 20 min when a sudden increase in MBP phosphorylation is seen. This is what one would predict after examining loading on the SDS-PA gel (Figure 20); there is a noticeably lower quantity of MBP in the 80 min lane than in the 60 min lane, yet the autoradiograph signal is approximately equal.

Co-expression with λ-phosphatase resulted in LmxMPK1 that had completed the majority of autophosphorylation in 30 min, although some did occur in the last 50 min of the assay. Quantification data matches what was observed visually (Figure 21): MBP phosphorylation initiates after a longer delay than is seen for singly expressed and PTP1B co-expressed kinase. The majority of MBP phosphorylation occurs between 40 and 60 min incubation, with a slight increase thereafter.

LmxMPK1 co-expressed with LmxPTP behaves in much the same manner as LmxMPK1 co-expressed with PTP1B (as was expected). Autophosphorylation was complete within 30-40 min and MBP phosphorylation occurred gradually and plateaued after 40-60 min.

The reaction slopes for MBP phosphorylation for each set of reactions was calculated using the data for 15 and 20 min. This was then used to calculate the 0 intercept for the y-axis, as a guide for the delay before MBP phosphorylation began. The

calculation is displayed on the graph, while the calculated 0 intercepts were 4 m 21 s, 13m 12 s, 10m 12 s and 9 min 14 s for singly expressed, λ-phosphatase, PTP1B and LmxPTP co-expressed LmxMPK1, respectively.

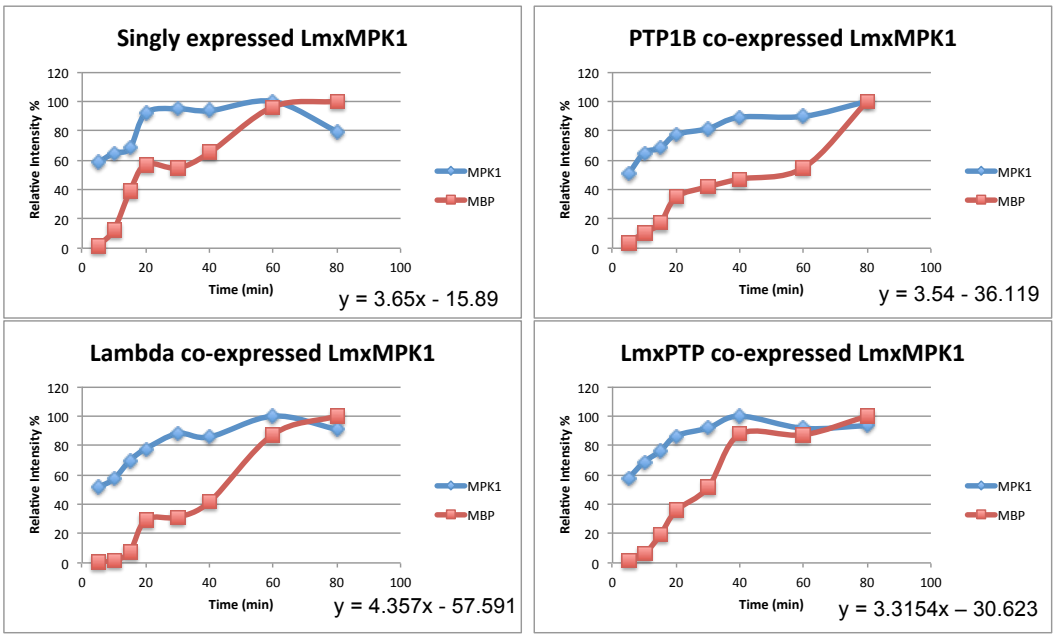

Figure 23: Autoradiograph data following quantification and normalisation.
For each graph the blue line denotes LmxMPK1 autophosphorylation and the red line denotes MBP phosphorylation. Equations are reaction slopes for MBP phosphorylation for each set of reactions, calculated using the data for 15 and 20 min (See preceding paragraph for full explanation).

4.2.4.2 Pre-incubation kinase assays

As mentioned previously, earlier work in the Wiese laboratory group had suggested that increasing autophosphorylation of LmxMPK1 led to a decrease in kinase activity (Melzer, PhD Thesis, 2007). A repeat of this experiment was performed to examine whether the same principle was observed (Figure 24) and also to show that the kinase was not being heat inactivated by extended incubations (lanes 7 and 8). A decrease in kinase autophosphorylation activity was observed as the length of pre-incubation increased (lanes 1-6); substrate phosphorylation also appeared to decrease. Kinase pre-incubated without ATP, but at 34°C, showed activity similar (lanes 7 and 8) to that of kinase not pre-incubated at all (lane 1), which confirms that the decrease in activity observed in lane 6 is indeed a result of autophosphorylation and not heat degradation of kinase.

The observed data was quantified using ImageJ and the trends that had been observed by visual analysis were confirmed (Figure 25).

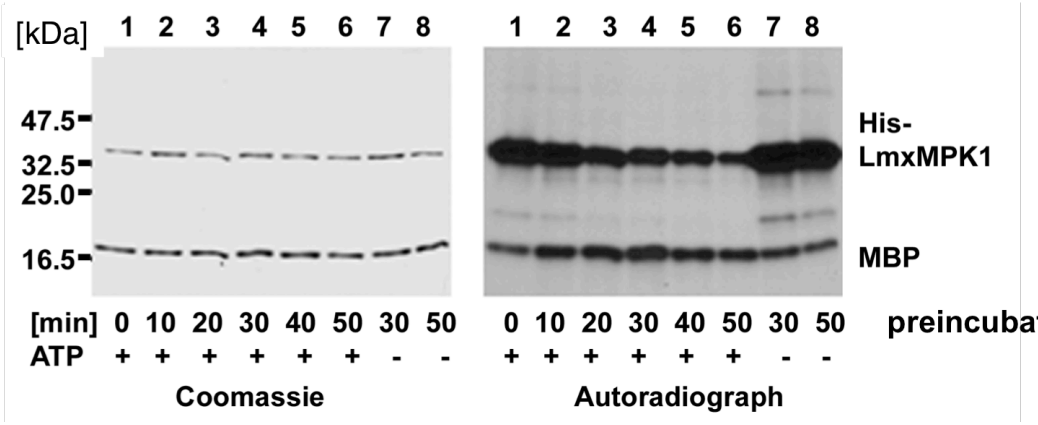

Figure 24: Effect of pre-incubation on LmxMPK1.
Recombinant LmxMPK1 was incubated with 100 µM ATP for between 0 and 50 min, following which it was incubated with MBP and γ-^{32}P ATP for 10 min. Left panel, Coomassie-stained SDS-PA gel; right panel, autoradiograph after 24 h exposure; His-LmxMPK1 and MBP are indicated; molecular masses of standard proteins are indicated in kDa.

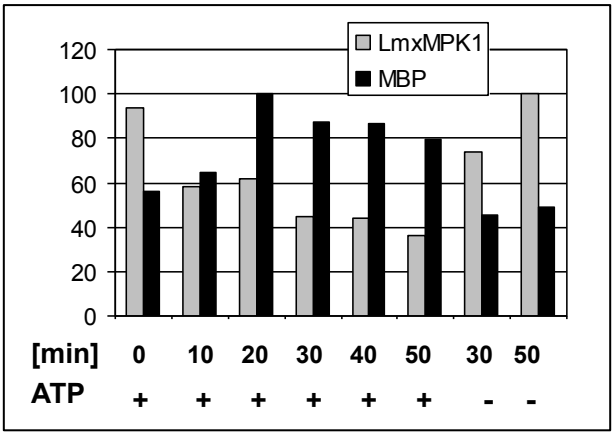

Figure 25: Autoradiograph data following quantification and normalisation.
Grey bars indicate LmxMPK1 autophosphorylation and black lines indicate MBP phosphorylation. The presence (+) or absence (-) of ATP in the kinase assay is indicated below each pair of bars. Analysis was performed as described in 4.2.4.1.

More detailed analysis was then carried out using fresh protein purified on the same day and used for assays at the same time, including kinase co-expressed with phosphatases. Assays shown are representative of three repeats.

Hexa-histidine tagged wild type LmxMPK1, and LmxMPK1 co-expressed with one of the phosphatases (PTP1B, λ-phosphatase and LmxPTP) were expressed in BL21 (DE3) [paplaclQ] cells and purified. While still bound to Co^{2+} sepharose beads approximately 1 µg of protein was incubated in 1 × Kinase Buffer with 100 µM ATP for varying lengths of time (0-90 min) at 34°C with end-over-end rotation in a total volume of 50 µl. The kinase-loaded beads were sedimented by centrifugation for 30 s at 11,000 × g, the supernatant was carefully removed then the kinase-loaded beads were incubated in 1 × Kinase Buffer, 5 µg MBP and 5 µl 1mM ATP containing 5 µCi γ-^{32}P ATP (6000 Ci/mmol) for 10 min at 34°C with end-over-end rotation in a total volume of 50 µl. The reaction was stopped by adding 12.5 µl SSB/DTT and heating at 95°C for ten minutes then placing on ice. Twenty-five µl of each sample was separated by SDS-PAGE, the gel was Coomassie-stained, dried and then exposed to X-ray film at -80°C.

As in the previous section, all subsequent results in this section are of kinase assays carried out simultaneously with radiation from a single stock to ensure equal levels of radioactive activity in each assay.

The effect of pre-incubating singly expressed LmxMPK1 in “cold” ATP is shown in Figure 26. As pre-incubation time increases, autophosphorylation when incubated with radiolabelled ATP decreases; MBP phosphorylation increases gradually as pre-incubation time increases and appears to reach a maximum velocity after 20 min pre-incubation, following which a decrease in activity is observed (30-90 min).

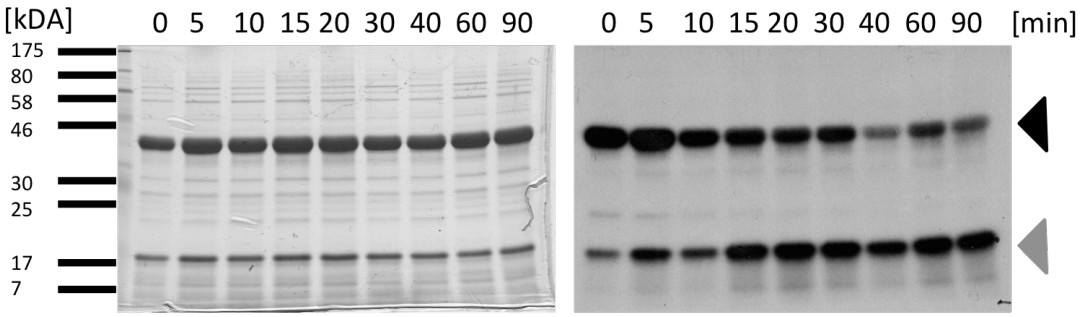

Figure 26: The effect of pre-incubation on phosphotransferase activity of singly expressed LmxMPK1. LmxMPK1 was incubated with 100 μM ATP for between 0 and 90 min, following which it was incubated with MBP and γ-^{32}P ATP for 10 min. Left panel, Coomassie-stained SDS-PA gel; right panel, autoradiograph after 6 h exposure; black arrowhead indicates His-LmxMPK1, grey arrowhead indicates MBP; molecular masses of standard proteins are indicated in kDa.

LmxMPK1 co-expressed with PTP1B (N-terminal triple-HA tag) was analysed in the same manner (Figure 27). As with singly expressed kinase, increasing pre-incubation time led to a decrease in autophosphorylation when incubated with the γ-^{32}P ATP. Substrate phosphorylation also appears to follow the same pattern as that of singly expressed kinase with maximum substrate phosphorylation acheived after 20-30 min pre-incubation; it then appears to decrease slightly to a steady rate for the remaining time (40-90 min).

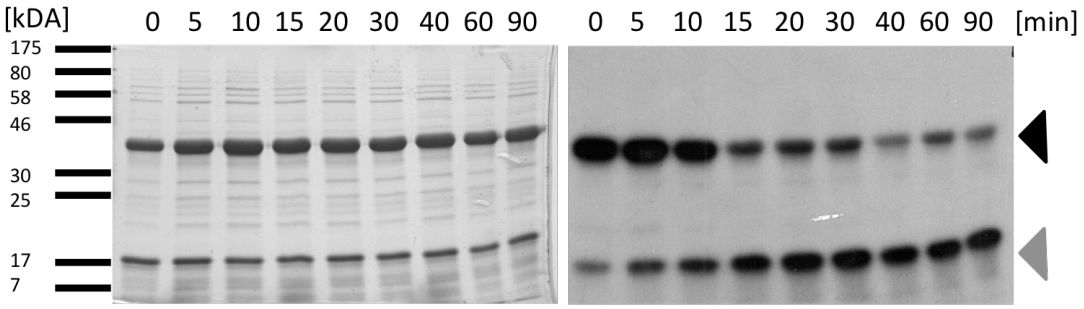

Figure 27: The effect of pre-incubation on phosphotransferase activity of PTP1B co-expressed LmxMPK1.

LmxMPK1 was incubated with 100 μM ATP for between 0 and 90 min, following which it was incubated with MBP and γ-^{32}P ATP for 10 min. Left panel, Coomassie-stained SDS-PA gel; right panel, autoradiograph after 6 h exposure; black arrowhead indicates His-LmxMPK1, grey arrowhead indicates MBP; molecular masses of standard proteins are indicated in kDa.

λ-phosphatase (C-terminal triple-HA tag) co-expressed LmxMPK1 (Figure 28) shows the same pattern of decreasing autophosphorylation activity as the length of the pre-incubation is extended. MBP phosphorylation is very weak for pre-incubation periods of less than 15 min; when pre-incubation is extended to 20 min or longer the degree of MBP phosphorylation appears to increase, with maximum MBP phosphorylation observed following 90 min pre-incubation.

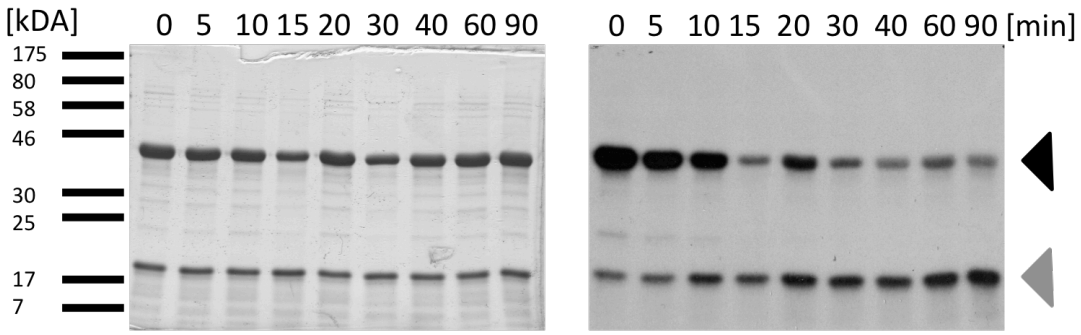

Figure 28: The effect of pre-incubation on phosphotransferase activity of λ-phosphatase co-expressed LmxMPK1.

LmxMPK1 was incubated with 100 μM ATP for between 0 and 90 min, following which it was incubated with MBP and γ-^{32}P ATP for 10 min. Left panel, Coomassie-stained SDS-PA gel; right panel, autoradiograph after 6 h exposure; black arrowhead indicates His-LmxMPK1, grey arrowhead indicates MBP; molecular masses of standard proteins are indicated in kDa.

LmxMPK1 co-expressed with LmxPTP (C-terminal triple-HA tag) was analysed in the same manner (Figure 29). As with singly expressed kinase, increasing pre-incubation time led to a decrease in autophosphorylation when incubated with the γ-^{32}P ATP. Substrate phosphorylation is slightly harder to comment on in this case, as the protein loading is not as even as for other gels in this section. Nonetheless, MBP loading for the 20 and 30 min pre-incubation lanes is lower than other lanes, this implies that the observed signal for these lanes should be higher and that substrate phosphorylation is likely to peak at one of these time points, before declining slightly.

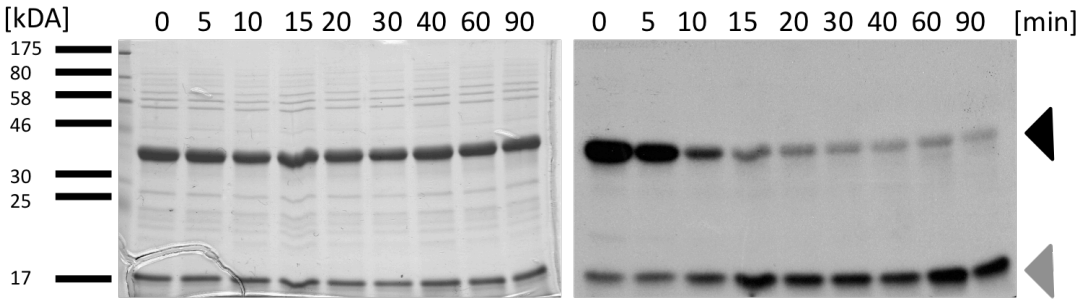

Figure 29: The effect of pre-incubation on phosphotransferase activity of LmxPTP co-expressed LmxMPK1.

LmxMPK1 was incubated with 100 μM ATP for between 0 and 90 min, following which it was incubated with MBP and γ-^{32}P ATP for 10 min. Left panel, Coomassie-stained SDS-PA gel; right panel, autoradiograph after 6 h exposure; black arrowhead indicates His-LmxMPK1, grey arrowhead indicates MBP; molecular masses of standard proteins are indicated in kDa.

ImageJ was used to adjust the results obtained from the pre-incubation assays in the same manner as was done for the time-course assays. Figure 30 shows the result of adjusting the results shown in Figures 26, 27, 28 and 29. As with the graphed, adjusted, time-course assay results (Figure 23), it should be borne in mind that the linearity of the adjusted signal is still compromised by the use of unflashed X-ray film.

For singly expressed and phosphatase co-expressed LmxMPK1 pre-incubation resulted in a decrease in autophosphorylation activity when incubated with γ-^{32}P ATP. Singly expressed kinase shows a gradual decrease in autophosphorylation activity, whereas autophosphorylation of kinase co-expressed with phosphatases rapidly decreases and is minimal in all three cases after 40 min and longer pre-incubation. MBP phosphorylation increases steadily in all cases as the length of the pre-incubation increases. It reaches a peak (30 min for singly expressed, λ-phosphatase and LmxPTP co-expressed kinase; 60 min for PTP1B co-expressed kinase) before declining.

An apparent error that was less obvious from only examining the SDS-PA gels and blots is that for all samples the results of 40 min pre-incubation are anomalous as both autophosphorylation and MBP phosphorylation are less than that of samples incubated for 60 min (except in the case of LmxPTP co-expression: autophosphorylation is already minimal after 30 min pre-incubation). It is possible that the samples that were pre-incubated for 40 min were not incubated with MBP and γ-^{32}P ATP for the full 10 min or that the beads loaded with LmxMPK1 were not agitated sufficiently to disperse them in the assay mixture.

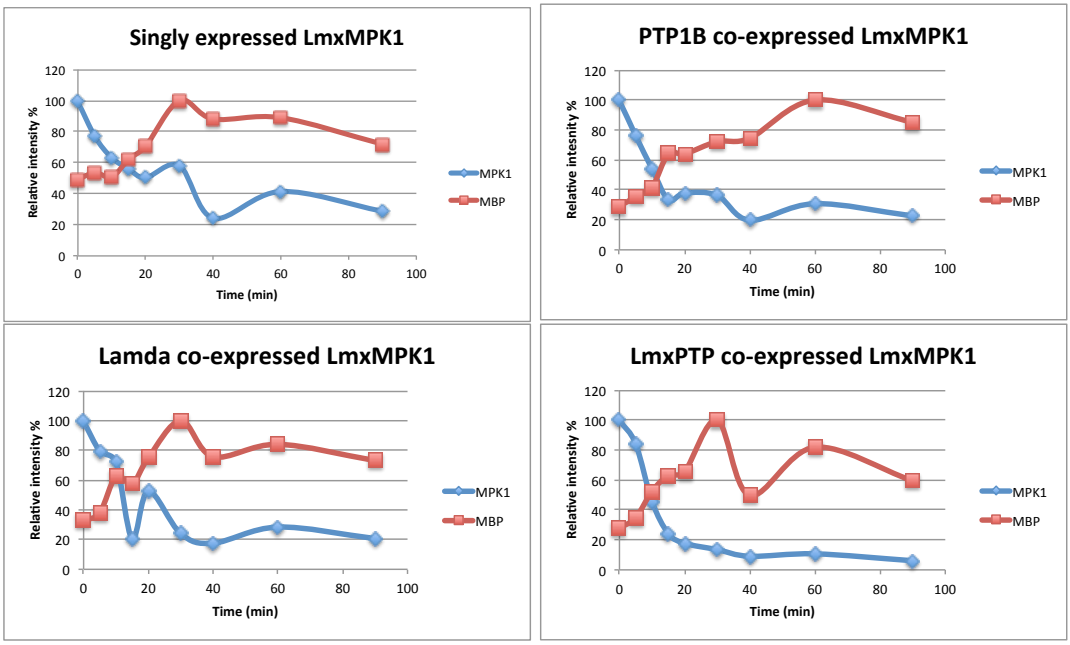

Figure 30: Autoradiograph data following quantification and normalisation. For each graph the blue line denotes LmxMPK1 autophosphorylation and the red line denotes MBP phosphorylation. Analysis was performed as described in 4.2.4.1.

4.3 Role of T224 in LmxMPK1

Mass spectrometry had indicated phosphorylation of threonine-224 both *in vivo* and for singly expressed recombinant LmxMPK1. In order to examine the potential role of the T224 residue with regards to cellular localisation and kinase activity it was decided to mutate this residue to either an alanine or a glutamate residue.

4.3.1 In vitro analysis

4.3.1.1 Generation of expression constructs

Two plasmids were ordered from Proteogenix (France), each containing a 444 bp section of the *LmxMPK1* gene except one plasmid encoded the mutation of threonine-224 to alanine (A) and one encoded a mutation to glutamate (E), these were pUC57-MPK1TA-MKK-DQED and pUC57-MPK1TE-MKK-AQEA, respectively. pUC57-MPK1TA-MKK-DQED, pUC57-MPK1TE-MKK-AQEA and pQE8W-MPK1 were all digested with *Bgl*II and *Kpn*I, this released the 444 bp fragment from the first two plasmids and a 4060 bp fragment from pQE8W-MPK1. The fragments were ligated to give pQE8W-MPK1(TA) and pQE8W-MPK1(TE).

The phosphatase/LmxMPK1 co-expression constructs (described in 4.2) pJC-MPK1-λ-phosphatase-3HA and pJC-MPK1-3HA-PTP1B were cleaved with *Eco*NI and *Sph*I, as were pQE8W-MPK1(TA) and pQE8W-MPK1(TE). The 4553 bp fragments from the pJC plasmids were ligated with the 917 bp fragments from the pQE8W plasmids to give four plasmids: pJC-MPK1(TA)-λ-phosphatase-3HA, pJC-MPK1(TE)-λ-phosphatase-3HA, pJC-MPK1(TA)-3HA-PTP1B and pJC-MPK1(TE)-3HA-PTP1B.

4.3.1.2 Assessment of phosphorylation state and phosphotransferase activity of T224 mutants

In order to determine if threonine-224 of LmxMPK1 is the only threonine residue that is autophosphorylated the following hexa-histidine tagged proteins were expressed and purified: 1) singly expressed LmxMPK1, 2) singly expressed T224A LmxMPK1, 3) Lambda-phosphatase co-expressed T224A LmxMPK1, 4) Lambda-phosphatase co-expressed LmxMPK1 and 5) PTP1B co-expressed LmxMPK1. While still bound to Co^{2+} sepharose beads approximately 1 µg of protein was incubated in 1 × Kinase Buffer, 100 µM ATP for 60 min at 34°C with end-over-end rotation in a total volume of 50 µl. The reaction was stopped by adding 12.5 µl SSB/DTT and heating at 95°C for ten minutes then placing on ice. Twenty-five µl of each sample was separated by

SDS-PAGE, blotted onto a PVDF membrane and probed using anti-phosphotyrosine (Figure 31) and anti-phosphothreonine (Figure 32) antibodies.

Figure 31 shows that tyrosine phosphorylation is present following purification for singly expressed wild type (Lane 2) and T224A LmxMPK1 (Lane 1), however not in the kinase co-expressed with phosphatase (Lanes 3-5). Following kinase assay increased tyrosine phosphorylation is observed for singly expressed kinase (Lanes 1' and 2') and tyrosine autophosphorylation has occurred for kinase that was co-expressed (Lanes 3'-5').

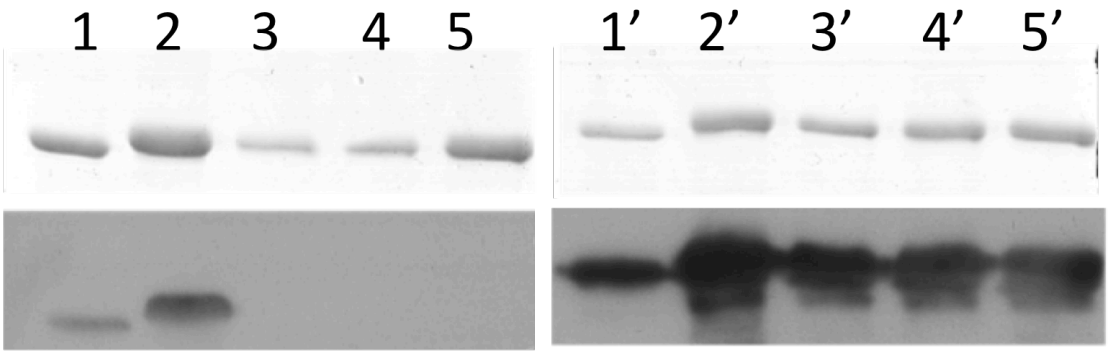

Figure 31: Tyrosine phosphorylation of singly and co-expressed LmxMPK1 and T224A mutant.
Left panels show kinase following purification from *E. coli*, right panels show kinase following 60 min kinase assay. Top panels show Coomassie-stained SDS-PA gel, bottom panels show result of immunoblot with anti-phosphotyrosine monoclonal antibody 4G10. 1, 1’, T224A LmxMPK1 mutant; 2, 2’ Wild type LmxMPK1; 3, 3’ λ-phosphatase co-expressed T224A mutant; 4, 4’ λ-phosphatase co-expressed LmxMPK1; 5, 5’ PTP1B co-expressed LmxMPK1.

Figure 32 shows that threonine phosphorylation is detectable in singly expressed wild type LmxMPK1 following purification (Lane 1), but not when co-expressed with phosphatases (Lanes 3, 4). The T224A mutant appears to have a very small amount of threonine phosphorylation when singly expressed (Lane 5) but none is detected following co-expression with phosphatase (Lane 2). Autophosphorylation on threonine is observed in all cases (Lanes 1', 2', 3', 4' and 5'), although only minimally for the singly expressed T224A mutant (Lane 5').

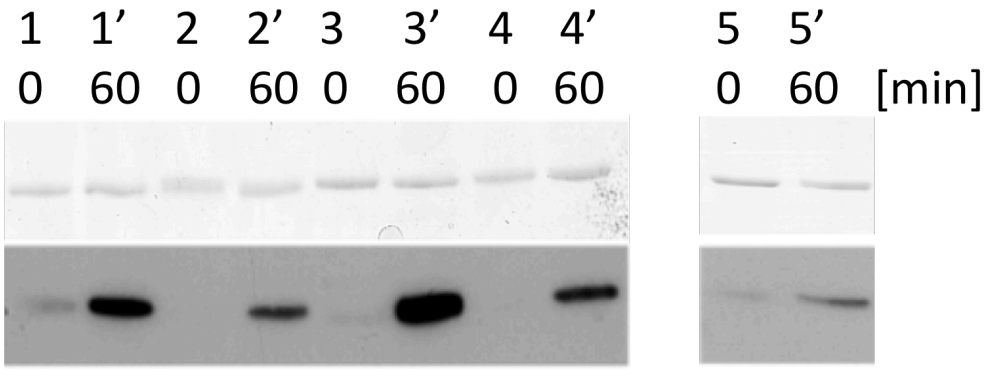

Figure 32: Threonine phosphorylation of singly and co-expressed LmxMPK1 and T224A mutant.
Top panel shows SDS-PA gel, bottom shows result of immunoblot with anti-phosphothreonine antibody. Time incubated with ATP is indicated in min. Lanes 1, 1’, Wild type, singly expressed; 2, 2’, λ-phosphatase co-expressed T224A mutant; 3, 3’, λ-phosphatase co-expressed LmxMPK1; 4, 4’, PTP1B co-expressed LmxMPK1; 5, 5’, singly expressed T224A mutant.

4.4 Analysis of the *in vivo* activity of LmxMPK1 through the use of GFP-tagged mutants

As mentioned in 4.2.4, one of the themes of this project was to generate data to support the hypothesis that LmxMPK1 was regulated in a novel manner by differential phosphorylation of the TDY motif in the activation loop. Various TDY mutants had been generated and expressed in a *L. mexicana LmxMPK1* null mutant background and the growth of these mutants was assessed (Figure 33; Wiese, unpublished). The EDY mutant showed growth that was essentially the same as the WT. The TDF exhibited better growth than the null mutant but not as good as the WT or EDY. The other cell types all displayed similar, slower growth with a final density of 10-20% of the WT by 120 hours.

Mutation of Thr224 was also combined with mutation of the TDY motif to assess whether a phosphomimicking glutamate was able to confer nuclear localisation in mutants that were inactive/showed no nuclear localisation. Thr224 was replaced with an alanine in some constructs to examine if the absence of a phosphothreonine prevented nuclear localisation.

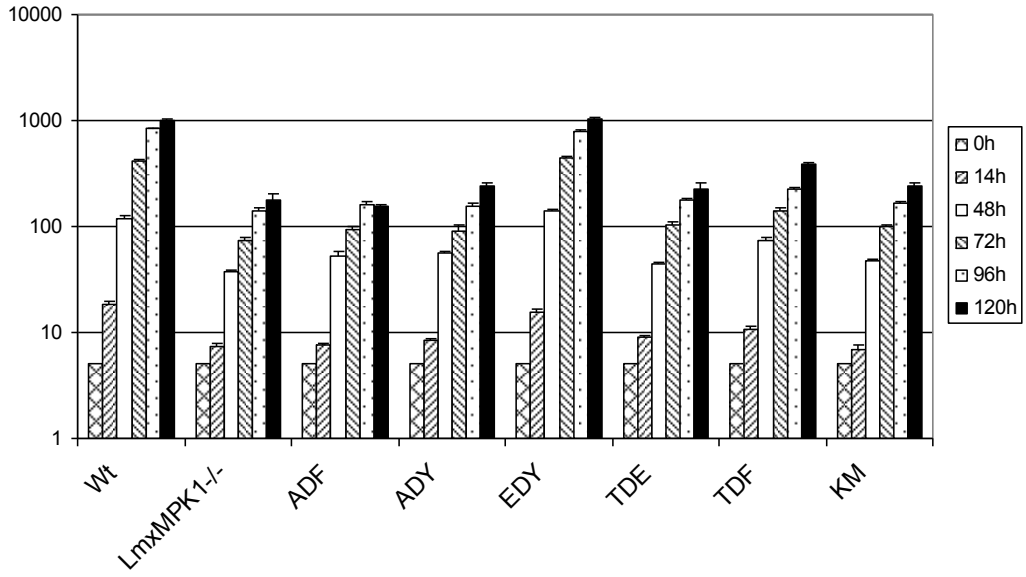

Figure 33: Growth of *L. mexicana* promastigotes.
Wt, wild type; LmxMPK1 -/-, Δ*LmxMPK1*; ADF, ADY, EDY, TDE, TDF & KM: Δ*LmxMPK1::* + pXLmxMPK1(ADF/ADY/EDY/TDE/TDF/KM). (Wiese, unpublished).

4.4.1 Generation of transfection constructs

The generation of the constructs involved multiple cloning steps and is somewhat convoluted. Figure 34 summarises it in an attempt to simplify the steps involved. Only the very last stage is omitted from the figure as it deals with DNA fragments that required different restriction enzymes to release the DNA fragment that encoded the mutation.

pX63polPhleo was cleaved using *Afe*I and *Hin*dIII, the 5207 bp fragment was isolated and treated using Klenow polymerase to fill in the 5'-overhang generated by the *Hin*dIII cleavage. The plasmid was then self-ligated to generate a circular 5207 bp plasmid, designated pX63polPhleoMOD. This removed one of the *Afe*I sites from pX63polPhleo and enabled the other one to be used in subsequent cloning steps.

A plasmid, pMK-MPK1HA, was obtained from Mr Gene (Regensburg, Germany) and cleaved with *Bam*HI to liberate a 635 bp fragment that contained the first 346 bp and last 85 bp of LmxMPK1 linked to a triple haemagglutinin (HA) tag. This fragment was ligated with pX63polPhleoMOD following digestion with *Bam*HI and *Bgl*II to remove a 12 bp fragment; the resulting plasmid was designated pX63polPhleoMODMPK1sHA.

To obtain the DNA coding for Green Fluorescent Protein (GFP) the plasmid pTH6nGFPc was digested sequentially with *Hpa*I and *Pme*I to release a 725 bp fragment. This was ligated with pX63polPhleoMODMPK1sHA, which had been linearised with *Pme*I, thus generating pX63polPhleoMODMPK1sHAgfp.

pX63polPhleoMODMPK1sHAgfp was cleaved with *Afe*I and *Bgl*II to release a 13 bp fragment, the major 6537 bp fragment was then ligated with the 649 bp fragment released by the digestion of the following plasmids with *Afe*I and *Bgl*II: pX5MPK1, pX5lmpkTDF, pX3lmpkADY, pX19lmpkADF, pX4MPK1T to E (EDY), pX1lmpkTDE and pX5lmpkEDF. This resulted in nine new plasmids with the general name pX63polPhleoMODMPK1(**)HAgfp, where ** was replaced with either WT or the activation lip mutation.

Due to difficulties with restriction sites (i.e. extra sites within the target fragment or no cut site) pcDNA3-MPK1 K43➔M, pX5lmpkF93G, pX5lmpkF93GF144L and pQE8W-MPK1F93A were cleaved with *Acc*65I and *Bam*HI to release 562 bp fragments which were ligated with the 6624 bp fragment released from

pX63polPhleoMODMPK1(WT)HAgfp, which had been cleaved with the same restriction enzymes. The resultant plasmids were named in accordance with the preceding paragraph.

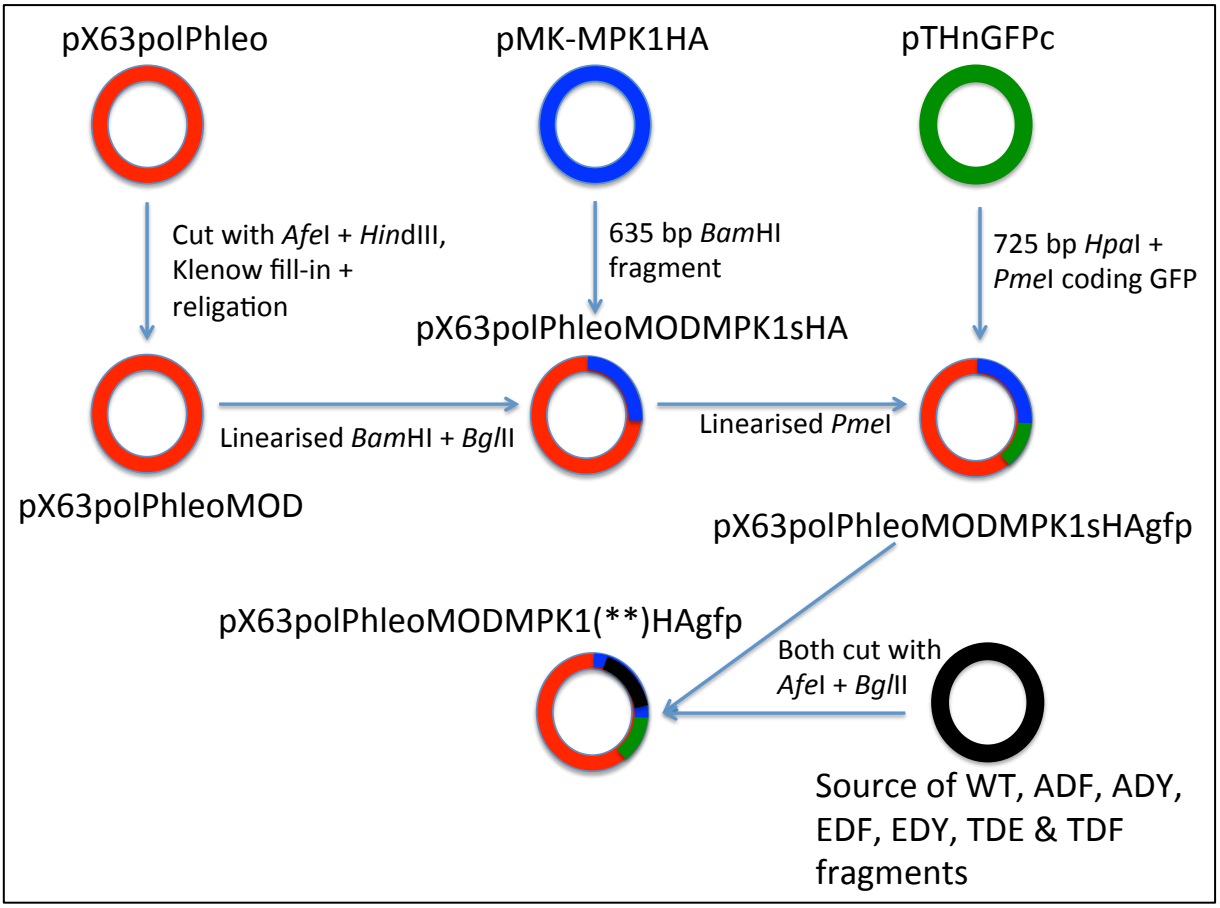

Figure 34: Cloning stages in the generation of GFP-tagged activation lip mutants.

4.4.1.1 T224 transfection constructs

pX63polPhleoMODMPK1(WT)HAgfp was cleaved with *Bgl*II and *Kpn*I. The resulting 6746 bp fragment was ligated with the 444 bp fragment from pUC57-MPK1TA-MKK-DQED and pUC57-MPK1TE-MKK-AQEA (see 4.3.1.1) to give pX63polPhleoMODMPK1(WT)HAgfp (T224A) and pX63polPhleoMODMPK1(WT)HAgfp (T224E).

The plasmids listed in the left column of table 1 were digested with *Bgl*II and *Kpn*I and the 6746 bp fragment was ligated with the 444 bp fragment(s) from the *Bgl*II and *Kpn*I digestion of pUC57-MPK1TA-MKK-DQED and pUC57-MPK1TE-MKK-AQEA (middle column) to generate the plasmid in the right column.

pX63polPhleoMODMPK1(WT)HAgfp	T224A T224E	pX63polPhleoMODMPK1(WT)HAgfp (T224A) pX63polPhleoMODMPK1(WT)HAgfp (T224E)
pX63polPhleoMODMPK1(KM)HAgfp	T224E	pX63polPhleoMODMPK1(KM)HAgfp (T224E)
pX63polPhleoMODMPK1(ADF)HAgfp	T224A T224E	pX63polPhleoMODMPK1(ADF)HAgfp (T224A) pX63polPhleoMODMPK1(ADF)HAgfp (T224E)
pX63polPhleoMODMPK1(ADY)HAgfp	T224A	pX63polPhleoMODMPK1(ADY)HAgfp (T224A)
pX63polPhleoMODMPK1(EDF)HAgfp	T224A	pX63polPhleoMODMPK1(EDF)HAgfp (T224A)
pX63polPhleoMODMPK1(EDY)HAgfp	T224A	pX63polPhleoMODMPK1(EDY)HAgfp (T224A)
pX63polPhleoMODMPK1(TDF)HAgfp	T224A	pX63polPhleoMODMPK1(TDF)HAgfp (T224A)

Table 1: Ligations to generate plasmids for transfection into *L. mexicana*.

4.4.2 Transfection and verification of obtained clones

The plasmids were transfected into an *LmxMPK1* deletion background (Δ*LmxMPK1::*) and three clones were selected for each mutant. The clones were selected for by continuous phleomycin pressure and verification of protein expression by fluorescent microscopy of live cells. The most fluorescent clone for each mutant was chosen for use in the growth curves. To confirm that GFP-tagged LmxMPK1 was being expressed an immunoblot was performed on cell lysates using an HRP-conjugated anti-GFP monoclonal antibody (130-091-833, Miltenyi, UK). The result of the immunoblot (Figure 35) shows a band of the expected size (68.8 kDa) for GFP (26.8 kDa) linked LmxMPK1 (42 kDa) for all clones. This shows that the fluorescence seen in cells is indeed tagged protein and not GFP alone.

2×10^7 cells were heated at 98°C for 10 min in *Leishmania* Lysis Buffer, cooled on ice for min then resolved by SDS-PAGE. Δ*PK4*:: + rPK4-eGFP cells were included as a positive control (lane 1). The gel was blotted onto a PVDF membrane, blocked for one hour at 37°C in Milk Powder/PBST then incubated for one hour at 37°C with the HRP-conjugated anti-GFP antibody (1:2500). The membrane was washed 3 times in PBST and 2 times in PBS then developed using chemiluminescence. The membrane

was then stripped and re-probed using an anti-IPS antibody (1:500 primary, 1:5000 goat anti-rabbit secondary) to illustrate loading between lanes.

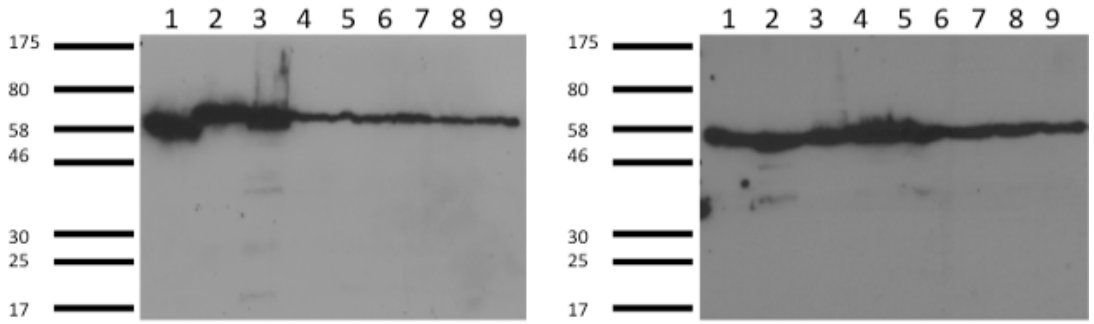

Figure 35: Immunoblot of *L. mexicana* cells expressing GFP-tagged LmxMPK1 mutants.Left panel shows immunoblot with anti-GFP antibody and right panel shows immunoblot with anti-IPS antibody. Molecular masses of standard proteins are indicated in kDa.
Lane 1, ΔPK4:: + rPK4-eGFP (positive control); (Lanes 2 – 9 were Δ*LmxMPK1::* with pX63polPhleoMODMPK1(**)Hagfp). 2, WT; 3, KM; 4, ADF; 5, ADY; 6, EDF; 7, EDY; 8, TDE; 9, TDF.

4.4.3 Localisation of LmxMPK1 mutants

Following transfection and verification of expression, localisation of the kinase was carried out using fluorescence microscopy. Cells were immobilised on poly-L-lysine treated microscopy slides and imaged at 100x magnification using a Nikon TE2000S inverted microscope and observed with a CFI Plan Fluor DLL-100X oil N.A. 1.3 objective lens. Images were captured using a Hamamatsu Orca-285 Firewire digital charge-coupled device camera and processed using ImageJ (NIH, USA). The image background was subtracted using a rolling ball radius of 1 pixel with the options to "Create background" and "Light background" selected. False colour was added using the Lookup Table setting.

Wild type kinase (Figure 36-top panels) exhibited diffuse localisation but with punctate aggregations. The WT-T224A mutant (Figure 36-middle panels) was not diffuse, it was principally concentrated as a "ring" around the nucleus. The WT-T224E (Figure 36-bottom panels) also showed the ring around the nucleus, although it had additional accumulations in "spots" and larger cellular structures.

The kinase dead mutant (K43M) (Figure 37-top panels) is localised to the cytoplasm and a dark spot is seen where the nucleus is. The KM-T224E mutant (Figure 37-bottom panels) displays a reticulate pattern with some spots also visible.

The activation lip mutant ADF (Figure 38-top panels) shows a diffuse distribution with punctate accumulation in cells. Both the T224A (Figure 38-middle panels) and T224E (Figure 38-bottom panels) ADF double mutants form a ring and show an accumulation in another cellular structure.

The ADY mutant (Figure 39-top panels) is distributed throughout the cell. The ADY-T224A (Figure 39-bottom panels) shows a ring-like accumulation around the nucleus in addition to some other large spots.

The LmxMPK1(EDF) is diffuse throughout the cell (Figure 40), however punctate spots are also seen.

The LmxMPK1(EDY) mutant shows diffuse localisation with spots throughout the cell (Figure 41-top panels). The EDY-T224A mutant (Figure 41-bottom panels) is less diffuse and forms a ring in addition to the spots.

Localisation of the TDE mutant (Figure 42) is diffuse with spots throughout the cell.

Finally, the TDF exhibits a diffuse but with spots localisation (Figure 43-top panels). The TDF-T224A mutant forms a ring around the nucleus but is also reticulate (Figure 43-bottom panels).

Although the principal aim of this microscopy was to examine the impact of the various mutations (activation lip and T224) on kinase localisation, the brightfield images of the cells also revealed alterations in cell morphology for the T224 mutants. Cells expressing kinase with a T224 mutation (A or E) were shorter and wider than cells with only a mutation in the TDY motif.

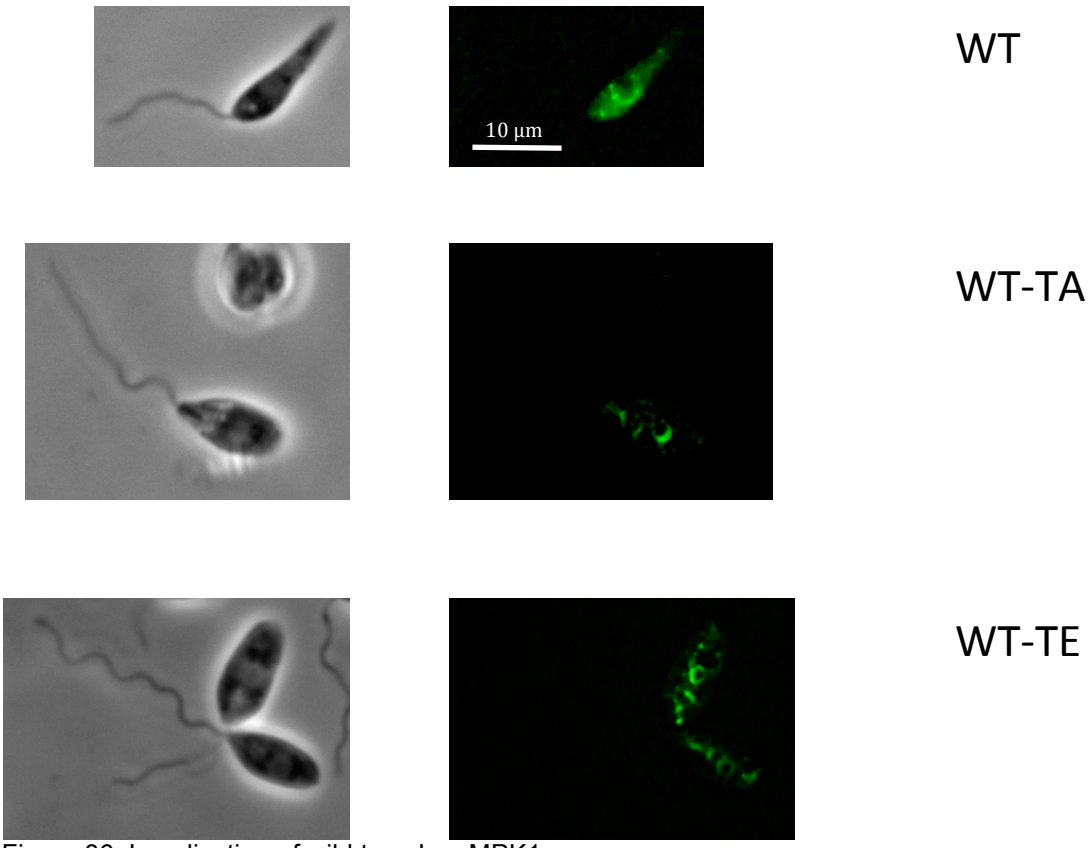

Figure 36: Localisation of wild type LmxMPK1.
Top panels, ΔLmxMPK1::LmxMPK1HAGFP; Middle, ΔLmxMPK1::LmxMPK1(T224A)HAGFP; Bottom, ΔLmxMPK1::LmxMPK1(T224E)HAGFP.
Left panels show brightfield, right panels are fluorescence micrographs.

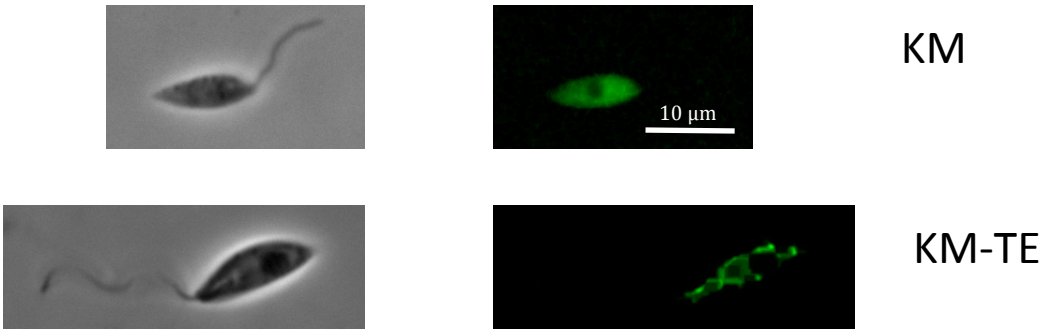

Figure 37: Localisation of LmxMPK1(K43M).
Top panels, ΔLmxMPK1::LmxMPK1(K43M)HAGFP;
Bottom panels, ΔLmxMPK1::LmxMPK1(K43M-T224E)HAGFP.
Left panels show brightfield, right panels are fluorescence micrographs.

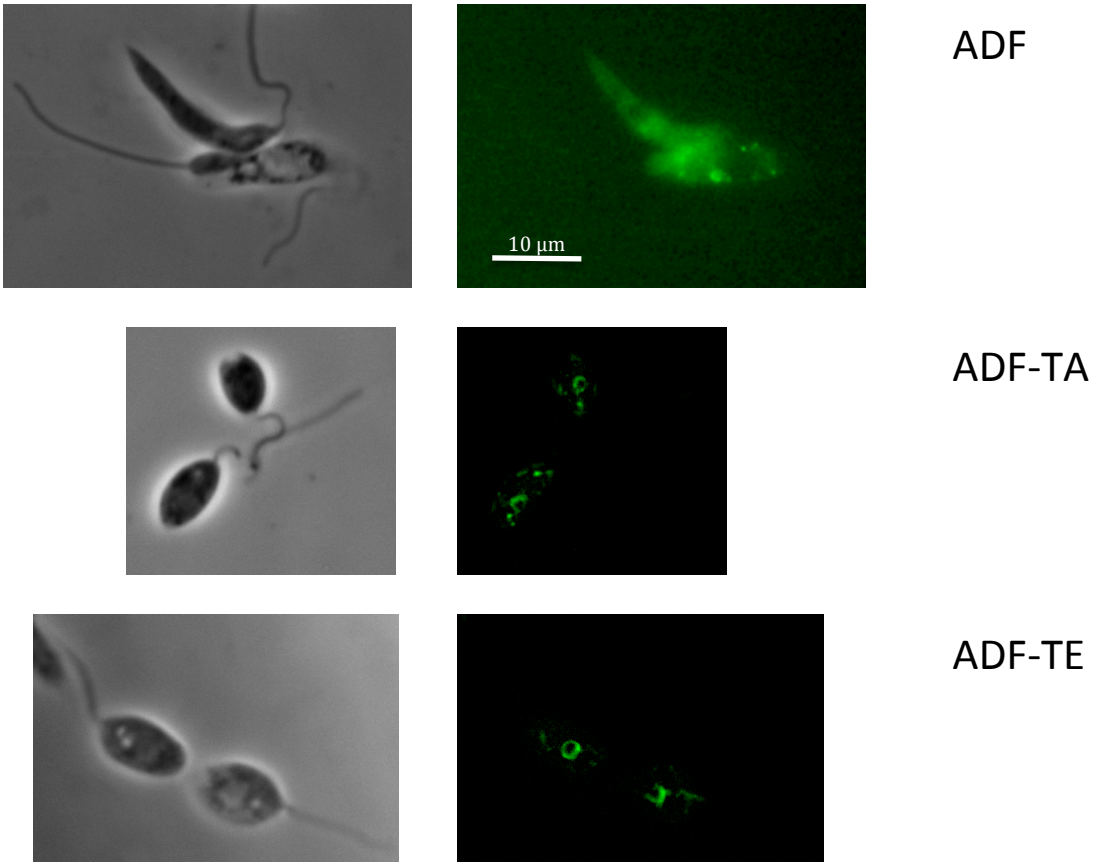

Figure 38: Localisation of LmxMPK1(ADF).
Top panels, ΔLmxMPK1::LmxMPK1(ADF)HAGFP;
Middle, ΔLmxMPK1::LmxMPK1(ADF-T224A)HAGFP;
Bottom, ΔLmxMPK1::LmxMPK1(ADF-T224E)HAGFP.
Left panels show brightfield, right panels are fluorescence micrographs.

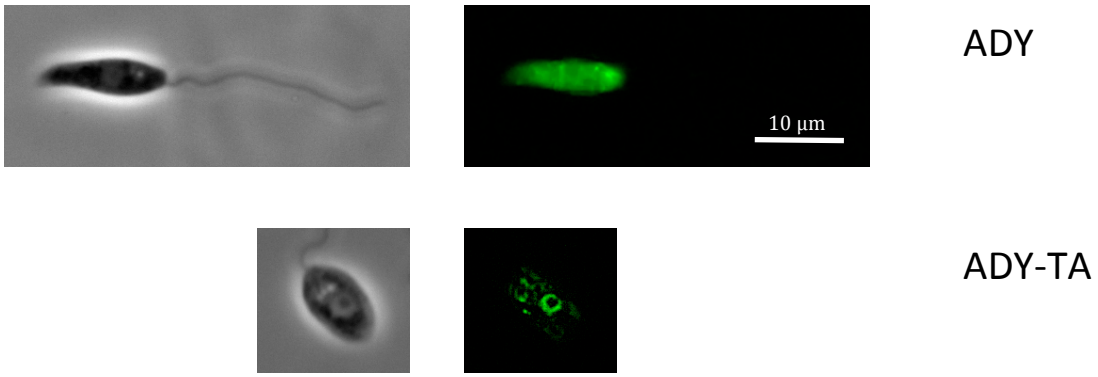

Figure 39: Localisation of LmxMPK1(ADY).
Top panels, ΔLmxMPK1::LmxMPK1(ADY)HAGFP;
Bottom, ΔLmxMPK1::LmxMPK1(ADY-T224E)HAGFP.
Left panels show brightfield, right panels are fluorescence micrographs.

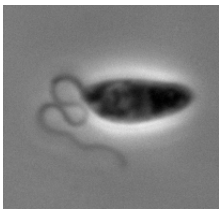

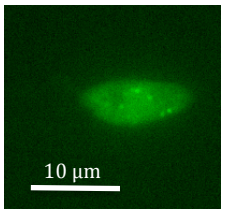

EDF

Figure 40: Localisation of LmxMPK1(EDF).
ΔLmxMPK1::LmxMPK1(EDF)HAGFP.
Left panels show brightfield, right panels are fluorescence micrographs.

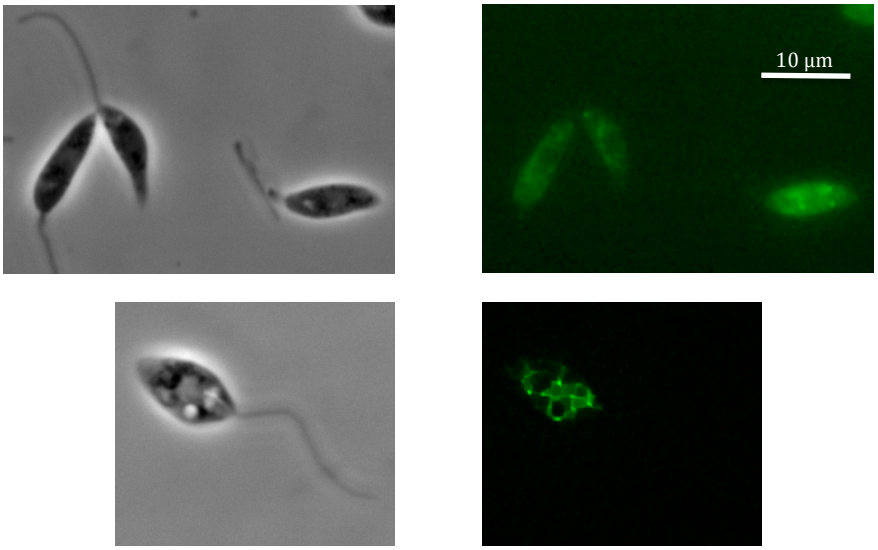

Figure 41: Localisation of LmxMPK1 (EDY).
Top panels, ΔLmxMPK1::LmxMPK1(EDY)HAGFP;
Bottom, ΔLmxMPK1::LmxMPK1(EDY-T224E)HAGFP.
Left panels show brightfield, right panels are fluorescence micrographs.

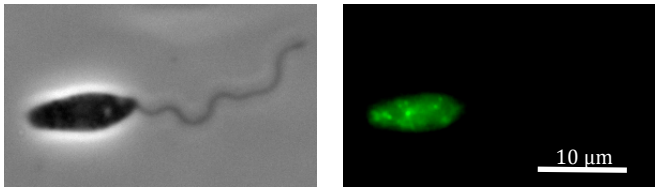

Figure 42: ΔLmxMPK1::LmxMPK1(TDE)HAGFP parasites.
Left panel shows brightfield, right panel is fluorescence micrograph.

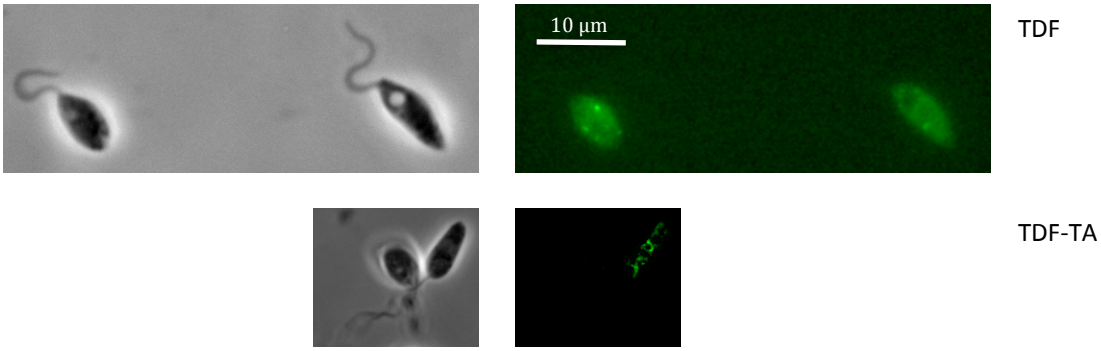

Figure 43: Localisation of LmxMPK1(TDF).
Top panels, ΔLmxMPK1::LmxMPK1(TDF)HAGFP;
Bottom, ΔLmxMPK1::LmxMPK1(TDF-T224E)HAGFP.
Left panels show brightfield, right panels are fluorescence micrographs.
.

4.5 LmxPTP: a *Leishmania mexicana* phosphatase

LmxPTP (accession number LmxM.05.0280, uniprot identifier E9AKD3) is encoded by a 675 bp gene, it is 224 amino acid in size, has a calculated molecular weight of 24.999 kDa and an isoelectric point of 9.69. It has a high degree of similarity to homologues in other *Leishmania* species: 92% to *L. donovani* and *L. infantum*, while *L. major* is 91% (Blast search on http://uniprotkb.org). Other trypanosomatid species are less similar: *T. cruzi* has a phosphatase with 66% similarity and *T. cruzi* has one with 61%. The most similar human proteins are PTP-like protein B (PTPLB) and PTPLA with a 37% and 34% match respectively. Intriguingly, PTPLA and PTPLB are not believed to have phosphatase activity and the trypanosomatid homologues of LmxPTP (listed above) have been classed as PTP-like (Andreeva & Kutuzov, 2008). (See appendix for sequence and alignment with homologues).

4.5.1 Localisation of LmxPTP *in vivo*

An extra-chromosomal copy of LmxPTP with a green fluorescent protein tag was used to visualise the sub-cellular location of the phosphatase.

4.5.1.1 Generation of transfection construct

The restriction enzymes *Eco*RI and *Eco*RV were used to liberate a 685 bp fragment from pCR2.1TOPO-LmxPTP that was then ligated with a 7690 bp fragment obtained by digesting pTH6nGFPc with *Mfe*I and *Hpa*I. This gave the plasmid pTH6nGFPc-LmxPTP, which was electroporated into wild type *Leishmania mexicana.*

4.5.1.2 Transfection and verification of obtained clones

The plasmid pTH6nGFPc-LmxPTP was transfected into wild type *L. mexicana* promastigotes and nine clones were selected. The clones were selected for by continuous hygromycin pressure and verification of protein expression by fluorescence microscopy of live cells. The three most fluorescent clones were chosen for use in microscopy.

4.5.1.3 Localisation of LmxPTP

Following transfection and verification of expression, localisation of the phosphatase was carried out using fluorescence microscopy as described in 4.4.3.

Figure 44 shows the results of fluorescence microscopy with *L. mexicana* + pTH6nGFPc-LmxPTP. All cells show a similar pattern of fluorescence “weaving” through the cell, with a particular accumulation around the nucleus.

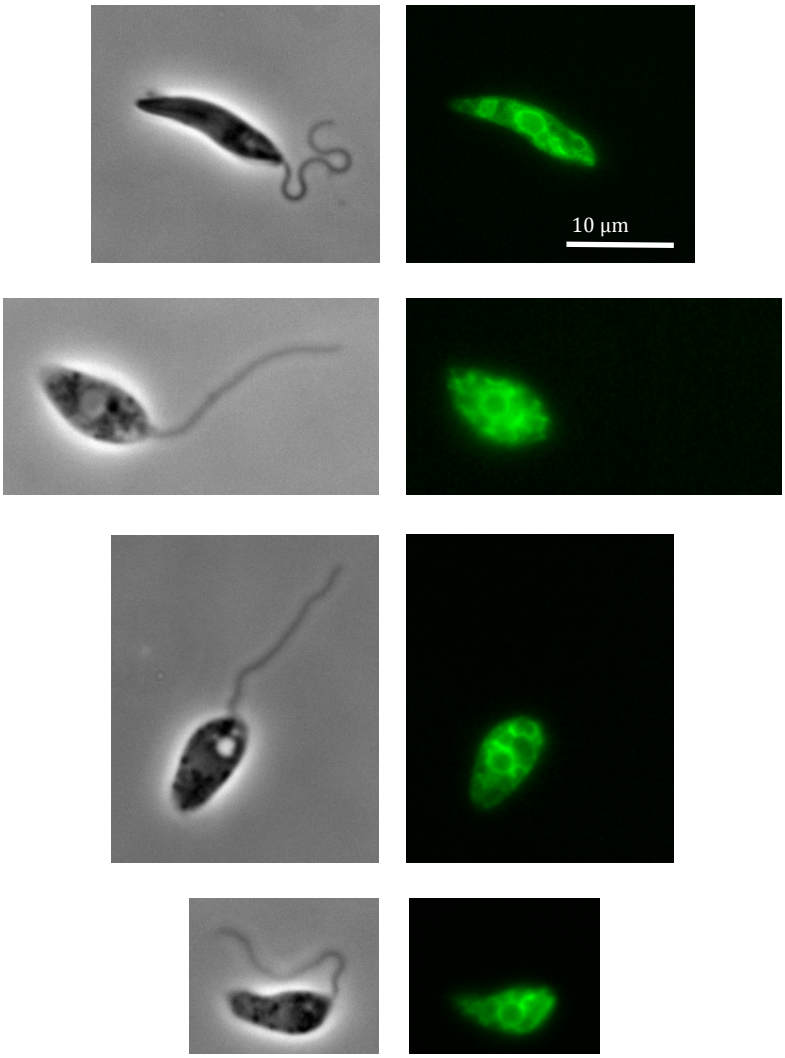

Figure 44: *Leishmania mexicana* cells expressing C-terminally GFP-tagged LmxPTP. Left panels show brightfield, right panels are fluorescence micrographs.

4.5.2 Deletion of *LmxPTP*

In order to assess the essentiality of LmxPTP to *L. mexicana* fragments of DNA that could homologously recombine with genomic DNA at the site of the gene for LmxPTP were generated. Instead of coding for LmxPTP the DNA fragments encode a resistance marker.

4.5.2.1 Generation of deletion construct

A plasmid pUC57-delLmxPTP was obtained from Proteogenix (Oberhausbergen, France). This contained the 327 bp upstream and 329 bp downstream DNA from the gene encoding LmxPTP. The plasmid was cleaved with *Nco*I and *Nhe*I and the 2333 bp fragment was ligated with two different resistance markers. The first ligation was with the 377 bp fragment generated by cleaving pCR2.1-Phleo with *Avr*II and *Nco*I to give pUC57-delLmxPTP-Phleo. The second ligation was with the 800 bp fragment from the cleavage of pCR2.1-Neo with *Bsp*HI and *Nhe*I to give pUC57-delLmxPTP-Neo.

Both pUC57-delLmxPTP-Phelo and pUC57-delLmxPTP-Neo were cleaved with *Eco*RV to liberate the DNA fragments for use in electroporation of wild type *L. mexicana*; these were named delLmxPTP-Phleo and delLmxPTP-Neo, respectively.

4.5.2.2 Transfection and verification of clones

The DNA fragments (4.5.2.1) were transfected into wild type *Leishmania mexicana* either one after another (first delLmxPTP-Neo, then delLmxPTP-Phleo) or simultaneously. Three clones were selected from each transfection by continuous antibiotic selection.

To confirm absence of the LmxPTP gene a PCR was performed using the LmexPTP.for and LmexPTP.rev primers (Figure 45) Wild type cells were used as a positive control (Lane 1). It was not possible to delete all alleles of the *LmxPTP* gene, although all lanes show a reduction in *LmxPTP* (with the exception of Lane 3). This is suggestive of polyploidy for the gene – a characteristic that has been observed for other *Leishmania* genes (see discussion).

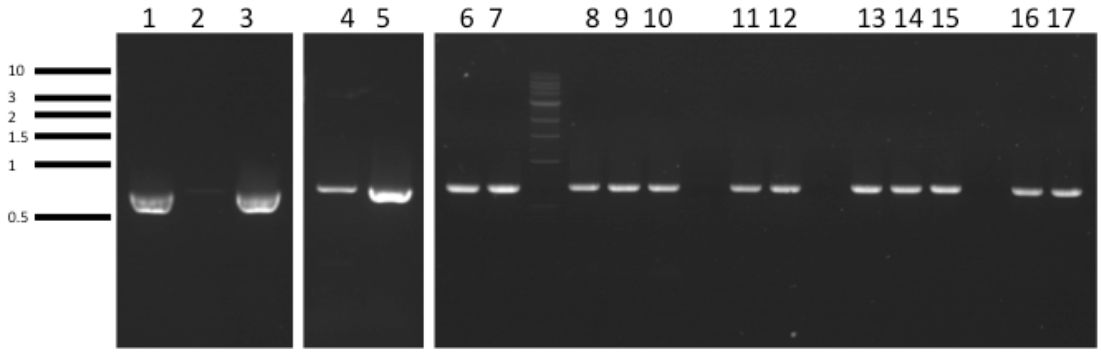

Transfection type	**Gel lanes**
Single Neomycin transfection (+/-)	5, 6, 7
Neomycin transfection followed by Phleomycin transfection	4, 8, 9, 10, 13, 14, 15, 16, 17
Phleomycin & Neomycin transfections simultaneously	2, 3, 11, 12

Figure 45: PCR of cells transfected with LmxPTP deletion fragments. Lane 1, WT0906; 2, Δ*LmxPTP* -/- Neo/Phleo F9; 3, Δ*LmxPTP* -/- Neo/Phleo D8; 4, Δ*LmxPTP* -/- Neo E11, Phelo C3; 5, Δ*LmxPTP* +/- Neo E11; 6, Δ*LmxPTP* +/- Neo B1; 7, Δ*LmxPTP* +/- Neo D5; 8, Δ*LmxPTP* -/- Neo B1, Phleo D2; 9, Δ*LmxPTP* -/- Neo B1, Phleo B10; 10, Δ*LmxPTP* -/- Neo B1, Phleo G7; 11, Δ*LmxPTP* -/- Neo/Phleo F5; 12, Δ*LmxPTP* -/- Neo/Phleo G4; 13, Δ*LmxPTP* -/- Neo D5, Phelo G6; 14, Δ*LmxPTP* -/- Neo D5, Phelo G5; 15, Δ*LmxPTP* -/- Neo D5, Phelo B6; 16, Δ*LmxPTP* -/- Neo E11, Phelo F10; 17, Δ*LmxPTP* -/- Neo E11, Phelo C6. Characters following fragments name indicate clone name. Sizes of standard DNA fragments are indicated in kilobases.

5 Discussion

5.1 Optimisation of an inhibitor-sensitised system for specific inhibition of LmxMPK1

Although it is possible to delete the gene for LmxMPK1 from the genome of the promastigote stage of the parasite (Wiese, 1998), this approach only gives information about the viability of the parasites in the absence of the protein. It does not give any indications as to what the substrates of LmxMPK1 are nor can it account for compensatory mechanisms that occur in the cell after an extended period without the protein. The use of RNAi is an obvious solution to this issue; however, only members of the *Viannia* subgenus of *Leishmania* possess the components of the RNAi pathway necessary to make this a viable option (*L. mexicana* is not part of the *Viannia* subgenus) (Lye *et al.*, 2010; Kolev *et al.*, 2011). The inhibitor-sensitive system allows this hurdle to be overcome; however retention of kinase activity and successful inhibition of kinase activity with the small molecule inhibitor is not assured (Zhang *et al.*, 2005). The initial development of the inhibitor-sensitive system relied on the mutation of the "gatekeeper" residue in the ATP binding pocket to a small glycine or alanine that would allow entry of the small inhibitor molecule (Bishop *et al.*, 2000). For v-Src this residue is isoleucine-338 (Bishop *et al.*, 2000), which corresponds to phenylalanine-93 in LmxMPK1, threonine-116 in LmxMPK3 (Erdmann, 2009) and methionine-111 in LmxMPK4 (John von Freyend, 2010b). Previous work in the Wiese group using GST-tagged LmxMPK1F93G demonstrated the potential to use this system in protozoan parasites (Melzer, 2007). As described in 4.1.1 we sought to determine whether substituting phenylalanine-93 for an alanine (instead of a glycine, as had previously been done) would affect kinase autophosphorylation and MBP phosphotransferase activity. We also wished to examine if substituting phenylalanine-144 for a leucine would stabilise the F93G mutant (LmxMPK1F93GF144L) as it has been shown that altering the gatekeeper residue can interfere with the tertiary structure of kinases and a second mutation can be required to stabilise the kinase (Zhang *et al.*, 2005).

As expected, wild type LmxMPK1 showed no sensitivity to any of the inhibitors (Figure 9). As with the GST-tagged kinase His-LmxMPK1F93G was active and amenable to concentration-dependent inhibition *in vitro* (Figure 10). 1Na showed the greatest inhibition at the lowest concentration; 10 µM 1Na reduced MBP

phosphorylation more than 10 μM of 1Nm did, whereas the same concentration of 2Nm only slightly inhibited MBP phosphorylation. 100 μM of 1Nm had no effect on autophosphorylation and inhibited MBP phosphorylation to the same (minimal) extent as 10 μM. Conversely, 100 μM of 1Na and 1Nm reduced autophosphorylation and completely inhibited MBP phosphorylation. As 1Na showed the greatest potential for inhibiting LmxMPK1F93G it was decided to use it in cell growth studies.

The kinase mutant in which phenylalanine-93 was replaced with an alanine residue (LmxMPK1F93A) displayed a similar trend of activity and inhibition with regards to autophosphorylation (Figure 11). However, only weak MBP phosphorylation could be detected for kinase incubated with DMSO alone, which was also the case for kinase incubated with 1 μM 1Na. For 10 μM 1Na even weaker MBP phosphorylation occurred, with no MBP phosphorylation observable at higher concentrations of 1Na, nor for any concentration of 1Nm or 2Nm. This suggests that the replacement of phenylalanine-93 with an alanine decreases the phosphotransferase activity of LmxMPK1 and that the F93G mutation is better suited for maintaining kinase activity while introducing susceptibility to the small molecule inhibitors. However, as MBP was used as a substrate in the absence of the as yet unknown *in vivo* substrate it is possible that phosphotransferase activity would be higher. For this reason it was decided to examine the effect of 1Na on Δ*LmxMPK1 L. mexicana* cells expressing LmxMPK1F93A.

The introduction of a second mutation to the F93G inhibitor-sensitised LmxMPK1 at phenylalanine-144 (LmxMPKF93GF144L) resulted in improved sensitivity to inhibition (Figure 12): even at the lowest tested concentrations of inhibitors a decrease in autophosphorylation was observed and sensitivity to 2Nm was seen. However, phosphorylation of MBP does not occur to the same extent seen for wild type kinase (Figure 9) or LmxMPK1F93G (Figure 10). Although it would have been interesting to test the effect of 2Nm *in vivo*, it was decided to only use 1Na, as this was the only inhibitor that consistently affected recombinant, inhibitor-sensitised mutants of LmxMPK1.

Expression of the three inhibitor-sensitised kinases linked to a C-terminal triple HA-GFP tag in an LmxMPK1 deletion background (Δ*LmxMPK1*) and incubation with varying concentrations of 1Na generated results that were broadly consistent with

what had been observed *in vitro* (Figure 13). After 5 days of growth in the presence of inhibitor, wild type *L. mexicana* (WT) exhibits growth of approximately 90% (relative to cells without inhibitor) for both 1 μM and 10 μM; however, although it is statistically significant, the standard deviation is too large for it to be considered relevant. This is somewhat in contrast to previous work (Melzer, 2007) where incubation of WT cells with 10 μM 1Na for 4 days resulted in 60% growth, relative to cells grown in the absence of inhibitor. This may be explained by the different batches of 1Na used: previous work used 1Na that had been synthesised by a collaborator (K Shah, Purdue University, USA) whereas the 1Na used in this study had been purchased from a commercial vendor (Tocris Bioscience, UK). However, the result in this study is more consistent with what would be expected and is encouraging for future work.

The F93G inhibitor-sensitised mutant shows promising susceptibility to *in vivo* selective inhibition by 1Na. After 5 days incubation with both 1 μM and 10 μM of inhibitor the cells show relative growth of approximately 55%. One of the most interesting aspects of this is an increase in inhibitor concentration of one order of magnitude only results in a slight decrease in growth. This suggests that use of 1 μM of inhibitor is sufficient to obtain valid *in vivo* results, excluding off-target effects as 1 μM of 1Na did not affect WT cells. The F93G results that were obtained in this work are not fully congruent with Melzer's work. They found that 0.1 μM, 1 μM and 10 μM of 1Na all inhibited growth to below 50% of the control, with 10 μM reducing growth to only 20% of the control. As described above, the most likely explanation for this discrepancy is the different batches of inhibitor that were used.

The results from the F93A mutant of LmxMPK1 were disappointing, although they did show that the F93G mutation was optimal for sensitisation to 1Na. Although cells grown in the presence of 10 μM 1Na showed growth of 80.2% compared to cells grown without inhibitor, this is with a standard deviation of ±9.5% and is not very impressive when considering that WT cells show growth of 88.6 ± 9.1% after 5 days in 10 μM of 1Na. Thus it seems reasonable to conclude that LmxMPK1F93A has little further value in inhibitor-sensitised studies.

The double mutant (LmxMPK1F93GF144L) is more susceptible than the F93A mutant to selective inhibition, although it does not perform as well as the single F93G

mutant. After 5 days incubation with inhibitor growth was 74.2 ± 3.4% and 65.2 ± 6.2% for cells grown in 1 μM and 10 μM of 1Na, respectively. Statistical analysis showed that there was a significant difference between these two results, which suggests that greater growth inhibition could be achieved using higher concentrations of inhibitor. However, this would have the disadvantage of higher concentrations of 1Na potentially affecting the WT (in experiments carried out in tandem with the same concentration of inhibitor), especially when the F93G mutant showed such strong performance at the lower concentration of 1 μM.

These results allow the conclusion to be drawn that the F93G mutation is the optimal mutation for creating inhibitor-sensitised LmxMPK1 as it retains a high degree of enzymatic activity when uninhibited and is amenable to inhibition both *in vitro* and *in vivo*.

The maximum effect that one would expect to observe for successful and specific inhibition of IS-LmxMPK1 is a decrease in growth to the level of the null mutant. Previous work in the Wiese group had examined the growth kinetics of the *LmxMPK1(-/-)* deletion mutant compared to wild type promastigote cells (Figure 33: Wiese, unpublished). The growth curve was started by inoculating SDM-79 medium with 5 x 10^5 cells/ml; 14 hours later the null mutant culture contained 60% less cells than the wild type, by 48 hours this had increased to 68% fewer cells and at the time points thereafter (72 h, 96 h and 120 h) there were 82% fewer cells in the null mutant culture than the wild type culture. This suggests that the maximum achievable level of growth inhibition in promastigotes using the IS system is approximately 80%. For the amastigote stage, catalytically active LmxMPK1 is essential and parasites lacking the protein are not viable, thus the IS system could be used to examine the effects of ablating LmxMPK1 activity at various points during differentiation from promastigotes to amastigotes and during proliferation of amastigotes. This could be done both for axenic amastigotes (those induced to differentiate by altering the pH and temperature of their environment) and for IS-LmxMPK1 expressing parasites used to infect macrophages.

The inhibitor-sensitised system has several applications that can be utilised to discover various aspects of the role of the sensitised kinase in the cell. These include metabolomics, phosphoproteomics and substrate identification.

Metabolomics is the study of the metabolic profile of an organism and entails monitoring the change in all or specific metabolites following an alteration in the cellular environment. The use of the inhibitor-sensitised system makes it possible to monitor the metabolic changes that occur in a cell following inactivation of the kinase of interest. This is preferable to deleting the kinase's gene from the genome and having to wait for up to 14 days to have confirmation of its absence and enough cells to analyse the metabolites. In the intervening time period the cells may have adapted to the loss of the kinase and compensated for the missing component(s) in the cell's signalling pathway(s) (Bishop *et al.*, 2000). The metabolic analysis of cells following specific kinase inhibition is likely to give indications as to what processes the kinase is involved in regulating.

Phosphoproteomic analysis of cells following specific inhibition of the kinase of interest would enable the identification of potential substrates of the kinase. A decrease in phosphorylation of particular proteins would be highly suggestive that they are the substrate(s) of the kinase of interest. The use of the inhibitor-sensitised system for phosphoproteomics has many of the same advantages as using it for metabolomics, specifically the shorter time period between inhibition of the kinase and analysis of the effect on the cell when compared to traditional gene deletion followed by analysis (Bishop *et al.*, 2000). The inhibitor-sensitised kinase system also has the advantage that it can be used to study the role of essential kinases, that is, kinases where deletion of the gene is fatal to cells. In these cases the inhibitor-sensitive kinase can be used to replace the genes for the kinase of interest and the effect of inhibition can be studied in the period before cell death (Bishop *et al.*, 2001; John von Freyend, 2010b).

Inhibitor-sensitised kinases can also be used in the search for the natural substrate of the kinase of interest (Kumar *et al.*, 2004; Blethrow *et al.*, 2008). This can be particularly useful if metabolomics data has been inconclusive or if phosphoproteomics has been unable to detect the substrate peptide. To do this a dephosphorylated wild type cell lysate is incubated with the inhibitor-sensitive kinase and an ATP analogue that can only be utilised by the inhibitor-sensitive kinase (Blethrow *et al.*, 2008). The ATP analogue is ATP that has been altered by the substitution of a benzyl group for the amine group normally present at N^6 in the adenine ring of ATP, this allows it to only be used by kinases where the gatekeeper

has been modified to a smaller amino acid. Substrates of the kinase are labelled by the transfer of a thiol group that has been generated by the replacement of an oxygen in the γ-phosphoryl of ATP (Blethrow *et al.*, 2008). Labelled substrates can then be purified from the reaction mix using iodoacetyl-agarose and elution with Oxone. They can then be identified by mass spectrometry. This technique has a particular advantage over the incubation of a large quantity of wild type recombinant kinase with a cell extract and "normal" ATP, namely that the result is not compromised by the possibility of autophosphorylation among kinases present in the lysate.

It would also be possible to use the GFP-tag to visualise the inhibitor-sensitised kinase in cells before and after addition of the specific inhibitor (here 1Na) to examine the effect on kinase localisation. When results that are discussed in 5.3 are considered, it seems probable that inhibition of the kinase would lead to a change in localisation. Furthermore, the effect of "washing out" the inhibitor afterwards could also be tested to see if the kinase localisation reverts to what was observed previously.

5.2 Dephosphorylation of LmxMPK1

LmxMPK1 is phosphorylated on tyrosine-178 of the TDY motif and threonine-224 (46 residues away from the TDY motif) when purified from *E. coli*. As MAP kinase activity in higher eukaryotes is modulated by phosphorylation on the threonine and tyrosine of the TDY motif, dephosphorylated kinase was needed to examine autophosphorylation and substrate phosphorylation dynamics. Although attempts had been made to dephosphorylate recombinant LmxMPK1 *in vitro* using commercial λ-phosphatase, these had proven inconsistent and it would have been expensive to use the quantities required to guarantee dephosphorylation of large quantities of recombinant LmxMPK1. Thus, LmxMPK1 was expressed in the two gene co-expression plasmid, pJC-duet (John von Freyend *et al.*, 2010a) with one of three phosphatases: the dual-specificity Lambda-phosphatase (λ-phosphatase), human Protein-Tyrosine Phosphatase-1B (PTP1B) and a novel *Leishmania mexicana* PTP homologue, LmxPTP (LmxM.05.0280). The phosphatases were expressed with a triple-haemagglutinin (HA) tag to enable separate purification if that were desired at a later date. The effect of the triple-HA tag was tested by generating two plasmids for

each phosphatase, with the triple-HA tag at either the C- or N-terminus of the phosphatase.

Following purification of LmxMPK1 co-expressed with the differentially tagged phosphatases, tyrosine phosphorylation was examined using the anti-phosphotyrosine monoclonal antibody, 4G10. This showed that N-terminally tagged PTP1B was superior in dephosphorylating LmxMPK1 to its C-terminally tagged version (Figure 15); that C-terminally tagged λ-phosphatase was better than N-terminally tagged (Figure 16) and that C-terminally tagged LmxPTP performed better than N-terminally tagged (Figure 17). Unexpectedly, the ability to autophosphorylate on tyrosine in subsequent kinase assays was not ablated by dephosphorylation of the kinase, which is unusual as autophosphorylation often requires the presence of a scaffold protein such as Ste5 for Fus3 autophosphorylation (Bhattacharyya *et al.*, 2006) and TAB1 (transforming growth factor-beta-activated protein kinase 1 (TAK1)-binding protein 1) for p38 autophosphorylation (Ge *et al*., 2002).

Threonine phosphorylation was also tested using an anti-phosphothreonine antibody, 71-8200 (Invitrogen, UK) (Figure 18). This confirmed that singly expressed LmxMPK1 is threonine phosphorylated when purified from *E. coli*, although no threonine phosphorylation was detected for kinase co-expressed with either λ-phosphatase or PTP1B. While it was expected that co-expression with λ-phosphatase would remove threonine phosphorylation it was not expected for kinase co-expressed with PTP1B. (Potential explanations for this are discussed below).

Co-expressed kinase activity was then assessed using two different types of kinase assays. The first, a time course assay, measured autophosphorylation and Myelin Basic Protein (MBP) phosphorylation over time by incubating the kinase with MBP and γ-^{32}P ATP in kinase assay buffer for various periods of time, stopping the reaction by heating to 95°C then separating the kinase and MBP by SDS-PAGE. Incorporation and transfer of ^{32}P was visualised by autoradiography and attempts were made to correct discrepancies in protein loading using ImageJ. The second, a pre-incubation assay, required incubation of the kinase alone with non-radiolabelled ATP for different lengths of time, removing this ATP and then incubating the kinase with MBP and γ-^{32}P ATP in kinase assay buffer for 10 min – regardless of how long

the pre-incubation was. ^{32}P incorporation was analysed in the same manner as for the time course assays.

Time course assays using singly expressed kinase (Figure 19) showed that it behaved in the same manner as had previously been observed (Melzer, 2007). The kinase autophosphorylated and phosphorylated MBP – although phosphorylation of the latter began after a short delay. ImageJ analysis (Figure 23) confirmed gradual autophosphorylation that plateaus after 20-30 min. MBP phosphorylation starts slowly but increases steadily from 10 min onwards, then reaches a maximum at 60 min. Although the autoradiograph (Figure 19) shows an increase in signal for both LmxMPK1 and MBP between 60 and 80 min, it is most likely due to the larger quantities of kinase and MBP present, as seen on the SDS-PA gel.

Immunoblots using anti-phospho amino acid antibodies had already shown that autophosphorylation of dephosphorylated LmxMPK1 occurs; this was confirmed in the time course assays (Figures 20, 21 and 22). However, dephosphorylated LmxMPK1 had a longer delay before MBP phosphorylation commenced.

LmxMPK1 co-expressed with either of the tyrosine-phosphatases (PTP1B and LmxPTP) appears to have reached maximum MBP phosphorylation after 40-60 min (although there is a higher value for 80 min PTP1B, this is likely to be an error from the adjusting process: both 60 and 80 min have very strong signals but both appear to be the maximum that the film can detect, thus adjusting the signal based on protein loading is redundant). λ-phosphatase co-expressed LmxMPK1 takes longer to reach maximum autophosphorylation and MBP phosphorylation takes longer to begin than LmxMPK1 singly expressed or with a tyrosine-phosphatase. This suggests that phosphorylation of threonine-224 may have a role in controlling LmxMPK1 autophosphorylation kinetics and/or substrate phosphorylation.

The work in this section was designed to help either confirm or refute an observation made by a previous member of the laboratory in their thesis (Melzer, 2007), namely that extended, intramolecular, autophosphorylation of LmxMPK1 results in slower substrate phosphorylation kinetics. This is linked to a broader hypothesis that monophosphorylation in the TDY motif on Tyr178 inactivates LmxMPK1. To do this, pre-incubation assays were performed, both with singly expressed kinase (as had

been done by Melzer) and with kinase that had been dephosphorylated by phosphatase co-expression.

Singly expressed kinase behaved as described previously (Melzer, 2007): kinase autophosphorylation in the 10 minutes radiometric assay decreased as the length of pre-incubation increased (due to the quantity of non-radioactive phosphate being incorporated increasing with longer pre-incubation) and MBP phosphorylation increased until 20 min, after which it decreased (Figure 24, 25 and 26). The “pilot” experiment (Figures 24, 25) supports the concept that this is due to phosphate incorporation rather than heat inactivation/degradation of the kinase.

Assays with phosphatase co-expressed LmxMPK1 display a similar trend (Figures 27, 28, 29), although kinase loading is somewhat uneven. ImageJ analysis eliminates the bias that adjusting protein loading by sight may introduce. Quantification and adjustment of the autoradiograph values (Figure 30) confirms that increasing the length of time that a kinase is pre-incubated with non-radioactive ATP decreases autophosphorylation activity when transferred to γ-^{32}P ATP. It also shows that after reaching maximum MBP phosphorylation following 30 min pre-incubation, MBP phosphorylation declines with increasing lengths of kinase pre-incubation. (For PTP1B this decline is seen following 60 min pre-incubation).

These data show that LmxMPK1 is an unusual kinase, as even when dephosphorylated it has the ability to autophosphorylate and subsequently phosphorylate a substrate (MBP). Autophosphorylation is on tyrosine of the phosphorylation lip and perhaps other tyrosine residues. Moreover, LmxMPK1 autophosphorylates on threonine residues outside the TDY motif with T224 appearing to be the predominant site.

It appears that phosphorylation of LmxMPK1 is essential for kinase activity as dephosphorylation by either a dual-specificity phosphatase (λ-phosphatase) or a protein-tyrosine phosphatase (PTP1B or LmxPTP) results in a longer delay before substrate phosphorylation commences, compared to singly expressed kinase. Furthermore, the increased delay before substrate phosphorylation commences as seen in λ-phosphatase co-expressed kinase, compared to the PTPs, suggests that threonine residues have some role in regulating kinase activity and either threonine

phosphorylation precedes substrate phosphorylation or threonine-dephosphorylated kinase is slower at substrate phosphorylation.

The results generated in this study have not enabled the definitive conclusion to be drawn that phosphorylation of Tyr178 leads to an inactive kinase. What can be said is that LmxMPK1 requires phosphorylation on at least one tyrosine residue and possibly one threonine also. These results also support the hypothesis that extended autophosphorylation leads to a less active kinase. Phosphorylation as a means of diminishing kinase activity has been established, Wee1 phosphorylates Cdc2 on two residues to inactivate it (Nurse & Thuriaux, 1980), while Wee1 is itself negatively regulated by phosphorylation (Wu & Russell, 1993). Glycogen synthase kinase 3 (GSK-3) is inactivated by monophosphorylation by a variety of kinases (Wang *et al.*, 2011). Autophosphorylation on tyrosine of the activation lip of the yeast MAPK, Hog1, has been suggested as an inactivating mechanism (Bell & Engelberg, 2003).

5.3 *In vivo* analysis of GFP-tagged LmxMPK1 mutants

5.3.1 Activation lip mutants

The *in vivo* expression of a protein of interest with a Green Fluorescent Protein (GFP) tag has the dual-advantage of allowing the protein's location in the cell to be observed by the use of fluorescent microscopy and is a convenient tag for the purification of the protein in its natural state (Morales *et al.*, 2007). Furthermore, by correlating the activity and phosphorylation status of the kinase with its cellular localisation, it may be possible to ascribe a role for it within a particular cellular process. The ability of C-terminally GFP-tagged LmxMPK1 to complement the null mutant had been tested successfully previously. Parasites expressing it were viable and as infective in mice as the wild type (Wiese, unpublished), thus demonstrating that the GFP-tag did not interfere with kinase functionality *in vivo*.

The hypothesis that this section of work sought to find data to support was that LmxMPK1 was regulated in a previously unreported manner. Namely, that dual phosphorylation of the activation lip TDY motif or monophosphorylation of the tyrosine inactivated the kinase. This had been suggested as only LmxMPK1 null mutant parasites expressing LmxMPK1 with an EDY or TDF motif were able to establish footpad infections in Balb/c mice – in addition to null mutants with a copy of wild type LmxMPK1 expressed from a plasmid (See introduction 1.4, Figure 8).

Furthermore, EDY and TDF promastigotes grew faster than the deletion mutant, with the EDY growing as well as WT cells (Figure 33). LmxMPK1 with an ADF, ADY or TDE motif were unable to rescue the ability of the null mutant to cause infection. Furthermore, in kinase assays with recombinant protein only wild type, ADY, EDF and EDY displayed autophosphorylation and MBP phosphorylation activity. Neither the ADF, TDE nor TDF displayed any *in vitro* activity (Wiese, unpublished). Additionally, separation of cell lysates into phosphorylated and non-phosphorylated fractions had shown that the wild type and K43M mutants were exclusively found in the phosphorylated fractions, the ADF was only found in the non-phosphorylated fraction and the ADY, EDY, TDE and TDF mutants were found in both (Melzer, 2007; Wiese, unpublished). For amastigotes wild type kinase and the TDF mutant were found only in the phosphorylated fraction, whereas the EDY was found in both. These data are summarised in Table 2.

Mutant	Active in assays	Infective	Phospho fraction (Promastigotes)		Phospho fraction (Amastigotes)	
WT	Y	Y	P		P	
KM	N	N	P		-	
ADF	N	N	N		-	
ADY	Y	Y (small)	BOTH		-	
EDF	Y	-	-		-	
EDY	Y	Y	BOTH	N≥P	BOTH	(equal)
TDE	N	N	BOTH	N<P	-	
TDF	N	Y	BOTH		P	

Table 2: Summary of previous work in the Wiese group with regard to LmxMPK1 and various mutants. WT, wild type kinase; KM, LmxMPK1K43M. 'Infective' is whether the mutant was capable of causing a footpad infection in Balb/c mice. 'Phospho fraction' refers to what fraction the kinase was found in following phosphoprotein purification: P, phosphorylated proteins; N, non-phosphorylated proteins. Green shading of boxes indicates that the result was the same as for WT kinase; red shading indicates that it is the opposite; yellow shading is for results that are not quite the same as the WT but are similar. Dashes indicate that this characteristic of the mutant was not examined (for some mutants amastigotes are not viable).

The transfection of Δ*LmxMPK1 L. mexicana* promastigote cells with plasmids expressing the wild type kinase, the “kinase dead” (K43M) and various TDY mutants resulted in the successful expression of the tagged proteins (Figure 35) and fluorescence micrographs were obtained (Figures 34 to 41).

If one were to consider that only kinase mutants displaying localisation to both the nucleus and the cytoplasm are active *in vivo* then the wild type, ADY, EDF, EDY and TDF display this characteristic. The KM, which is known to be inactive, is only found in the cytoplasm (Figure 37) as is the ADF (Figure 38). No mutant showed exclusively nuclear localisation. The kinase localisation combined with previous data that showed slower growth kinetics for the LmxMPK1 null mutant (Melzer, 2007) appears to confirm that LmxMPK1 has a dynamic role in the promastigote stage of the life cycle, although not an indispensable one given that the null mutant can still proliferate.

Work on the *L. major* MAP kinases 4, 7 and 10, showed that all three were confined to the cytosol during the promastigote stage of the life cycle (Morales *et al.*, 2007), moreover they did not show any change in localisation in response to the heat and temperature changes that mimic the change in environment that the parasites experience when transmitted to the mammalian host. Evidence was found that they are unphosphorylated in the promastigote stage and phosphorylated following the environmental shift that induces differentiation to amastigotes. Wild type LmxMPK1 is phosphorylated in both stages of the life cycle (Table 2) but in different patterns: both threonine-176 and tyrosine-178 of the activation lip of LmxMPK1 are phosphorylated in promastigotes and axenic amastigotes. In lesion-derived amastigotes only single tyrosine-phosphorylation could be detected so far. Mono-phosphorylation of tyrosine-178 as well as threonine-224 phosphorylation was found in promastigotes, axenic amastigotes and lesion-derived amastigotes (mass spectrometry performed by H Rosenqvist – see appendix).

5.3.2 Role of threonine-224

5.3.2.1 *In vitro* analysis

The *in vitro* analysis of threonine-224 shows that LmxMPK1(T224A) is capable of autophosphorylation on tyrosine, even if dephosphorylated by co-expression with a phosphatase (Figure 31) – the same as wild type LmxMPK1. Singly expressed wild

type LmxMPK1 is very weakly threonine-phosphorylated following purification from *E. coli* (Figure 32) and no threonine phosphorylation could be detected if co-expressed with phosphatases, both λ-phosphatase and, curiously, PTP1B. The absence of threonine phosphorylation following co-expression with a tyrosine phosphatase is an unexpected result that suggests autophosphorylation on tyrosine-178 precedes that of threonine-224 and that threonine-224 phosphorylation does not occur in the absence of tyrosine autophosphorylation. Strong threonine autophosphorylation in kinase assays is observed for wild type kinase, both singly expressed and co-expressed with phosphatases. Singly expressed LmxMPK1(T224A) showed a very faint signal for threonine phosphorylation following purification, which increased to a more definite signal following kinase assay. λ-phosphatase co-expressed T224A showed no threonine phosphorylation following purification but did show a moderate signal after kinase assay.

Threonine autophosphorylation by mutants lacking the T224 was surprising, although it is possible that this is an experimental artefact of *in vitro* work that does not mimic the cellular situation. It has been shown that kinases can autophosphorylate on residues prior to folding into their tertiary structure that they do not autophosphorylate on if expressed with a phosphatase prior to purification (Shreshta *et al*., 2011). However, given that lambda-phosphatase co-expressed LmxMPK1T224A (Figure 32, Lanes 2 and 2') showed autophosphorylation on threonine only after kinase assay suggests that a further threonine is autophosphorylated. Homology modelling of LmxMPK1 with mammalian ERK1/2 shows the existence of a threonine close to the active site (T198) that is a good candidate for further autophosphorylation (Figure 46). Current work in the Wiese group is seeking to confirm if this residue is a true autophosphorylation target.

The essentiality of T224 (and potentially T198) and its phosphorylation can be tested *in vivo* by observing if null mutant cells expressing the mutant kinases are capable of differentiating into amastigotes and – crucially for an LmxMPK1 mutant – proliferating.

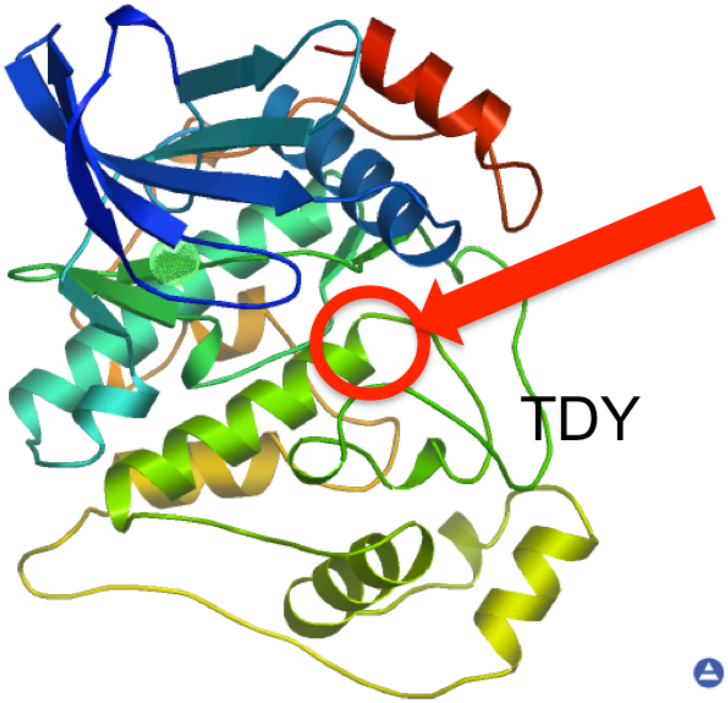

Figure 46: Homology model of LmxMPK1.
T198 is indicated by the red arrow and circle. Model was retrieved from the SWISS-MODEL database by searching with the sequence of LmxMPK1. (http://swissmodel.expasy.org) (Arnold *et al.*, 2006; Kiefer *et al.*, 2009)

5.3.2.2 *In vivo* analysis

Mass spectrometry had detected phosphorylation of threonine-224 in both promastigotes and amastigotes so the role of this residue *in vivo* was analysed. It was anticipated that replacing the threonine with a glutamate (T224E) would mimic a phosphorylated threonine and restore the ability of mutants such as the KM and the ADF to enter the nucleus if this phosphorylation is required for nuclear import. In some activation lip mutants threonine-224 was exchanged for an alanine (T224A), as this would enable the effect of a non-phosphorylated threonine to be examined. Curiously, both threonine-224 mutations resulted in very similar localisation phenotypes, regardless of what variation of the TDY motif was present in the activation loop: kinase was permanently excluded from the nucleus and often a fluorescent ring was observed around the nucleus (Figures 34 to 41: bottom and middle panels). This suggests that T224 is critical for nuclear translocation of LmxMPK1 and that for this to occur it is essential that the 224th residue is a threonine, as glutamate was unable to replicate the effect of phosphothreonine. Dimerisation of Polo-like kinase 4 (Plk4) involves phosphorylation of a threonine (Thr289); replacement with phosphomimicking aspartic acid is not sufficient to restore dimerisation (Guderian *et al.*, 2010), which may also be the case for Thr224 in LmxMPK1.

The mutation of T224 also appeared to cause alterations to the shape of the *Leishmania* cells. Cell length was diminished and width was greater for cells expressing T224A/E LmxMPK1, compared to WT, KM or TDY mutations alone. The volume and dimensions of eukaryotic cells have been linked to cell-cycle progression and DNA content, and an association has been demonstrated in *Leishmania* also (Wheeler *et al.*, 2011). Disruption of these attributes has been caused by kinase mutations in yeast (wee1 and Pom1 in *Schizosaccharomyces pombe (S. pombe*) (Nurse, 1975; Montagne *et al.*, 1999)). It is possible that mutation of T224 interferes with some aspect of DNA replication control, which in turn results in smaller *Leishmania* cells. Testing this rationale would simply entail staining and analysing the DNA content of WT cells, cells with a TDY mutation only, and cells with the T224A and T224E mutants of LmxMPK1. Indeed, a trypanosomatid kinase causing defects in DNA replication has been previously documented for TbECK1 (Ellis *et al.*, 2004).

The *Leishmania* homologue of GSK3β autophosphorylates on Ser232 (Ojo *et al*., 2011), which corresponds to Thr224 in LmxMPK1, suggesting that auto-phosphorylation outwith the activation loop is a regulatory mechanism also found in higher eukaryotes and trypanosomatids. Studies in mammalian cells that analysed the localisation of ERK1/2 found that disruption of residues outwith the TDY motif affected the ability of the kinase to localise to the nucleus, specifically serine-244, proline-245 and serine-246 (Caunt and McArdle, 2010; Chunderland *et al*., 2008) and threonine-188 (Lorenz *et al*., 2008). Although it should be noted that the ERK1/2 T188 is only 3 residues away from the tyrosine of the activation lip, and not 46 as T224 is in LmxMPK1. However, considering that the SPS sequence (in ERK1/2) and threonine-224 (LmxMPK1) are located within the tenth MAP kinase domain it is possible to speculate that they may have equivalent roles within their respective kinases with regard to facilitating nuclear entry.

Mammalian ERK1/2 is predominately localised to the cytosol in the absence of an upstream activation signal (Adachi *et al*., 1999; Cobb & Goldsmith, 2000; Caunt & McArdle, 2010). Following phosphorylation on the threonine and tyrosine of the activation loop by MEK (MAPK/ERK Kinase) ERK1/2 dimerises and translocates to the nucleus (Cobb & Goldsmith, 2000; Caunt and McArdle, 2010). The residues involved in ERK dimerisation, leucine-333, 336, 341 and 344 are all found in the C-terminal extension (L16) (Roskoski, 2012). A search of the sequence of LmxMPK1 for non-sequential leucines in the carboxy-terminal region of the enzyme revealed the presence of four leucine residues starting at leucine-320 (L320-X_2-L-X-L-X-L) (See appendix for highlighted sequence), suggesting that dimerisation is a process that might be important for LmxMPK1 function.

The nuclear pores in eukaryotic cells are typically limited to only allow proteins smaller than 40 kDa to diffuse through. If this is also the case in trypanosomatid organisms then dimerisation of LmxMPK1 (41.1 kDa as a monomer) would require active transport of some form. Although recognition of the residues on LmxMPK1 phosphorylated by its activator(s) may act as a sufficient signal for nuclear transport proteins to initiate shuttling of LmxMPK1 into the nucleus, it is suggested by the retention of the K43M and ADF mutants in the cytosol that some sort of kinase activity is necessary for nuclear translocation to occur. For mammalian ERK1/2 autophosphorylation of Thr188 promotes translocation to the nucleus (Lorenz *et al*.,

2009), so it may be that LmxMPK1 also requires autophosphorylation to undergo nuclear translocation. On the other hand, it may need to phosphorylate a nuclear transporter. Phosphorylation of nucleoporins in higher eukaryotes leading to translocation of cytosolic proteins has been reported (Kosako & Imamoto, 2010), although generally it is not the molecule that phosphorylates the nucleoporin that is imported (Matsubayashi *et al.*, 2001).

5.4 Analysis of LmxPTP *in vivo*

Phosphatase activity of the *Leishmania mexicana* PTP homologue, LmxPTP, *in vitro* has already been demonstrated (4.2), work was undertaken to analyse what the *in vivo* localisation of LmxPTP was and to attempt the deletion of the phosphatase from the genome.

LmxPTP showed a localisation that often appeared “thread like” throughout the cell (Figure 44). It was non-nuclear but appeared to be present as a “ring” around the nuclear membrane. The cellular body that this corresponds to is unknown, however, analysis of the sequence of LmxPTP shows an endoplasmic reticulum retention sequence, KKXX, at the C-terminus of the phosphatase (KKSA) (Vincent *et al.*, 1998). Indeed, support for the idea of LmxPTP localising to the ER is the localisation of SHERP (small hydrophilic endoplasmic reticulum-associated protein) in *L. major*. SHERP has been shown to be ER localised and immunofluorescence revealed the same pattern as was seen for LmxPTP (Knuepfer *et al.*, 2001).

H. sapiens PTPLB, the human homologue of LmxPTP, also contains an ER retention sequence in its C-terminus (KKFE) and is consequently found localised to the ER (Wang *et al.*, 2004). However, the presence of the GFP-tag at this terminus of the phosphatase makes it unlikely that the localisation of LmxPTP is being directed by this motif in the case of tagged LmxPTP, untagged phosphatase may localise in the same position as a result of the KKSA motif.

Mammalian PTP1B is also found localised to the endoplasmic reticulum (ER) (Frangioni *et al.*, 1992; Tonks, 2003; Monteleone *et al.*, 2012) in a manner controlled by the 35 terminal amino acids at the C-terminus, which form a hydrophobic “anchor” (Frangioni *et al.*, 1992). As previously discussed, the GFP-tag is likely to disrupt any cellular targeting properties of the C-terminus, however, analysis of the first 35 amino acids of the N-terminus of LmxPTP reveals a highly hydrophobic region

(http://www.pepcalc.com; using the Hopp-Woods scale). The pTHGFP plasmid adds a His-tag to the N-terminus of the protein, although it is unlikely to affect the hydrophobicity of this part of the molecule. N-terminal ER retention sequences have been described in proteins from other organisms including the Hepatitis B virus and humans (Kuroki *et al.*, 1989; Vander Heyden *et al.*, 2011).

Future work to determine the exact nature of the localisation signal of LmxPTP is intriguing as it could confirm either the C- or the N-terminus as the source of the localisation signal for LmxPTP or indicate that they are both involved, as is the case for cytochrome P450 (Szczesna-Skorupa *et al.*, 1995), which is an uncommon property for a protein.

Although not specific to phosphatases, acylating post-translational modifications have also been reported to control the sub-cellular localisation of *Leishmania* proteins (as they do in higher eukaryotes). For example hydrophilic acylated surface proteins (HASPs) must be myristoylated and palmitoylated in order to ensure correct membrane localisation (Denny *et al.*, 2000). Likewise, correct localisation of the *Plasmodium falciparum* calcium-dependent kinase, PfCDPK1, is dependent on both myristoylation and palmitoylation (Möskes *et al.*, 2004).

The N-terminus of LmxPTP could be myristoylated (Gly2), however, it does not appear that there are any residues suitable for palmitoylation within the first ten amino acids of the phosphatase (MGIKDMYLLA, see appendix for full sequence), suggesting that myristoylation alone may be the PTM that controls the localisation of LmxPTP. Single acylation-type modifications have been shown to be sufficient to direct ER localisation of a protein (Lu & Hrabak, 2002). However, the N-terminal His-tag that is attached to LmxPTP when expressed in pTH6nGFPc precludes myristoylation occurring, as the glycine is no longer adjacent to the terminal methionine. This leads to the probable conclusion that it is the hydrophobicity of the C-terminus that is directing the localisation of GFP-tagged LmxPTP, although for the untagged protein it may be one or several of the previously discussed localisation mechanisms.

Relatively little work has been done to examine the cellular localisation of *Trypanosoma* and *Leishmania* phosphatases (Szoor, 2010), however of those that have been studied the majority (9 out of the 11) are non-nuclear.

Deletion of the *LmxPTP* gene was attempted by homologous integration of DNA deletion fragments. Although resistance to the selective antibiotics was observed and PCR indicated a reduction in LmxPTP genetic content compared to wild type cells (Figure 45), it was not possible to fully eliminate the gene. Gene polyploidy has been observed in *Leishmania spp.* for certain genes (Cruz *et al.*, 1993; Rogers *et al.*, 2011) and can cause difficulties when attempting to delete genes, particularly in the case of tetraploid genes where one can encounter difficulties with having a sufficient number of selective antibiotics. Although the *Leishmania* genome is naturally aneuploidic, chromosome duplication has also been observed as a result of attempts to delete essential genes: in these cases the deletion construct integrates to one of the target alleles but the parasite merely duplicates the chromosome being targeted, thus achieving resistance to the selective antibiotic and maintaining an essential gene (Cruz *et al.*, 1993). It is possible that this may be hindering efforts to delete the *LmxPTP* gene as PTPs have already been shown to be essential in *Trypanosoma* species (Szoor *et al.*, 2006) and *Leishmania* (Nascimento *et al.*, 2006). TbPTP1 prevents the trypomastigote (bloodstream form) of the parasite from differentiating into the procyclic (insect gut) form. A *Leishmania* PTP (LmPTP1) is dispensable for the procyclic form of the parasite but is essential for the amastigote stage (Nascimento *et al.*, 2006).

Given the ability of LmxPTP to dephosphorylate LmxMPK1 *in vitro* it seems reasonable to speculate that the same may also be true *in vivo*. PTP1B dephosphorylates substrates that are “presented” to it in punctate vesicles (Tonks, 2003; Issad *et al.*, 2005; Yip *et al.*, 2010) and we have seen bright “spots” of GFP-tagged LmxMPK1 *in vivo*, which supports the hypothesis that LmxPTP is localised to the ER and dephosphorylates LmxMPK1. Strategies are available to identify the *in vivo* substrates of mammalian phosphatases, principally by mutating certain residues of the phosphatase such that it “traps” its substrate while trying to dephosphorylate it (Flint *et al.*, 1997; refinements of the technique reviewed in Blanchetot *et al.*, 2005). Substrate trapping has been successfully used to identify NOPP44/46 as the *in vivo* substrate of TbPTP1 (Chou *et al.*, 2010), validating this as a technique for use with trypanosomatid phosphatases.

However, many of the residues used in mammalian phosphatases to confer the trapping capability are absent in LmxPTP or, curiously, are already the amino acid

that the trapping mutant has (see Appendix section, 6.2.4 for alignment). For example, changing glutamate-115 in PTP1B for an alanine has been examined as a potential trapping mutation (Flint *et al.*, 1997), yet when aligned with LmxPTP an alanine is already present at the equivalent position (Ala-31), the same is also true for the D181A mutation: the equivalent LmxPTP residue is an alanine. The most surprising of the missing/altered residues are those of the active site. The PTP consensus motif is [I/V]HCXXGXXR[S/T], yet LmxPTP only has four of these residues at the equivalent positions: His61, Gly65, Arg67 and Ser68. As mentioned previously, LmxPTP had been categorised as a PTP-like phosphatase (PTPL) due to the divergence of the active site residues from the PTP consensus sequence (Andreeva *et al.*, 2008). For mammalian PTPLs, the arginine of the active site is replaced by a proline and even mutating it to an arginine does not restore significant phosphatase activity (Wang *et al.*, 2004). However, phosphatase activity of LmxPTP has been shown (see 4.2), suggesting that for trypanosomatid PTPLs the presence of arginine at this position may be sufficient for phosphatase activity. Furthermore, the inability to delete LmxPTP provides further weight to the argument that it is an active and essential phosphatase.

Although the essentiality of trypanosomatid PTPs suggests that they should be promoted as drug targets for treatment of leishmaniasis and trypanosomiasis, *in silico* modelling has suggested that the active site has strong similarity to that of human PTP (Nascimento *et al.*, 2006) indicating that an inhibitor that targeted these enzymes would have a high risk of cross-inhibition of mammalian PTP, with the associated risk of side effects.

Conclusions and future perspectives

This study has optimised an inhibitor-sensitised method for studying LmxMPK1 both *in vitro* and *in vivo*; this should allow future work to identify the substrate(s) of the kinase and the dissection of the role of LmxMPK1 within the *L. mexicana* cellular environment.

Dephosphorylated recombinant LmxMPK1 was generated using a phosphatase co-expression system. This was used in kinase assays to assess the role of phosphorylation in regulating kinase activity. It showed that phosphorylation is necessary for kinase activity but also that extended autophosphorylation decreases phosphotransferase activity towards MBP, as had been predicted in the hypothesis (Introduction, section 1.4). Moreover, autophosphorylation on threonine-224 was confirmed but the role this plays in activity regulation is unclear.

The expression of GFP-tagged LmxMPK1 mutants in a null mutant background was not quite the panacea to correlating activation lip phosphorylation and activity with cellular localisation. However, they did yield new data that showed that localisation is dynamic for LmxMPK1 and that nuclear localisation was possible, however, the KM and ADF mutants were never found in the nucleus.

Analysis of Thr224 showed that it is critical for nuclear translocation of active kinase as mutants that had previously been found in the nucleus ceased to be following mutation of this residue. Replacement of this residue and assessment of threonine phosphorylation after kinase assays suggested autophosphorylation on at least one other threonine residue.

LmxPTP was shown to be an active phosphatase, despite previous assignment as a PTP-like protein, which are known to be enzymatically inactive. It appears to associate to the ER and might be attached to the cytosolic face of the ER membrane, although the precise manner by which this is mediated remains to be established. Although LmxMPK1 has been dephosphorylated *in vitro* by it, phosphatases are promiscuous so further work is needed to establish whether this is also the case *in vivo*. Substrate-trapping would be the most definitive, although the residues normally used to confer the ability to trap are missing. An *in vitro* method would entail

expressing other kinases that autophosphorylate in the pJC-duet vector with LmxPTP and assess their phosphorylation-status following purification.

The proposed mechanism of activation and regulation of LmxMPK1 can be updated to say: that phosphorylation of Thr176 by an upstream kinase is necessary for *in vivo* activation of LmxMPK1; that LmxMPK1 autophosphorylates on Tyr178, Thr224 and at least one other threonine residue (not threonine-176) with increased autophosphorylation leading to a less active kinase. It still appears valid to say that dual-phosphorylation of the TDY motif leads to an inactive kinase. It may be that cytosolic LmxMPK1 is phosphorylated on threonine-176 by an upstream kinase and autophosphorylates on tyrosine-178 followed by threonine-224 autophosphorylation. Tyr178 is dephosphorylated by a phosphatase (potentially LmxPTP), which allows nuclear translocation of LmxMPK1 and phosphorylation of its substrate(s) (currently unknown).

This shows that LmxMPK1 is an unusual kinase with an activation mechanism that is different to that of MAPKs in higher eukaryotes. Understanding fully how this essential kinase is regulated would allow for better drug design for the treatment of leishmaniasis.

References

Adachi, M., Fukuda, M., & Nishida, E. (1999). Two co-existing mechanisms for nuclear import of MAP kinase: passive diffusion of a monomer and active transport of a dimer. *The EMBO journal*, *18*(19), 5347-58.

Alexander, J., & Russell, D. G. (1992). The interaction of *Leishmania* species with macrophages. *Advances in parasitology*, *31*, 175-254.

Alvar, J., Vélez, I. D., Bern, C., Herrero, M., Desjeux, P., Cano, J., Jannin, J., et al. (2012). Leishmaniasis Worldwide and Global Estimates of Its Incidence. (M. Kirk, Ed.) PLoS ONE, 7(5), e35671.

Ambit, Audrey, Kerry L Woods, Benjamin Cull, Graham H Coombs, and Jeremy C Mottram. 2011. "Morphological events during the cell cycle of *Leishmania major*." Eukaryotic cell 10 (11) (November): 1429-38.

Andreeva, A. V., & Kutuzov, M. A. (2008). Protozoan protein tyrosine phosphatases. International journal for parasitology, 38(11), 1279-95.

Antoine, J. C., Prina, E., Lang, T., & Courret, N. (1998). The biogenesis and properties of the parasitophorous vacuoles that harbour *Leishmania* in murine macrophages. *Trends in microbiology*, *6*(10), 392-401.

Arnold, K., Bordoli, L., Kopp, J., & Schwede, T. (2006). The SWISS-MODEL workspace: a web-based environment for protein structure homology modelling. *Bioinformatics (Oxford, England)*, *22*(2), 195-201.

Ashutosh, Garg, M., Sundar, S., Duncan, R., Nakhasi, H. L., & Goyal, N. (2012). Downregulation of mitogen-activated protein kinase 1 of *Leishmania donovani* field isolates is associated with antimony resistance. *Antimicrobial agents and chemotherapy*, *56*(1), 518-25.

Aslett, M., Aurrecoechea, C., Berriman, M., Brestelli, J., Brunk, B. P., Carrington, M., Depledge, D. P., et al. (2010). TriTrypDB: a functional genomic resource for the Trypanosomatidae. *Nucleic acids research*, *38*(Database issue), D457-62.

Avruch, J. (2007). MAP kinase pathways: the first twenty years. *Biochimica et biophysica acta*, *1773*(8), 1150-60.

Barhoumi, M., Tanner, N. K., Banroques, J., Linder, P., & Guizani, I. (2006). *Leishmania infantum* LeIF protein is an ATP-dependent RNA helicase and an eIF4A-like factor that inhibits translation in yeast. *The FEBS journal*, *273*(22), 5086-100.

Bates, P. A. (2008). *Leishmania* sand fly interaction: progress and challenges. *Current Opinion in Microbiology*, *11*(4), 340-344.

Bell, M., & Engelberg, D. (2003). Phosphorylation of Tyr-176 of the yeast MAPK Hog1/p38 is not vital for Hog1 biological activity. *The Journal of biological chemistry*, *278*(17), 14603-6.

Bengs, F., Scholz, A., Kuhn, D., & Wiese, M. (2005). LmxMPK9, a mitogen-activated protein kinase homologue affects flagellar length in *Leishmania mexicana*. *Molecular microbiology*, *55*(5), 1606-15.

Berman, J. (2006). Visceral leishmaniasis in the New World & Africa. *The Indian journal of medical research*, *123*(3), 289-94.

Berzunza-Cruz, M., Bricaire, G., Salaiza Suazo, N., Pérez-Montfort, R., & Becker, I. (2009). PCR for identification of species causing American cutaneous leishmaniasis. *Parasitology research*, *104*(3), 691-9.

Bhattacharyya, R. P., Reményi, A., Good, M. C., Bashor, C. J., Falick, A. M., & Lim, W. A. (2006). The Ste5 scaffold allosterically modulates signaling output of the yeast mating pathway. *Science*, *311*(5762), 822-6.

Bishop, A C, Ubersax, J. A., Petsch, D. T., Matheos, D. P., Gray, N. S., Blethrow, J., Shimizu, E., et al. (2000). A chemical switch for inhibitor-sensitive alleles of any protein kinase. *Nature*, *407*(6802), 395-401.

Bishop, Anthony C, Buzko, O., & Shokat, K. M. (2001). Magic bullets for protein kinases. *Trends in Cell Biology*, *11*(4), 167-172.

Blanchetot, C., Chagnon, M., Dubé, N., Hallé, M., & Tremblay, M. L. (2005). Substrate-trapping techniques in the identification of cellular PTP targets. *Methods (San Diego, Calif.)*, *35*(1), 44-53.

Blethrow, J. D., Glavy, J. S., Morgan, D. O., & Shokat, K. M. (2008). Covalent capture of kinase-specific phosphopeptides reveals Cdk1-cyclin B substrates. *Proceedings of the National Academy of Sciences of the United States of America*, *105*(5), 1442-7.

Bogdan, C., & Röllinghoff, M. (1998). The immune response to *Leishmania*: mechanisms of parasite control and evasion. *International journal for parasitology*, *28*(1), 121-34.

Brenchley, R., Tariq, H., McElhinney, H., Szöor, B., Huxley-Jones, J., Stevens, R., Matthews, K., et al. (2007). The TriTryp phosphatome: analysis of the protein phosphatase catalytic domains. *BMC genomics*, *8*, 434. doi:10.1186/1471-2164-8-434

Brun, R., & Schönenberger. (1979). Cultivation and in vitro cloning or procyclic culture forms of *Trypanosoma brucei* in a semi-defined medium. Short communication. *Acta tropica*, *36*(3), 289-92.

Cabello, I., Caraballo, A., & Millan, Y. (2002). Leishmaniasis in the genital area. *Rev Inst Med Trop Sao Paulo*, *44*(2), 105-107.

Cai, Z., Chehab, N. H., & Pavletich, N. P. (2009). Structure and activation mechanism of the CHK2 DNA damage checkpoint kinase. *Molecular cell*, *35*(6), 818-29.

Caunt, C. J., & Mcardle, C. A. (2010). Stimulus-induced uncoupling of extracellular signal-regulated kinase phosphorylation from nuclear localization is dependent on docking domain interactions. *Journal of Cell Science*, 4310-4320.

Caunt, C. J., & Mcardle, C. A. (2012). ERK phosphorylation and nuclear accumulation : insights from single-cell imaging. *Biochemical Society Transactions*, *40*, 224-229. doi:10.1042/BST20110662

Chou, S., Jensen, B. C., Parsons, M., Alber, T., & Grundner, C. (2010). The *Trypanosoma brucei* life cycle switch TbPTP1 is structurally conserved and dephosphorylates the nucleolar protein NOPP44/46. *The Journal of biological chemistry*, *285*(29), 22075-81. doi:10.1074/jbc.M110.108860

Chuderland, D., Konson, A., & Seger, R. (2008). Identification and characterization of a general nuclear translocation signal in signalling proteins. *Molecular cell*, *31*(6), 850-61. doi:10.1016/j.molcel.2008.08.007

Cobb, M. H., & Goldsmith, E. J. (2000). Dimerization in MAP-kinase signalling. *Trends in biochemical sciences*, *25*(1), 7-9.

Committee, W. E. (2010). Control of the leishmaniases. *World Health Organization technical report series*, (949), xii-xiii, 1-186, back cover.

Cruz, A. K., Titus, R., & Beverley, S. M. (1993). Plasticity in chromosome number and testing of essential genes in *Leishmania* by targeting. *Proceedings of the National Academy of Sciences of the United States of America*, *90*(4), 1599-603.

Da Silva, R. P., Hall, B. F., Joiner, K. A., & Sacks, D. L. (1989). CR1, the C3b receptor, mediates binding of infective *Leishmania major* metacyclic promastigotes to human macrophages. *Journal of immunology (Baltimore, Md. : 1950)*, *143*(2), 617-22.

Desjeux, P. (2004). Leishmaniasis: current situation and new perspectives. *Comparative immunology, microbiology and infectious diseases*, *27*(5), 305-18.

Donovan, C. (1903). On the possibility of the occurrence of trypanosomiasis in India. *British Medical Journal*, *2*(2219), 79.

Ellis, J., Sarkar, M., Hendriks, E., & Matthews, K. (2004), A novel ERK-like, CRK-like protein kinase that modulates growth in *Trypanosoma brucei* via an autoregulatory C-terminal extension. *Molecular microbiology*, *53*(5), 1487-99.

Erdmann, M. (2009). *LmxMPK3, a mitogen-activated protein kinase involved in length control of a eukaryotic flagellum*. PhD Thesis, University of Hamburg, Germany.

Erdmann, Maja, Scholz, A., Melzer, I. M., Schmetz, C., & Wiese, M. (2006). Interacting Protein Kinases Involved in the Regulation of Flagellar Length, *17*(April), 2035-2045.

Flint, A. J., Tiganis, T., Barford, D., & Tonks, N. K. (1997). Development of "substrate-trapping" mutants to identify physiological substrates of protein tyrosine phosphatases. *Proceedings of the National Academy of Sciences of the United States of America*, *94*(5), 1680-5.

Frangioni, J. V., Beahm, P. H., Shifrin, V., Jost, C. A., & Neel, B. G. (1992). The nontransmembrane tyrosine phosphatase PTP-1B localizes to the endoplasmic reticulum via its 35 amino acid C-terminal sequence. *Cell*, *68*(3), 545-60.

Ge, B., Gram, H., Di Padova, F., Huang, B., New, L., Ulevitch, R. J., Luo, Y., et al. (2002). MAPKK-independent activation of p38alpha mediated by TAB1-dependent autophosphorylation of p38alpha. Science (New York, N.Y.), 295(5558), 1291-4.

Gramiccia, M., & Gradoni, L. (2005). The current status of zoonotic leishmaniases and approaches to disease control. *International journal for parasitology*, *35*(11-12), 1169-80.

Guderian, G., Westendorf, J., Uldschmid, A., & Nigg, E. A. (2010). Plk4 trans-autophosphorylation regulates centriole number by controlling betaTrCP-mediated degradation. *Journal of cell science*, *123*(Pt 13), 2163-9.

Ha, D. S., Schwarz, J. K., Turco, S. J., & Beverley, S. M. (1996). Use of the green fluorescent protein as a marker in transfected *Leishmania*. *Molecular and biochemical parasitology*, *77*(1), 57-64.

Hanks, S. (2003). Genomic analysis of the eukaryotic protein kinase superfamily: a perspective. *Genome Biology*, *4*(5), 111.

Hanks, S. K., & Hunter, T. (1995). Protein kinases 6. The eukaryotic protein kinase superfamily: kinase (catalytic) domain structure and classification. *FASEB journal : official publication of the Federation of American Societies for Experimental Biology*, *9*(8), 576-96.

Hermoso, T., Fishelson, Z., Becker, S. I., Hirschberg, K., & Jaffe, C. L. (1991). Leishmanial protein kinases phosphorylate components of the complement system. *The EMBO journal*, *10*(13), 4061-7.

Ilg, T. (2000). Lipophosphoglycan is not required for infection of macrophages or mice by *Leishmania mexicana*. *Embo J*, *19*(9), 1953-1962.

Ilg, T. (2002). Generation of myo-inositol-auxotrophic *Leishmania mexicana* mutants by targeted replacement of the myo-inositol-1-phosphate synthase gene. *Molecular and biochemical parasitology*, *120*(1), 151-6.

Issad, T., Boute, N., Boubekeur, S., & Lacasa, D. (2005). Interaction of PTPB with the insulin receptor precursor during its biosynthesis in the endoplasmic reticulum. *Biochimie*, *87*(1), 111-6.

Ivens, A. C., & Blackwell, J. M. (1999). The *Leishmania* genome comes of Age. *Parasitol Today*, *15*(6), 225-231. doi:S0169-4758(99)01455-6 [pii]

Jeffrey, K. L., Camps, M., Rommel, C., & Mackay, C. R. (2007). Targeting dual-specificity phosphatases: manipulating MAP kinase signalling and immune responses. *Nature reviews. Drug discovery*, *6*(5), 391-403. doi:10.1038/nrd2289

John von Freyend, Simona, Rosenqvist, H., Fink, A., Melzer, I. M., Clos, J., Jensen, O. N., & Wiese, M. (2010a). LmxMPK4, an essential mitogen-activated protein kinase of *Leishmania mexicana* is phosphorylated and activated by the STE7-like protein kinase LmxMKK5. *International journal for parasitology*, *40*(8), 969-78.

John von Freyend, S. (2010b). *Analysis of LmxMPK4 and LmxMPK6, two mitogen-activated protein kinases of Leishmania mexicana*. PhD Thesis, University of Hamburg, Germany.

Kamhawi, S. (2006). Phlebotomine sand flies and *Leishmania* parasites: friends or foes? *Trends in parasitology*, *22*(9), 439-45.

Kiefer, F., Arnold, K., Künzli, M., Bordoli, L., & Schwede, T. (2009). The SWISS-MODEL Repository and associated resources. *Nucleic acids research*, *37*(Database issue), D387-92.

Knuepfer, E., Stierhof, Y. D., McKean, P. G., & Smith, D. F. (2001). Characterization of a differentially expressed protein that shows an unusual localization to intracellular membranes in *Leishmania major*. The Biochemical journal, 356(Pt 2), 335-44.

Kolev, N. G., Tschudi, C., & Ullu, E. (2011). RNA interference in protozoan parasites: achievements and challenges. *Eukaryotic cell*, *10*(9), 1156-63.

Kosako, H., & Imamoto, N. (2010). Phosphorylation of nucleoporins: signal transduction-mediated regulation of their interaction with nuclear transport receptors. *Nucleus (Austin, Tex.)*, *1*(4), 309-13.

Krupa, A., Preethi, G., & Srinivasan, N. (2004). Structural modes of stabilization of permissive phosphorylation sites in protein kinases: distinct strategies in Ser/Thr and Tyr kinases. *Journal of molecular biology*, *339*(5), 1025-39.

Kuhn, D., & Wiese, M. (2005). LmxPK4, a mitogen-activated protein kinase kinase homologue of *Leishmania mexicana* with a potential role in parasite differentiation. *Mol Microbiol*, *56*(5), 1169-1182.

Kumar, N. V., Eblen, S. T., & Weber, M. J. (2004). Identifying specific kinase substrates through engineered kinases and ATP analogs. *Methods (San Diego, Calif.)*, *32*(4), 389-97.

Kuroki, K., Russnak, R., & Ganem, D. (1989). Novel N-terminal amino acid sequence required for retention of a hepatitis B virus glycoprotein in the endoplasmic reticulum. *Molecular and cellular biology*, *9*(10), 4459-66.

Lainson, R., Shaw, J. J., Peters, W., & Killick-Kendrick, R. (1987). Evolution, classification and geographical distribution., 1-120. Academic Press.

Leifso, K., Cohen-Freue, G., Dogra, N., Murray, A., & McMaster, W. R. (2007). Genomic and proteomic expression analysis of *Leishmania* promastigote and amastigote life stages: the *Leishmania* genome is constitutively expressed. *Mol Biochem Parasitol*, *152*(1), 35-46.

Leishman, W. B. (1903). ON THE POSSIBILITY OF THE OCCURRENCE OF TRYPANOSOMIASIS IN INDIA. *BMJ*, *1*(2213), 1252-1254. doi:10.1136/bmj.1.2213.1252

Lorenz, K., Schmitt, J. P., Schmitteckert, E. M., & Lohse, M. J. (2009). A new type of ERK1/2 autophosphorylation causes cardiac hypertrophy. *Nature medicine*, *15*(1), 75-83. Nature Publishing Group.

Lu, S. X., & Hrabak, E. M. (2002). An Arabidopsis calcium-dependent protein kinase is associated with the endoplasmic reticulum. Plant physiology, 128(3), 1008-21.

Lucas, C. M., Franke, E. D., Cachay, M. I., Tejada, A., Cruz, M. E., Kreutzer, R. D., Barker, D. C., et al. (1998). Geographic distribution and clinical description of leishmaniasis cases in Peru. *Am J Trop Med Hyg*, *59*(2), 312-317.

Lye, L.-F., Owens, K., Shi, H., Murta, S. M. F., Vieira, A. C., Turco, S. J., Tschudi, C., et al. (2010). Retention and loss of RNA interference pathways in trypanosomatid protozoans. *PLoS pathogens*, *6*(10), e1001161.

Mallinson, D. J., & Coombs, G. H. (1989). Biochemical characteristics of the metacyclic forms of *Leishmania major* and L. mexicana mexicana. *Parasitology*, *98 (Pt 1)*, 7-15.

Mandal, G., Sharma, M., Kruse, M., Sander-Juelch, C., Munro, L. A., Wang, Y., Vilg, J. V., et al. (2012). Modulation of *Leishmania major* aquaglyceroporin activity by a mitogen-activated protein kinase. *Molecular microbiology*.

Manning, G., Whyte, D. B., Martinez, R., Hunter, T., & Sudarsanam, S. (2002). The protein kinase complement of the human genome. *Science (New York, N.Y.)*, *298*(5600), 1912-34.

Matsubayashi, Y., Fukuda, M., & Nishida, E. (2001). Evidence for existence of a nuclear pore complex-mediated, cytosol-independent pathway of nuclear translocation of ERK MAP kinase in permeabilized cells. *The Journal of biological chemistry*, *276*(45), 41755-60.

McFarlane, E., Perez, C., Charmoy, M., Allenbach, C., Carter, K. C., Alexander, J., & Tacchini-Cottier, F. (2008). Neutrophils contribute to development of a protective immune response during onset of infection with *Leishmania donovani*. *Infect Immun*, *76*(2), 532-541.

Melzer, I. M. (2007). *Biochemische Charakterisierung von LmxMPK1, einer essentiellen MAP Kinase aus Leishmania mexicana*. PhD Thesis, University of Hamburg, Germany.

Miguel, D. C., Yokoyama-Yasunaka, J. K., & Uliana, S. R. (2008). Tamoxifen Is Effective in the Treatment of *Leishmania amazonensis* Infections in Mice. *PLoS Negl Trop Dis*, *2*(6), e249.

Miranda-Saavedra, D., Stark, M. J. R., Packer, J. C., Vivares, C. P., Doerig, C., & Barton, G. J. (2007). The complement of protein kinases of the microsporidium Encephalitozoon cuniculi in relation to those of *Saccharomyces cerevisiae* and *Schizosaccharomyces pombe*. *BMC genomics*, *8*, 309.

Mojtahedi, Z., Clos, J., & Kamali-Sarvestani, E. (2008). *Leishmania major*: identification of developmentally regulated proteins in procyclic and metacyclic promastigotes. *Exp Parasitol*, *119*(3), 422-429.

Monteleone, M. C., González Wusener, A. E., Burdisso, J. E., Conde, C., Cáceres, A., & Arregui, C. O. (2012). ER-Bound Protein Tyrosine Phosphatase PTP1B Interacts with Src at the Plasma Membrane/Substrate Interface. *PloS one*, *7*(6), e38948.

Morales, M. A., Renaud, O., Faigle, W., Shorte, S. L., & Späth, G. F. (2007). Over-expression of *Leishmania major* MAP kinases reveals stage-specific induction of phosphotransferase activity. *International journal for parasitology*, *37*(11), 1187-99.

Möskes, C., Burghaus, P. A., Wernli, B., Sauder, U., Dürrenberger, M., & Kappes, B. (2004). Export of Plasmodium falciparum calcium-dependent protein kinase 1 to the parasitophorous vacuole is dependent on three N-terminal membrane anchor motifs. *Molecular microbiology*, *54*(3), 676-91.

Muskus, C. E., & Marin Villa, M. (2002). Metacyclogenesis: a basic process in the biology of Leishmania. *Biomedica*, *22*(2), 167-177.

Nascimento, M., Zhang, W.-W., Ghosh, A., Houston, D. R., Berghuis, A. M., Olivier, M., & Matlashewski, G. (2006). Identification and characterization of a protein-tyrosine phosphatase in *Leishmania*: Involvement in virulence. *The Journal of biological chemistry*, *281*(47), 36257-68. doi:10.1074/jbc.M606256200

Naula, C., Schaub, R., Leech, V., Melville, S., & Seebeck, T. (2001). Spontaneous dimerization and leucine-zipper induced activation of the recombinant catalytic domain of a new adenylyl cyclase of *Trypanosoma brucei,* GRESAG4.4B. *Molecular and biochemical parasitology*, *112*(1), 19-28.

Neuber, H. (2008). Leishmaniasis. *J Dtsch Dermatol Ges*, *6*(9), 754-765.

Nugent, P. G., Karsani, S. A., Wait, R., Tempero, J., & Smith, D. F. (2004). Proteomic analysis of *Leishmania mexicana* differentiation. *Mol Biochem Parasitol*, *136*(1), 51-62.

Nurse, P. (1975), Genetic control of cell size at cell division in yeast. *Nature*, *256*(5518), 547-551.

Nurse, P., & Thuriaux, P. (1980). Regulatory genes controlling mitosis in the fission yeast Schizosaccharomyces pombe. *Genetics*, *96*(3), 627-37.

Ojo, K. K., Arakaki, T. L., Napuli, A. J., Inampudi, K. K., Keyloun, K. R., Zhang, L., Hol, W. G. J., et al. (2011). Structure determination of glycogen synthase kinase-3 from *Leishmania major* and comparative inhibitor structure-activity relationships with *Trypanosoma brucei* GSK-3. *Molecular and biochemical parasitology*, *176*(2), 98-108.

Olivier, M., Gregory, D. J., & Forget, G. (2005). Subversion mechanisms by which *Leishmania* parasites can escape the host immune response: a signalling point of view. *Clinical microbiology reviews*, *18*(2), 293-305.

Pandey, K., Sinha, P. K., Rabidas, V., Kumar, N., Bimal, S., Verma, N., Lal, C., et al. (2008). HIV, visceral leishmaniasis and Parkinsonism combined with diabetes mellitus and hyperuricaemia: A case report. *Cases J*, *1*(1), 183.

Parsons, M., & Ruben, L. (2000). Pathways Involved in Environmental Sensing in Trypanosomatids. *Parasitology Today*, *16*(2), 56-62. doi:10.1016/S0169-4758(99)01590-2

Parsons, M., Worthey, E. A., Ward, P. N., & Mottram, J. C. (2005). Comparative analysis of the kinomes of three pathogenic trypanosomatids: *Leishmania major*, *Trypanosoma brucei* and *Trypanosoma cruzi*. *BMC genomics*, *6*, 127.

Pearson, G., Robinson, F., Beers Gibson, T., Xu, B. E., Karandikar, M., Berman, K., & Cobb, M. H. (2001). Mitogen-activated protein (MAP) kinase pathways: regulation and physiological functions. *Endocrine reviews*, *22*(2), 153-83.

Pimenta, P. F., da Silva, R. P., Sacks, D. L., & da Silva, P. P. (1989). Cell surface nanoanatomy of *Leishmania major* as revealed by fracture-flip. A surface meshwork of 44 nm fusiform filaments identifies infective developmental stage promastigotes. *Eur J Cell Biol*, *48*(2), 180-190.

Puentes, S. M., Da Silva, R. P., Sacks, D. L., Hammer, C. H., & Joiner, K. A. (1990). Serum resistance of metacyclic stage *Leishmania major* promastigotes is due to release of C5b-9. *Journal of immunology (Baltimore, Md. : 1950)*, *145*(12), 4311-6.

Puig, L., & Pradinaud, R. (2003). *Leishmania* and HIV co-infection: dermatological manifestations. *Ann Trop Med Parasitol*, *97 Suppl 1*, 107-114.

Quinnell, R. J., & Courtenay, O. (2009). Transmission, reservoir hosts and control of zoonotic visceral leishmaniasis. *Parasitology*, *136*(14), 1915-34.

Rogers, M. B., Hilley, J. D., Dickens, N. J., Wilkes, J., Bates, P. A., Depledge, D. P., Harris, D., et al. (2011). Chromosome and gene copy number variation allow major structural change between species and strains of *Leishmania*. *Genome research*, *21*(12), 2129-42.

Roskoski, R. (2012). ERK1/2 MAP kinases: Structure, function, and regulation. *Pharmacological research : the official journal of the Italian Pharmacological Society*, *66*(2), 105-143.

Salman, S. M., Rubeiz, N. G., & Kibbi, A. G. (1999). Cutaneous leishmaniasis: clinical features and diagnosis. *Clin Dermatol*, *17*(3), 291-296.

Sarkar, A., Aga, E., Bussmeyer, U., Bhattacharyya, A., Möller, S., Hellberg, L., Behnen, M., et al. (2012). Infection of neutrophil granulocytes with *Leishmania major* activates ERK 1/2 and modulates multiple apoptotic pathways to inhibit apoptosis. *Medical microbiology and immunology*. doi:10.1007/s00430-012-0246-1

Schubach, A., Cuzzi-Maya, T., Goncalves-Costa, S. C., Pirmez, C., & Oliveira-Neto, M. P. (1998). Leishmaniasis of glans penis. *J Eur Acad Dermatol Venereol*, *10*(3), 226-228.

Seaman, J., Mercer, A. J., & Sondorp, E. (1996). The epidemic of visceral leishmaniasis in western Upper Nile, southern Sudan: course and impact from 1984 to 1994. *International journal of epidemiology*, *25*(4), 862-71.

Shio, M. T., Hassani, K., Isnard, A., Ralph, B., Contreras, I., Gomez, M. A., Abu-Dayyeh, I., et al. (2012). Host cell signalling and *Leishmania* mechanisms of evasion. Journal of tropical medicine, 2012, 819512.

Shrestha, A., Hamilton, G., O'Neill, E., Knapp, S., & Elkins, J. M. (2012). Analysis of conditions affecting auto-phosphorylation of human kinases during expression in bacteria. *Protein expression and purification*, *81*(1), 136-43.

Simpson, L, and P Braly. 1970. "Synchronization of *Leishmania tarentolae* by hydroxyurea." The Journal of protozoology 17 (4) (November): 511-7.

Singh, G., Chavan, H. D., & Dey, C. S. (2008). Proteomic analysis of miltefosine-resistant *Leishmania* reveals the possible involvement of eukaryotic initiation factor 4A (eIF4A). *Int J Antimicrob Agents*, *31*(6), 584-586.

Szczesna-Skorupa, E., Ahn, K., Chen, C. D., Doray, B., & Kemper, B. (1995). The cytoplasmic and N-terminal transmembrane domains of cytochrome P450 contain independent signals for retention in the endoplasmic reticulum. *The Journal of biological chemistry*, *270*(41), 24327-33.

Szöor, B., Wilson, J., McElhinney, H., Tabernero, L., & Matthews, K. R. (2006). Protein tyrosine phosphatase TbPTP1: A molecular switch controlling life cycle differentiation in trypanosomes. *The Journal of cell biology*, *175*(2), 293-303.

Szöör, B. (2010). Trypanosomatid protein phosphatases. *Molecular and biochemical parasitology*, *173*(2), 53-63.

Sørensen, A. L., Hey, A. S., & Kharazmi, A. (1994). *Leishmania major* surface protease Gp63 interferes with the function of human monocytes and neutrophils in vitro. *APMIS : acta pathologica, microbiologica, et immunologica Scandinavica*, *102*(4), 265-71.

Tolia, N. H., & Joshua-Tor, L. (2006). Strategies for protein coexpression in Escherichia coli. *Nature methods*, *3*(1), 55-64.

Tonks, N. K. (2003). PTP1B: From the sidelines to the front lines! *FEBS Letters*, *546*(1), 140-148.

Vander Heyden, A. B., Naismith, T. V., Snapp, E. L., & Hanson, P. I. (2011). Static retention of the lumenal monotopic membrane protein torsinA in the endoplasmic reticulum. *The EMBO journal*, *30*(16), 3217-31.

Vincent, M. J., Martin, A. S., & Compans, R. W. (1998). Function of the KKXX motif in endoplasmic reticulum retrieval of a transmembrane protein depends on the length and structure of the cytoplasmic domain. *The Journal of biological chemistry*, *273*(2), 950-6.

Wang, B., Pelletier, J., Massaad, M. J., Herscovics, A., & Shore, G. C. (2004). The yeast split-ubiquitin membrane protein two-hybrid screen identifies BAP31 as a regulator of the turnover of endoplasmic reticulum-associated protein tyrosine phosphatase-like B. *Molecular and cellular biology*, *24*(7), 2767-78.

Wang, H., Brown, J., & Martin, M. (2011). Glycogen synthase kinase 3: a point of convergence for the host inflammatory response. *Cytokine*, *53*(2), 130-40.

Wheeler, R. J., Gluenz, E., & Gull, K. (2011), The cell cycle of *Leishmania*: morphogenetic events and their implications for parasite biology. *Molecular microbiology*, *79*(3), 647-62.

Wheeler, R. J., Gull, K., & Gluenz, E. (2012). Detailed interrogation of trypanosome cell biology via differential organelle staining and automated image analysis. *BMC biology*, *10*, 1.

Wiese, M. (1998). A mitogen-activated protein (MAP) kinase homologue of *Leishmania mexicana* is essential for parasite survival in the infected host. *The EMBO journal*, *17*(9), 2619-28.

Wiese, Martin. (2007). *Leishmania* MAP kinases – Familiar proteins in an unusual context. *International Journal for Parasitology*, *37*, 1053-1062. doi:10.1016/j.ijpara.2007.04.008

Wiese, Martin, Kuhn, D., & Grünfelder, C. G. (2003). Protein kinase involved in flagellar-length control. *Eukaryotic cell*, *2*(4), 769-77.

Wiese, Martin, Wang, Q., & Go, I. (2003). Identification of mitogen-activated protein kinase homologues from *Leishmania mexicana*. *International Journal for Parasitology*, *33*, 1577-1587.

Wu, L., & Russell, P. (1993). Nim1 kinase promotes mitosis by inactivating Wee1 tyrosine kinase. *Nature*, *363*(6431), 738-41.

Yip, S.-C., Saha, S., & Chernoff, J. (2010). PTP1B: a double agent in metabolism and oncogenesis. *Trends in biochemical sciences*, *35*(8), 442-9.

Zhang, C., Kenski, D. M., Paulson, J. L., Bonshtien, A., Sessa, G., Cross, J. V., Templeton, D. J., et al. (2005). A second-site suppressor strategy for chemical genetic analysis of diverse protein kinases. *Nature Methods*, *2*(6), 435-441.

Zhou, C., Yang, Y., & Jong, A. Y. (1990). Mini-prep in ten minutes. *BioTechniques*, *8*(2), 172-3.

Zilberstein, D. (1993). Transport of nutrients and ions across membranes of trypanosomatid parasites. *Advances in parasitology*, *32*, 261-91.

Zilberstein, D., Blumenfeld, N., Liveanu, V., Gepstein, A., & Jaffe, C. L. (1991). Growth at acidic pH induces an amastigote stage-specific protein in *Leishmania* promastigotes. *Molecular and biochemical parasitology*, *45*(1), 175-8.

6 Appendices

6.1 LmxMPK1

6.1.1 Genetic sequence of LmxMPK1 (Genbank: Z95887)

ATGACCTCATACGGCATCGACGGTGAGGTTGAGCAACGCTACCGCATTCTCCGCCACA
TCGGCAGCGGTGCCTACGGAGTCGTCTGGTGTGCCCTCGACCGCCGCACGGGCAAGTG
CGTTGCCCTCAAAAAGGTCTACGACGCCTTTGGCAACGTTCAAGATGCGCAGCGCACC
TATCGGGAAGTGATGCTTTTGCAGCGACTGCGGCACAACCCCTTCATTGTCGGCATCC
TCGACGTGATTCGTGCGGCCAACAACATTGACCTGTACCTCGTCTTTGAGTTGATAGA
GACCGATCTCACAGCCATTATCCGTAAAAACCTTCTGCAACGCGATCACAAGCGCTTC
CTCACCTATCAGTTACTTCGCACAGTGGCACAGCTCCACGCACAGAACATCATTCACC
GGGATTTGAAGCCGGCCAACGTATTTGTGAGCAGCGACTGCTCCATCAAGCTCGGGGA
CTTTGGTCTGGCTCGAACGTTTCGCAGTGGCTACGACAACGAACAGGAGTTTCTCGAC
CTGACCGACTACATCGCAACTAGGTGGTACCGGTCGCCGGAGATTTTGGTCAAGTCGC
GCGCCTATTCCACAGCGATGGACATGTGGGCCATCGGGTGTGTGATTGGGGAGATGCT
GCTAGGCCGCCCACTCTTCGAGGGCCGCAACACGCTGGATCAACTCCGCCTGATCATT
GAGGCTATCGGCGTGCCGAGCGACGCAGATGTGCGCAGCCTTCACTCGCCCGAGCTCG
AGAAGCTCATCAACTCCCTTCCGACCCCGTTGATCTTCTCTCCGCTTGTGGGGAACAA
GAACCTGAAGGATAGCGAGGCGACAGACTTGATGATGAAGCTCATTGTCTTCAATCCA
AAGAGGCGGCTTTCCGCGGTGGAGGCGCTGCAGCACCCCTACGTCGCCCCGTTTGTGC
AGCATGGTGAGCTGGAGAAGATCCAAGGCCTCGACCCACTCGTGCTGCCCCTCGTGGA
TGAGAAGATCTACACCAAGGAGGAGTACAAGGCGAATCTGTACGACGAGATCGGCATG
CGCTACCGCTATCACATAACAGACGTGTATTAG

Sequence Length: 1077 bp

6.1.2 Amino acid sequence of LmxMPK1

MTSYGIDGEVEQRYRILRHIGSGAYGVVWCALDRRTGKCVALKKVYDAFGNVQDAQRT
YREVMLLQRLRHNPFIVGILDVIRAANNIDLYLVFELIETDLTAIIRKNLLQRDHKRF
LTYQLLRTVAQLHAQNIIHRDLKPANVFVSSDCSIKLGDFGLARTFRSGYDNEQEFLD
LTDYIATRWYRSPEILVKSRAYSTAMDMWAIGCVIGEMLLGRPLFEGRNTLDQLRLII
EAIGVPSDADVRSLHSPELEKLINSLPTPLIFSPLVGNKNLKDSEATDLMMKLIVFNP
KRRLSAVEALQHPYVAPFVQHGELEKIQGLDPLVLPLVDEKIYTKEEYKANLYDEIGM
RYRYHITDVY

Sequence Length: 358 aa

6.2 LmxPTP

6.2.1 Genetic sequence of LmxPTP (LmxM.05.0280)

ATGGGCATCAAGGACATGTACCTGCTCGCCTACAACGCGGGCATGTGTGCTGGCTGGGCC
ACAATCCTCGTAAAGGTCATCGGGCATTTGGCGGAGGGTCGAGACGTCGCCTCGGTGTAC
CCCGAGATTGCGCGGCTGCTGTGCGTTGCGCAGACCGGCGCCATTGTCGAAATCTTTCAT
GCCGCCTTCGGGGTCGTGCGCAGCCCAGTCGGCACGACCTTCCTGCAGGTCCTGTCGCGC
CTCATCGTACTGTACGGTGCCGTGCGCATCGGAGACACGGACTCCACGAAGAGCCTCGTC
TTTGTTCAGATGCTGGTCGCCTGGTGCCTGAGCGAAGTAATTCGCTACTCCTTCTACGGC
GCGAACCTCCTCAGCGTCAGTGTTGCGCCGCTGACGTGGCTGCGCTACTCCGCCTTCATG
GTGCTCTACCCTGTCGGCATCACCGGAGAGATCGGCTGCCTTTACAAGGCGCTGCCGTAC
ATCCAGAAGCACAAGCCGTGGACCGTGGAACTGCCGAACAAGTTGAACTTCACCTTCTCG
TGGTACAACTCCGTGTGGTTTATCCTCCTCGGCGTATACCCCTACGGCAGCTACGTCATG
TACTCGTACATGCTCGCGCAGCGCCGCAAGACTTTGGCGAAGGCCGCGTCCGAGAGGTCG

Sequence length: 675 bp

6.2.2 Predicted amino acid sequence of LmxPTP

MGIKDMYLLAYNAGMCAGWATILVKVIGHLAEGRDVASVYPEIARLLCVAQTGAIVEI
FHAAFGVVRSPVGTTFLQVLSRLIVLYGAVRIGDTDSTKSLVFVQMLVAWCLSEVIRY
SFYGANLLSVSVAPLTWLRYSAFMVLYPVGITGEIGCLYKALPYIQKHKPWTVELPNK
LNFTFSWYNSVWFILLGVYPYGSYVMYSYMLAQRRKTLAKAASERSKKSA

Sequence Length: 224 aa

6.2.3 Alignment of LmxPTP with homologues

The amino acid sequence for LmxPTP (E9AKD3) was aligned with that of its homologues in *L. donovani* (E9B8B8), *L. braziliensis* (A4H472), *T. cruzi* (Q4CTD5) and *H. sapiens* (PTPLB, Q6Y1H2).

```
                                      :   **: **  * .**  * . :
1    ----------------------------------MGIKDMYLLAYNAGMCAGWATILVKV   26  E9AKD3   E9AKD3_LEIMU
1    ----------------------------------MGIKDMYLLAYNAGMCVGWGTILVKV   26  E9B8B8   E9B8B8_LEIDB
1    ----------------------------------MGIRDMYLLAYNASMCVGWGAILVKV   26  A4H472   A4H472_LEIBR
1    -----------------------------------MLKKAYLLAYNGSMLTGWALILFKV   25  Q4CTD5   Q4CTD5_TRYCC
1    MAAVAATAAAKGNGGGGGRAGAGDASGTRKKKGPGPLATAYLVIYNVVMTAGWLVIAVGL   60  Q6Y1H2   HACD2_HUMAN

     :       .  .:*  * : * . * **: **:*. :*:* * *  * :** **::::::.
27   IGHLAEGRDVASVYPEIARLLCVAQTGAIVEIFHAAFGVVRSPVGTTFLQVLSRLIVLYG   86  E9AKD3   E9AKD3_LEIMU
27   IGHLAEGRDPASVYPGIARLLCVAQTGAVAEILHAAFGVVRSPVGTTFLQVLSRLIVLYG   86  E9B8B8   E9B8B8_LEIDB
27   VKHFVDGGDAASVYPEIAQLLCVAQTGALAEILHAAFGIVRSPVGTTLLQVLSRLIVLYG   86  A4H472   A4H472_LEIBR
26   VNHVASGKNIWDVYPLIARLLLVFQGGAVMEIIHAMLGLVRSPVPTTFMQVSSRLIVLFG   85  Q4CTD5   Q4CTD5_TRYCC
61   VRAYLAKGSYHSLYYSIEKPLKFFQTGALLEILHCAIGIVPSSVVLTSFQVMSRVFLIWA  120  Q6Y1H2   HACD2_HUMAN

       :   .:   .  .  :::** ::*:***:**  .**      :.* **: *::***:*
87   AVRIGDTDSTKSLVFVQMLVAWCLSEVIRYSFYGANLLSVSVAPLTWLRYSAFMVLYPVG  146  E9AKD3   E9AKD3_LEIMU
87   AVRIGDTDSTKSLVFVQMLVAWCLSEIIRYSFYGANLLRVNLASLTWLRYSAFMVLYPVG  146  E9B8B8   E9B8B8_LEIDB
87   AVRLGDTEATRSLAFVQMVVAWCLSEVIRYSFYGANLLNTTAPPLTWLRYSAFMVLYPVG  146  A4H472   A4H472_LEIBR
86   SLRIGPTESRHSPFFTQMVVAWSLSEIIRYAFYATNLLDFKPKILTWLRYTAFMLLYPVG  145  Q4CTD5   Q4CTD5_TRYCC
121  VTHSV-KEVQSEDSVLLFVIAWTITEIIRYSFYTFSLLNHLPYLIKWARYTLFIVLYPMG  179  Q6Y1H2   HACD2_HUMAN

     ::**:  :* ***:::    :::.:**: *::*.:*  : :*::.  *     :* :*:
147  ITGEIGCLYKALPYIQKHKPWTVELPNKLNFTFSWYNSVWFILLGVYPYGSYVMYSYMLA  206  E9AKD3   E9AKD3_LEIMU
147  ITGEIGCLYKALPYIKKHKPWTVELPNKLNFTFSWYNTVWFILLGIYPYGSYVMYSYMLA  206  E9B8B8   E9B8B8_LEIDB
147  ITGEIGCLYKALPYIKKHKPWTVEMPNKLNFTFSWYNSVWFILLGVYPYGSYVMYSYMLA  206  A4H472   A4H472_LEIBR
146  ISGEIGCFYKALPYIKANKPWSMELPNRYNWTFSWYNTVWLILLGLYPYGSYVMYTYMLQ  205  Q4CTD5   Q4CTD5_TRYCC
180  VSGELLTIYAALPFVRQAGLYSISLPNKYNFSFDYYAFLILIMISYIPIFP-QLYFHMIH  238  Q6Y1H2   HACD2_HUMAN

     **** :. :
207  QRRKTLAKAASERSKKSA-----------  224  E9AKD3   E9AKD3_LEIMU
207  QRRKTFAKSASERSKKSA-----------  224  E9B8B8   E9B8B8_LEIDB
207  QRRKMFAKAASERAKKSA-----------  224  A4H472   A4H472_LEIBR
206  QRRKVLGFTTRTAPPASGATTATKSSKKQ  234  Q4CTD5   Q4CTD5_TRYCC
239  QRRKILSHTEEHKKFE-------------  254  Q6Y1H2   HACD2_HUMAN
```

6.2.4 Alignment of LmxPTP with *H. sapiens* PTP1B

The amino acid sequence for LmxPTP (E9AKD3) was aligned with that of PTP1B (PTN1, P18031).

```
     * ::. :    :   ...**:*  .:  .
1    MEMEKEF---EQIDKSGSWAAIYQDIRHEASDFPCRVAKLPKNKNRNRYRDVSPFDHSRI   57  P18031   PTN1_HUMAN
1    MGIKDMYLLAYNAGMCAGWATILVKVIGHL------------------------------   30  E9AKD3   E9AKD3_LEIMU

                                                                  :
58   KLHQEDNDYINASLIKMEEAQRSYILTQGPLPNTCGHFWEMVWEQKSRGVVMLNRVMEKG  117  P18031   PTN1_HUMAN
31   ------------------------------------------------------------AE-   32  E9AKD3   E9AKD3_LEIMU

                                 ..*: * *      *    *    **:*
118  SLKCAQYWPQKEEKEMIFEDTNLKLTLISEDIKSYYTVRQLELENLTTQETREILHFHYT  177  P18031   PTN1_HUMAN
33   ----------------------------GRDVASVYPEIARLLCVAQTGAIVEIFH----   60  E9AKD3   E9AKD3_LEIMU

         *** .**..  **:.*      : . . *. .  :. *.*:          ::**::
178  TWPDFGVPESPAS--FLNFL------FKVRESGSLSPEHGPVVVHCSAGIGRSGTFCLAD  229  P18031   PTN1_HUMAN
61   --AAFGVVRSPVGTTFLQVLSRLIVLYGAVRIGDTDSTKSLVFVQ------MLVAWCLSE  112  E9AKD3   E9AKD3_LEIMU

                                       :*:*: .    *:: :. * .
230  TCLLLMDKRKDPSSVDIKKVLLEMRKFRMGLIQTADQLRFSYLAVIEGAKFIMGDSSVQD  289  P18031   PTN1_HUMAN
113  -------------------------------------VIRYSFYG----ANL-LSVSVAPL  131  E9AKD3   E9AKD3_LEIMU

      * . *   :  *                                            *. *
290  QWKELSHEDLEPPPEHIPPPPRPPKRILEPHNGKCREFFPNHQWVKEETQEDKDCPIKEE  349  P18031   PTN1_HUMAN
132  TWLRYSAFMVLYPV-----------------------------------------GITGE  150  E9AKD3   E9AKD3_LEIMU

      *.  :* **  :                         *     .**:*  :.::*:::
350  KGSPLNAAPYGIESMSQDTEVRSRVVGGSLRGAQAASPAKGEPSLPEKDEDHALSYWKPF  409  P18031   PTN1_HUMAN
151  IGCLYKALPYIQKHK----------------------PW--TVELPNK-LNFTFSWYNS-  184  E9AKD3   E9AKD3_LEIMU

      * : :  *   *:*: * ::: ..
410  LVNMCVATVLTAGAYLCYRFLFNSNT---------------  435  P18031   PTN1_HUMAN
185  -VWFILLGVYPYGSYVMYSYMLAQRRKTLAKAASERSKKSA  224  E9AKD3   E9AKD3_LEIMU
```

6.3 Results of mass spectrometry analyses

Peptides identified from LmxMPK1 by MS/MS analysis

Identified peptides are marked in red and bold in the displayed sequence of LmxMPK1. Sequence Coverage: 72.3%

```
  1 MTSYGIDGEV EQRYRILRHI GSGAYGVVWC ALDRRTGKCV ALKKVYDAFG
 51 NVQDAQRTYR EVMLLQRLRH NPFIVGILDV IRAANNIDLY LVFELIETDL
101 TAIIRKNLLQ RDHKRFLTYQ LLRTVAQLHA QNIIHRDLKP ANVFVSSDCS
151 IKLGDFGLAR TFRSGYDNEQ EFLDLTDYIA TRWYRSPEIL VKSRAYSTAM
201 DMWAIGCVIG EMLLGRPLFE GRNTLDQLRL IIEAIGVPSD ADVRSLHSPE
251 LEKLINSLPT PLIFSPLVGN KNLKDSEATD LMMKLIVFNP KRRLSAVEAL
301 QHPYVAPFVQ HGELEKIQGL DPLVLPLVDE KIYTKEEYKA NLYDEIGMRY
351 RYHITDVY
```

MS/MS spectrum of LmxMPK1 from amastigotes showing the presence of threonine and tyrosine phosphorylation of the TDY motif

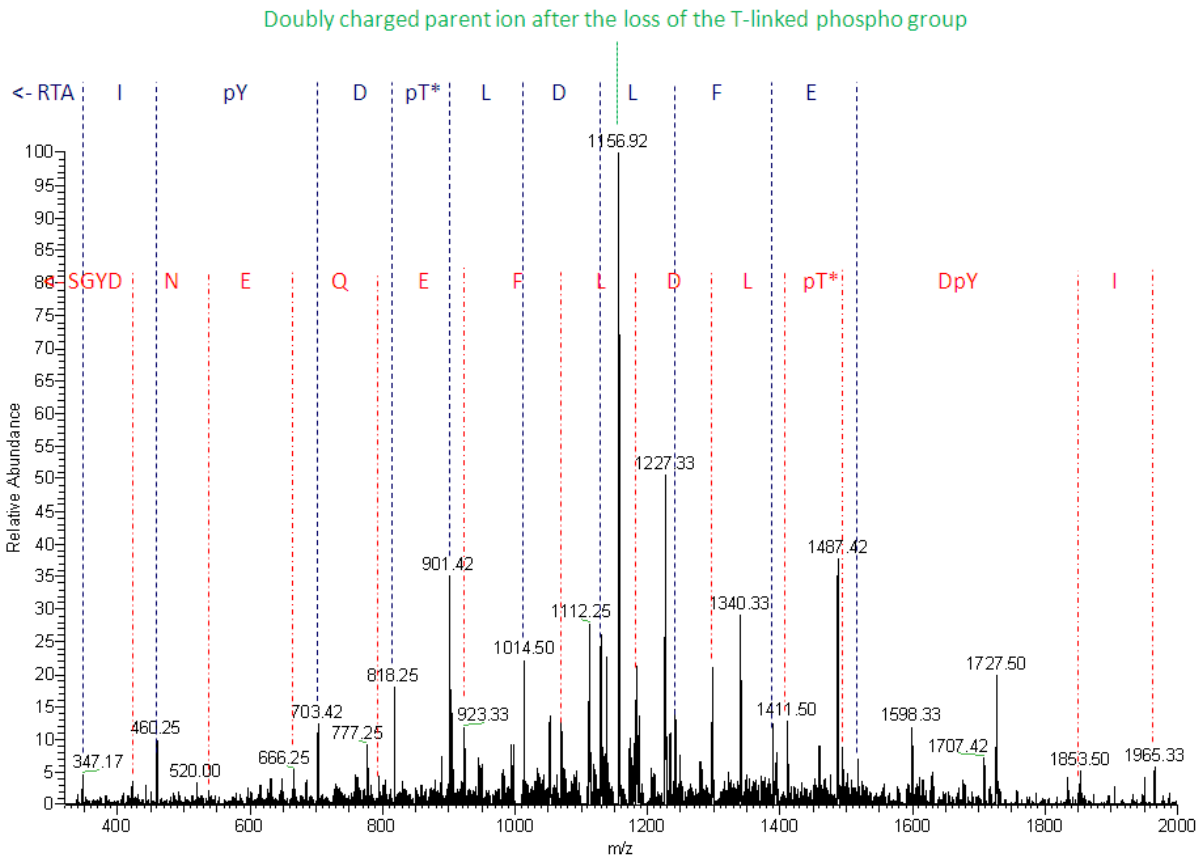

MS/MS spectrum of LmxMPK1 from promastigotes showing the presence of threonine and tyrosine phosphorylation of the TDY motif

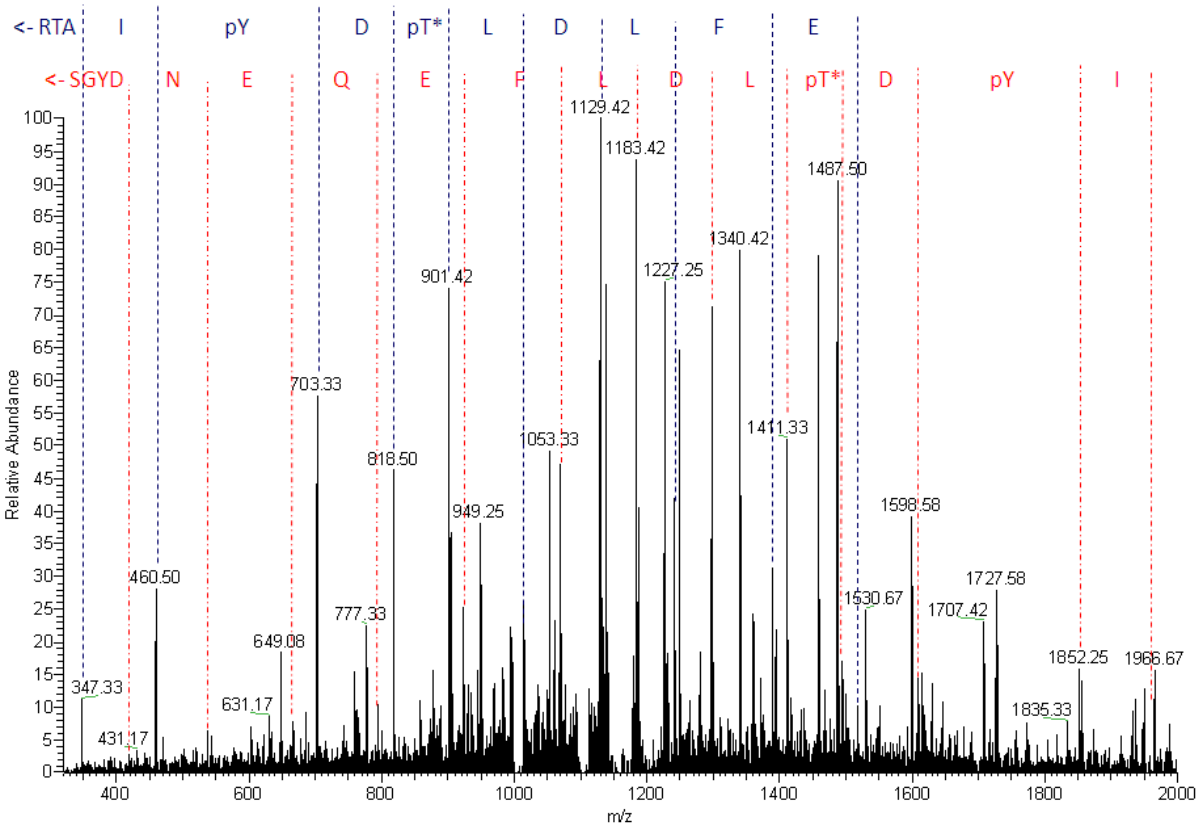

MS/MS spectrum of LmxMPK1 showing phosphorylation of Thr224 (Promastigotes/Amastigotes and recombinant protein display this pattern)

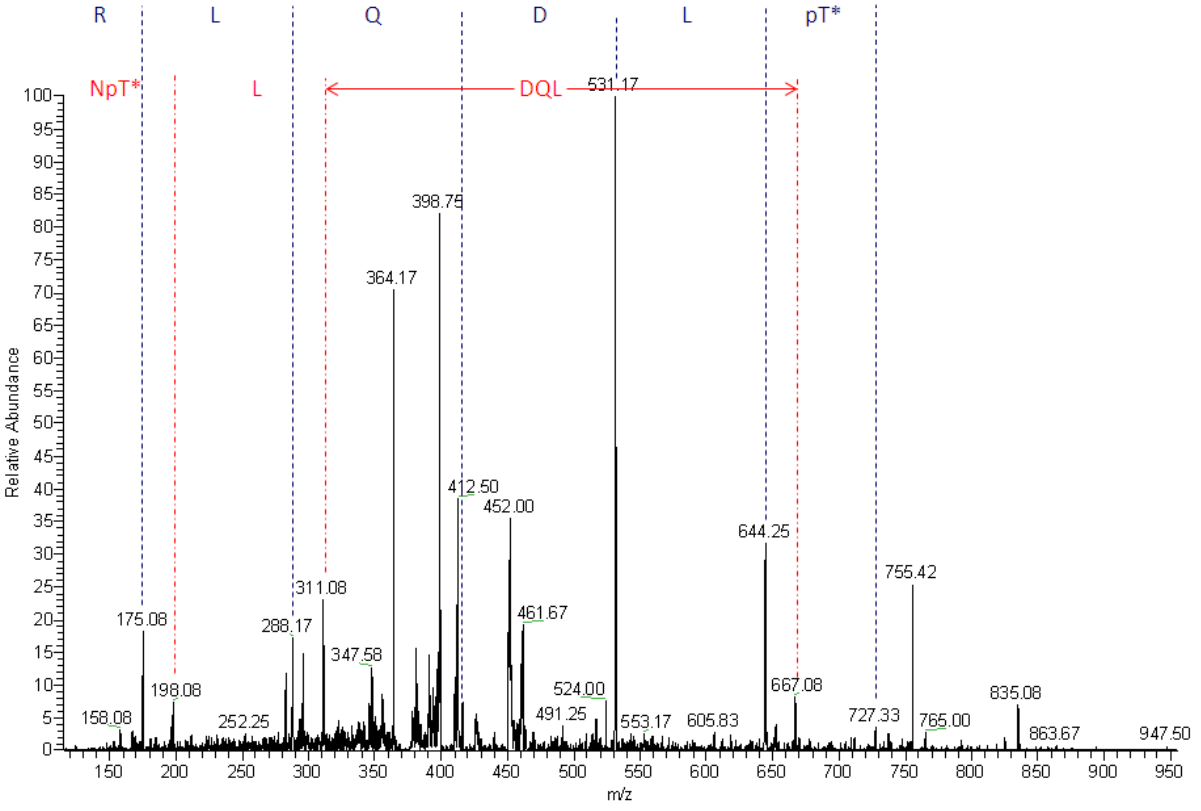

6.4 DNA fragments generated by *de novo* synthesis

6.4.1 Triple-haemagglutinin tag

AAGCTTTCGCGACTCGAGTTTAAACCCTCAGATATCACCCAATTGGCCGCTAGCAGCG
TAATCTGGAACGTCATACGGATATGAGCCTGCATAGTCCGGGACATCATAGGGATAGG
AGCCCGCATAGTCAGGAACATCGTATGGGTAGTTAACGCCACTAGTTGCCATATG

Fragment contained within the plasmid pMA-triple-HA

6.4.2 Partial LmxMPK1 sequence tagged with triple-HA

GGATCCTAGGGTTTAAACCCTCGCGACCCACCTCCACCGCCACCGGACCCACGCGGAA
CCAGCAACGCGTAATCTGGAACGTCGTACGGATAGCTGCCTGCATAGTCCGGGACATC
ATAGGGATAGGACCCGGCATAGTCAGGCACGTCGTATGGGTAGGGCCCCTGGAACAGA
ACTTCCAGTACGTAATACACGTCTGTTATGTGATAGCGGTAGCGCATGCCGATCTCGT
CGTACAGATTCGCCTTGTACTCCTCCTTGGTGTAGATCTTCCGCCTCCAGCGCTTGTG
ATCGCGTTGCAGAAGGTTTTTACGGATAATGGCTGTGAGATCGGTCTCTATCAACTCA
AAGACGAGGTACAGGTCAATGTCGTTGGCCGCACGAATCACGTCGAGGATGCCGACAA
TGAAGGGGTTGTGCCGCAGTCGCTGCAAAAGCATCACTTCCCGATAGGTGCGCTGCGC
ATCTTGAACGTTGCCAAAGGCGTCGTAGACCTTTTTGAGGGCAACGCACTTGCCCGTG
CGGCGGTCGAGGGCACACCAGACGACTCCGTAGGCACCGCTGCCGATGTGGCGGAGAA
TGCGGTAGCGTTGCTCAACCTCACCGTCGATGCCGTATGAGGTCATGGTCAATTGGGA
TCC

Fragment contained within the plasmid pMK-MPK1HA

6.4.3 Fragments encoding T224 mutations

T224A:

GGTACCGGTCGCCGGAGATTTTGGTCAAGTCGCGCGCCTATTCCACAGCGATGGACAT
GTGGGCGATCGGGTGTGTGATTGGGGAGATGCTGCTAGGCCGCCCACTCTTCGAGGGC
CGCAACGCGCTGGATCAACTCCGCCTGATCATTGAGGCTATCGGCGTGCCGAGCGACG
CAGATGTGCGCAGCCTTCACTCGCCCGAGCTCGAGAAGCTCATCAACTCCCTTCCGAC
CCCGTTGATCTTCTCTCCGCTTGTGGGGAACAAGAACCTGAAGGATAGCGAGGCGACA
GACTTGATGATGAAGCTCATTGTCTTCAATCCAAAGAGGCGGCTTTCCGCGGTGGAGG
CGCTGCAGCACCCCTACGTCGCCCCGTTTGTGCAGCATGGTGAGCTGGAGAAGATCCA
AGGCCTCGACCCACTCGTGCTGCCCCTCGTGGATGAGAAGATCTCTCGAGCGTGACCC
GGACGCCCGCCCCACGTGCGCGGAGTTGCTTCAGCACCAATTCTTCGATGGGATAACC
ACCGAAAGTGCTGTGGCGATGGTCAAGATGGCAGTGGAGCAGATGACCCGCCTCATCA
ATAACAACGCACAGAAGGAGAAGGAAGTGGCTCGGGATCAGGAGGACCTGGAGAATGA
CGTCAAGGCACAGCTTGATAAGATGGTGTTGTACGTA

675 bp

Fragment contained within the plasmid pUC-57-MPK1TA-MKK-DQED

T224E:

GGTACCGGTCGCCGGAGATTTTGGTCAAGTCGCGAGCCTATTCCACAGCGATGGACAT
GTGGGCCATCGGGTGTGTGATTGGGGAGATGCTGCTAGGCCGCCCACTCTTCGAGGGC
CGCAACGAGCTGGATCAACTCCGCCTGATCATTGAGGCTATCGGCGTGCCGAGCGACG
CAGATGTGCGCAGCCTTCACTCGCCCGAGCTCGAGAAGCTCATCAACTCCCTTCCGAC
CCCGTTGATCTTCTCTCCGCTTGTGGGGAACAAGAACCTGAAGGATAGCGAGGCGACA
GACTTGATGATGAAGCTCATTGTCTTCAATCCAAAGAGGCGGCTTTCCGCGGTGGAGG
CGCTGCAGCACCCCTACGTCGCCCCGTTTGTGCAGCATGGTGAGCTGGAGAAGATCCA
AGGCCTCGACCCACTCGTGCTGCCCCTCGTGGATGAGAAGATCTCTCGAGCGTGACCC
GGACGCCCGCCCAACCTGCGCGGAGTTGCTTCAGCACCAATTCTTCGATGGGATAACC
ACCGAAAGTGCTGTGGCGATGGTCAAGATGGCAGTGGAGCAGATGACCCGCCTCATCA
ATAACAACGCACAGAAGGAGAAGGAAGTGGCTCGTGCGCAGGAGGCCTTGGAGAATGA
CGTCAAGGCACAGCTTGATAAGATGGTGTTGTACGTA

675 bp

Fragment contained within the plasmid pUC57-MPK1TE-MKK-AQEA

6.4.4 LmxPTP deletion fragment

GATATCTCTGTGAGCTTGTGCGTGACTGCGCGTCTGCACGTGGAGGCCGAAGAACACA
CGCTTGCCTCCACACGCACACAGACACAGACACACCCTTCCTCCTGTTCTCGCTTGCC
GGCTCACGCTCCCGCTCTTAGTGTACGTTGCCTTCTTCAACACTGCCATCGTTTTCCT
CGCCCCTTCTCCCCACCACCACCACCACAACCACCACCACACACACACATCATCGTCG
CCACCATCTCGCAGAGATCTACGCTCTCTTCACTCCTCTCTGCGTCGCCTCTTCCGCC
TTTTAACGCTCCCCGAATTCACGAACACACGCTCACAGCCATGGCCTAGGGCTAGCTA
AGACGACCGCCCACGTCACGCCTGTGCGCGCGTGGGGACGGGACGCAGTACGGTGGGG
GCGCACCGAAGACAGCGCAAGCGTCGGGAAAACGTTGGGGGTAATGCGCAGGTAAAGA
GAAGGGAAGGGGAACGCCATGTGCGTATTGTATGTATATCGACGTCTATCGAGGTGAA
GACACGGCGTGGCGGGCGCGGTCGGTGCACCAATAGGGGGCCGCCGCGCCCCTTCTTC
ATCGCTGTTCTCGCTTCTGTGTACCTCTCGTCGAATGCATGCAAGCGTGCGAAGGGCA
CGGTGCAGCTGGAGTCGAGATGGTATGAAGACGTGGGGATATC

681 bp

Fragment contained within the plasmid pUC57-delLmxPTP

6.5 Plasmid maps

Plasmids from inhibitor-sensitised chapter:

Restriction map of pQE8W-mpk1WT - 4500 nt
<Serial Cloner V2.5> -- <30 Jul 2012 21:28>

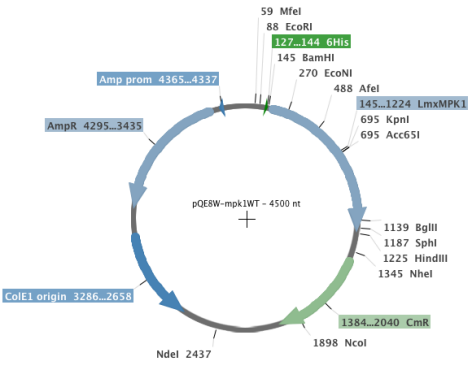

Restriction map of pCR2.1-TOPO-mpk1F93A - 4676 nt
<Serial Cloner V2.5> -- <30 Jul 2012 21:35>

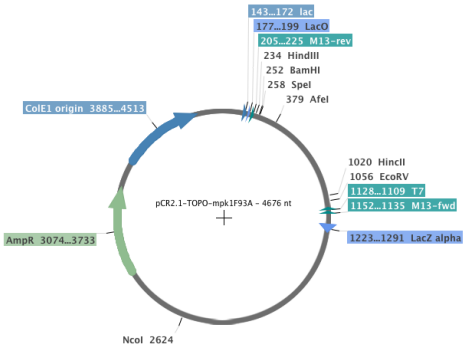

Restriction map of pGEX-KG-mpk1F93A - 6149 nt
<Serial Cloner V2.5> -- <30 Jul 2012 21:42>

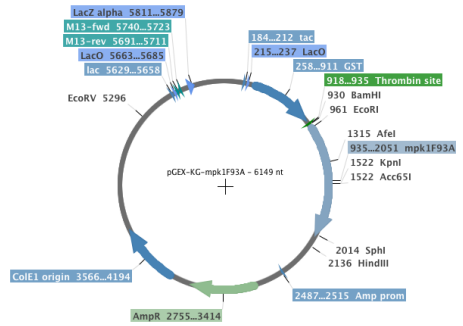

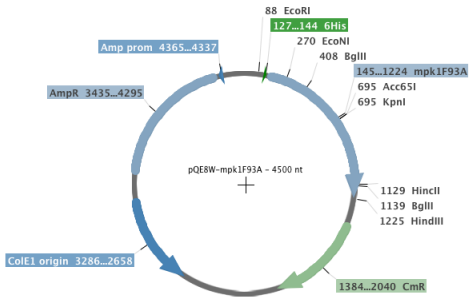

Restriction map of pQE8W-mpk1F93G - 4500 nt
<Serial Cloner V2.5> -- <30 Jul 2012 22:16>

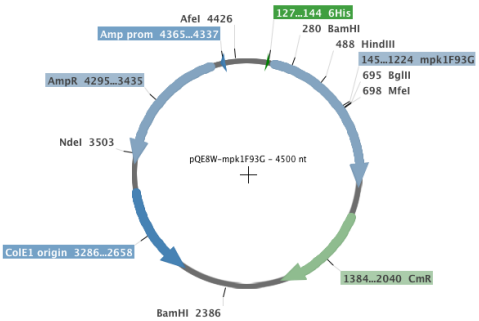

Plasmids from dephosphorylation chapter:

Restriction map of pMA-triple-HA - 2543 nt
<Serial Cloner V2.5> -- <30 Jul 2012 20:05>

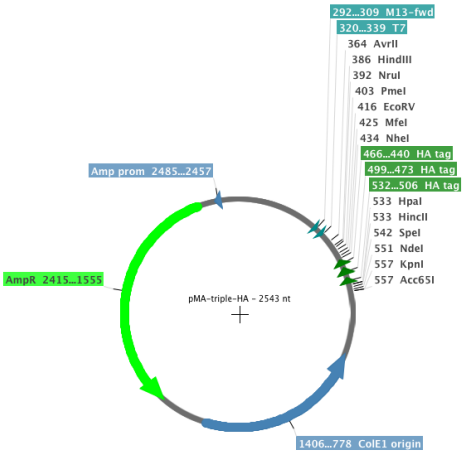

Restriction map of pJC-LmxMPK1-3HA - 4516 nt
<Serial Cloner V2.5> -- <30 Jul 2012 19:32>

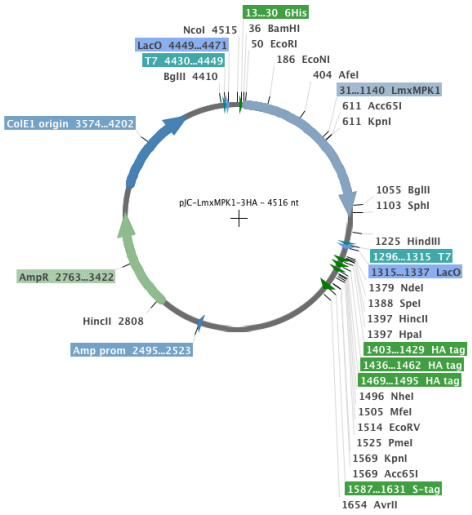

Restriction map of pJC-LmxMPK1-lambda-3HA - 5173 nt
<Serial Cloner V2.5> -- <30 Jul 2012 16:57>

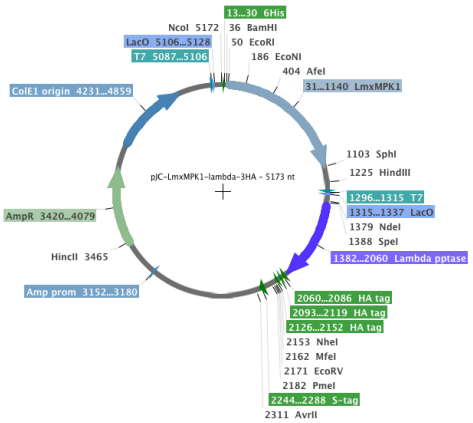

Restriction map of pJC-LmxMPK1-3HA-Lambda - 5164 nt
<Serial Cloner V2.5> -- <30 Jul 2012 17:47>

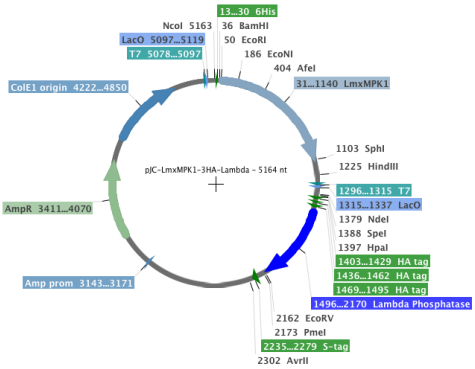

Restriction map of pJC-LmxMPK1-PTP1B-3HA - 5479 nt
<Serial Cloner V2.5> -- <30 Jul 2012 20:56>

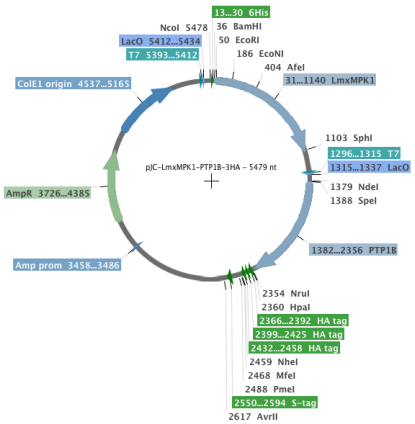

Restriction map of pJC-LmxMPK1-3HA-PTP1B - 5470 nt
<Serial Cloner V2.5> -- <30 Jul 2012 20:42>

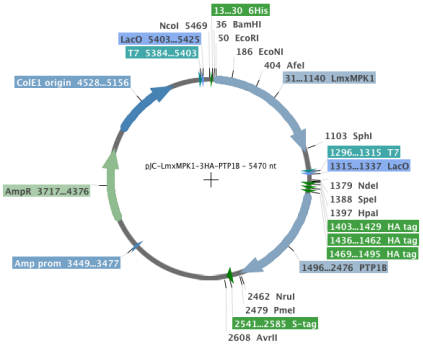

Restriction map of pJC-LmxMPK1-LmxPTP-3HA.xdna - 5182 nt
<Serial Cloner V2.5> -- <30 Jul 2012 21:04>

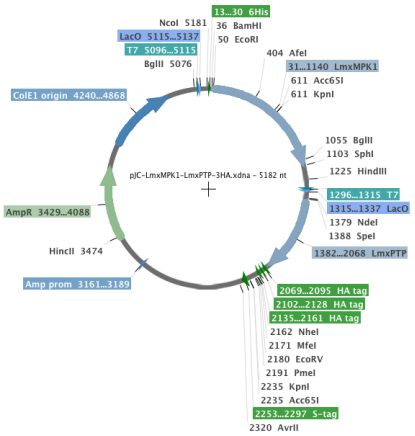

Restriction map of pJC-LmxMPK1-3HA-LmxPTP - 5173 nt
<Serial Cloner V2.5> -- <30 Jul 2012 21:17>

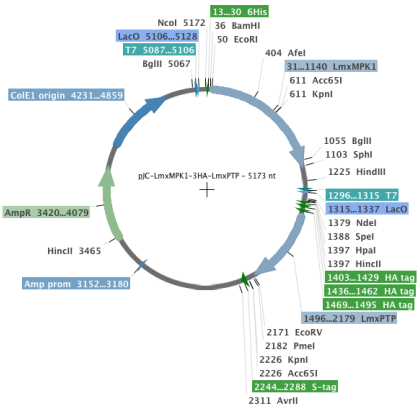

GFP-tagged localisation of activation lip mutants:

Restriction map of pX63polPheloMOD - 5207 nt
<Serial Cloner V2.5> -- <30 Jul 2012 22:22>

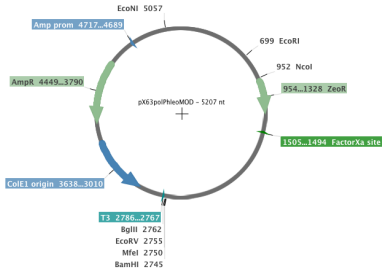

Restriction map of pMA-mpk1HA - 3011 nt
<Serial Cloner V2.5> -- <30 Jul 2012 22:39>

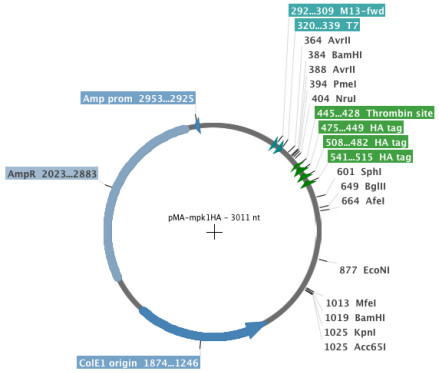

Restriction map of pX63polPheloMODmpk1sHAgfp - 6550 nt
<Serial Cloner V2.5> -- <30 Jul 2012 23:03>

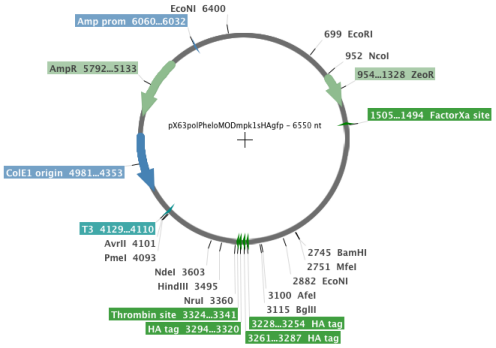

Restriction map of pTH6nGFPc.xdna - 7699 nt
<Serial Cloner V2.5> -- <30 Jul 2012 23:12>

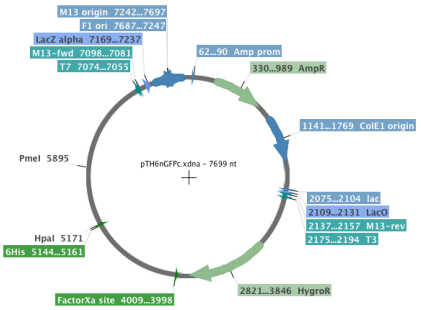

Restriction map of pX63polPheloMODmpk1(WT)HAgfp - 7186 nt
<Serial Cloner V2.5> -- <30 Jul 2012 23:23>

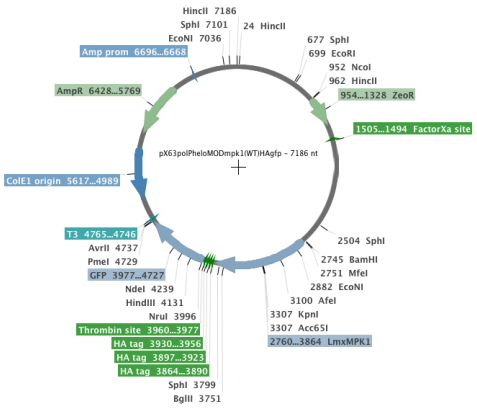

T224 mutants:

Restriction map of pUC57-MPK1TA-MKK-DQED - 3391 nt
<Serial Cloner V2.5> -- <30 Jul 2012 23:36>

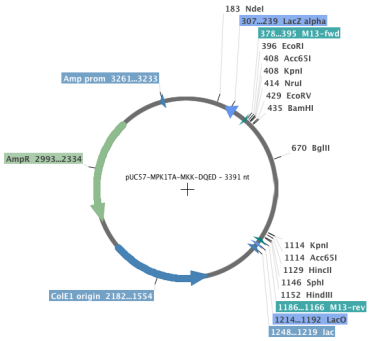

Restriction map of pUC57-MPK1TE-MKK-AQEA - 3388 nt
<Serial Cloner V2.5> -- <30 Jul 2012 23:37>

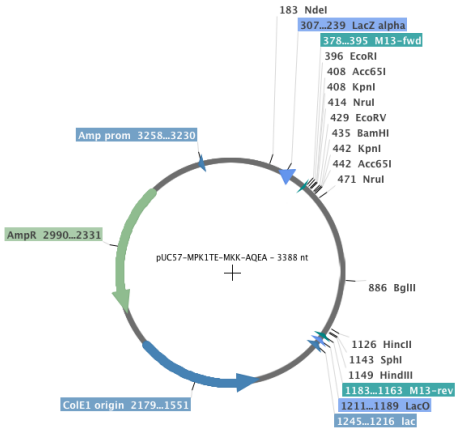

Restriction map of pQE8W-mpk1(T224A) - 4500 nt
<Serial Cloner V2.5> -- <31 Jul 2012 12:21>

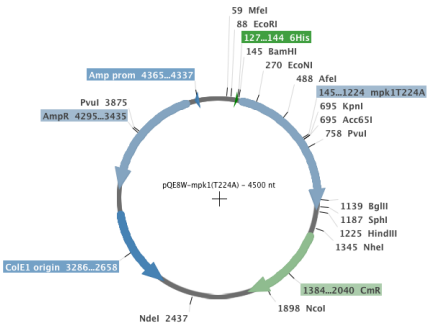

Restriction map of pQE8W-mpk1(T224E) - 4500 nt
<Serial Cloner V2.5> -- <31 Jul 2012 12:22>

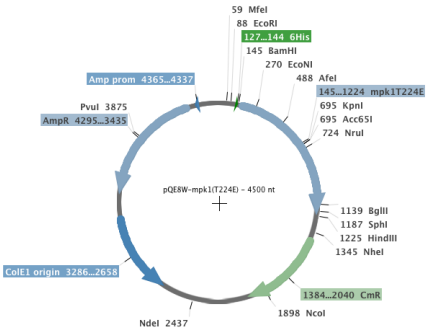

Restriction map of pJC-mpk1T224A-3HA-PTP1B - 5470 nt
<Serial Cloner V2.5> -- <31 Jul 2012 12:44>

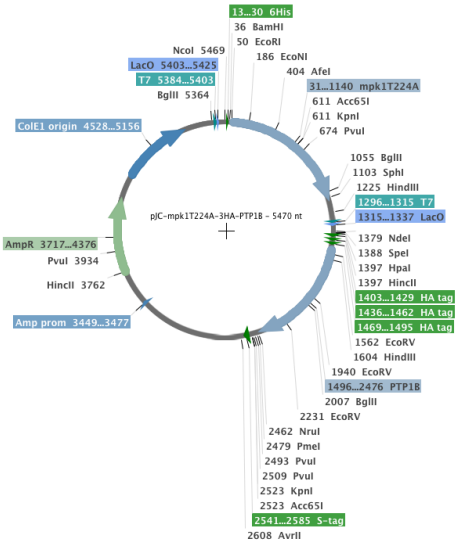

Restriction map of pJC-mpk1T224E-3HA-PTP1B.xdna - 5470 nt
<Serial Cloner V2.5> -- <31 Jul 2012 13:06>

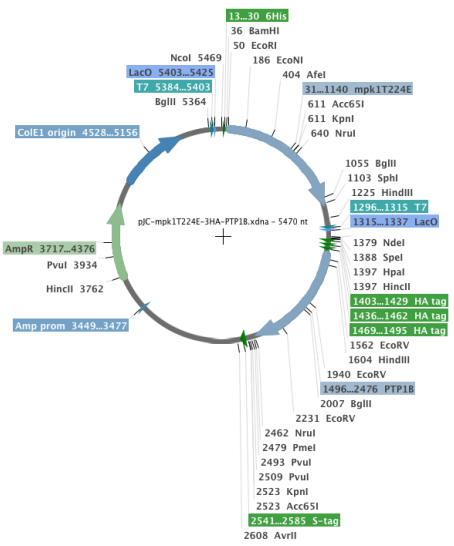

Restriction map of pJC-mpk1T224A-lambda-3HA - 5173 nt
<Serial Cloner V2.5> -- <31 Jul 2012 13:15>

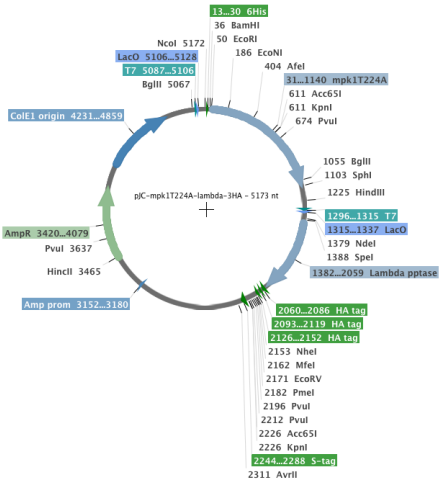

Restriction map of pJC-mpk1T224E-lambda-3HA - 5173 nt
<Serial Cloner V2.5> -- <31 Jul 2012 13:31>

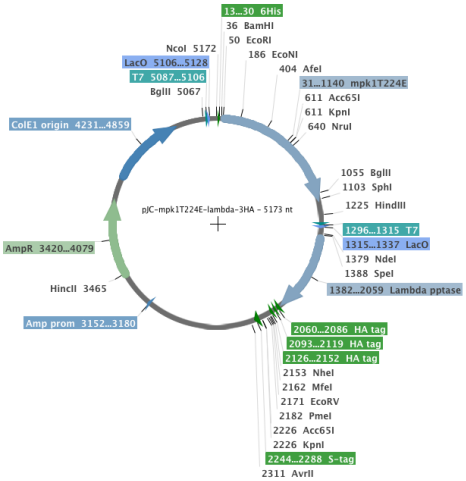

Restriction map of pX63polPhleoMODmpk1(T224A)HAgfp.xdna - 7186 nt
<Serial Cloner V2.5> -- <31 Jul 2012 13:39>

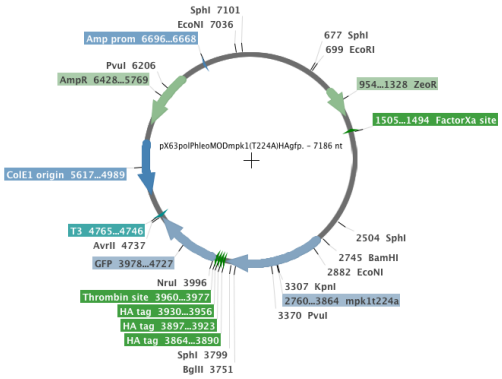

LmxPTP deletion and localisation:

Restriction map of pUC57-delLmxPTP - 3385 nt
<Serial Cloner V2.5> -- <31 Jul 2012 13:42>

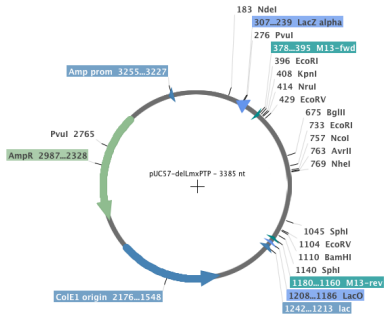

Restriction map of pUC57-delLmxPTP-Phleo - 3750 nt
<Serial Cloner V2.5> -- <31 Jul 2012 13:45>

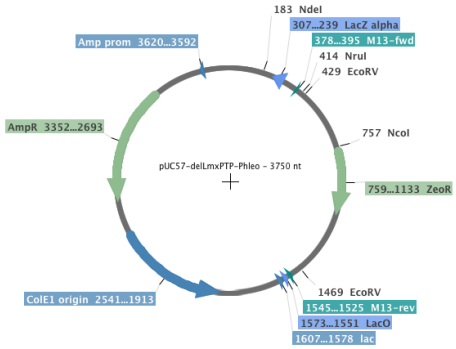

Restriction map of pCR2.1-Phleo - 4298 nt
<Serial Cloner V2.5> -- <31 Jul 2012 13:48>

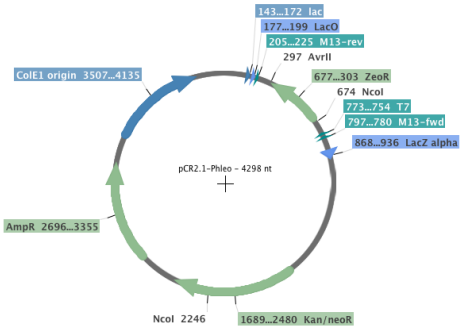

Restriction map of pUC57-delLmxPTP-Neo - 4179 nt
<Serial Cloner V2.5> -- <1 Aug 2012 10:51>

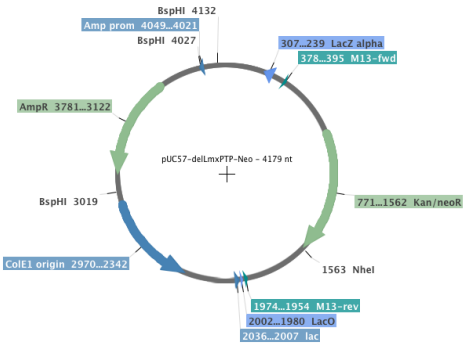

Restriction map of pCR2.1-Neo - 4727 nt
<Serial Cloner V2.5> -- <1 Aug 2012 10:29>

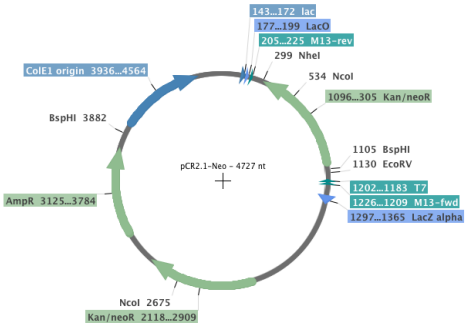

Acknowledgments

I would primarily like to thank my supervisor Dr Martin Wiese for giving me the opportunity to carry out my PhD in his lab group. His encouragement, guidance and patience when examining results and planning new experiments were invaluable to the success of my project.

A note of thanks is due to Dr Paul Herron (Microbiology, SIPBS) who very kindly allowed me to use his fluorescent microscope for the capturing of images that were essential for this thesis. Thanks also to Adrienne McGachy for technical assistance with aspects of running the lab and helping our lab group with the move between buildings. Lucia Krott provided technical assistance for the cloning of the LmxPTP deletion constructs and T224 mutants.

For my first year in the lab I was extremely fortunate to have the company of Mona John von Freyend, both to show me techniques, explain what I was doing wrong (not much, obviously!) and have some excellent discussions with.

From second year onwards the Wiese group shrank to Laura Munro and I. We've had some excellent laughs, a wee trip to Hamburg (not just to see the BNI!) and a bigger trip to Boston/NYC (with the KMCB meeting at Woods Hole squeezed in too). Thanks for proof-reading this before submission!

Other members of 253/HW601 were excellent company for working with, not to mention the odd trip to the pub. Stuart, Selina, Bharath, Craig, Sara, Karen, Caroline, Kirstyn and Chris: thanks for your support and friendship!

A massive thank-you to Heidi Rosenqvist for performing the mass spectrometry included in this thesis! Not only for the practical running of the samples but also her unending patience for explaining what the results meant to a mass/charge philistine like myself.

Lastly, thanks to my family for your support and belief in me during what was at times a long three years. I'm sure one day I'll work out a way of explaining to you what it was I was doing in the lab all that time!

Patrick McAleer, Glasgow, September 2012